Functional investigation of cannabinoid receptors

Thesis

Submitted for a Doctoral Degree in Natural Sciences

(Dr. rer. nat.)

Mathematics and Natural Sciences Faculty,

Rheinische Friedrich Wilhelms University, Bonn, Germany

Submitted by

Date Rahul Anant

Bonn, 2007

Supervisor: Prof. Dr. Andreas Zimmer
First reviewer: Prof. Dr. Michael Famulok
Second reviewer: Prof. Dr. Jörn Piel
Third reviewer: Prof. Dr. Christa E. Müller

Date of Submission: 21/11/2007
Date of Examination: 18/01/2008

Thesis work completed at:
Institute for Molecular Psychiatry,
Sigmund Freud Str. 25,
53127, Bonn, Germany.

Publication year: 2008

Declaration

I solemnly declare that the work submitted here is result of my own investigation, except where otherwise stated. This work has not been submitted to any other university or institute towards the partial fulfilment of any degree.

Date Rahul Anant

Dedicated to mother, father and teachers

मातृदेवो भव । पितृदेवो भव । आचार्यदेवो भव ।

Matru devo bhava | Pitru devo bhava | Acharya devo bhava |

(Sanskrit Verse from Taittiriya Upanishad, Siksa Valli I, XI Anuvaka, II)

Worship your mother, father and teachers

Abbreviations

2-AG	2-Arachidonylglycerol (5Z,8Z,11Z,14Z)-5,8,11,14-Eicosatetraenoic acid, 2-hydroxy-1-(hydroxymethyl) ethyl ester
2-LinoG	2-linoleoylglycerol
2-PalmG	2-palmitoylglycerol
ACPA	Arachidonylcyclopropylamide *N*-(Cyclopropyl)-5Z,8Z,11Z,14Z-eicosatetraenamide
AEA	Arachidonylethanolamide, *N*-(2-Hydroxyethyl)-5Z,8Z,11Z,14Z-eicosatetraenamide
AM-630	6-Iodo-2-methyl-[2-(4-morpholinyl)ethyl]-1H-indol-3-yl(4-methoxyphenyl)methanone
APS	Ammonium persulfate
bp	Basepair
CB1	Cannabinoid receptor 1
CB2	Cannabinoid receptor 2
CDP Star	Disodium 4-chloro-3-(methoxy spiro {1,2-dioxethan- 3,2-(5-chloro)tricyclo[3.3.1.13,7] decan}-4-yl) phenylphosphate
CFP	Cyan fluorescent protein
CNS	Central nervous system
CP55,940	(-)-cis-3-[2-Hydroxy-4-(1,1-dimethylheptyl)phenyl]-trans-4-(3-hydroxypropyl) cyclohexanol
cAMP	Cyclic adenosine-3', 5'-monophosphate
DMSO	Dimethylsulfoxide
DNFB	2,4-Dinitroflurobenzene
dNTP	Deoxynucleotides
dsRed	*Discosoma sp.* red fluorescent protein
EDTA	Disodium ethylendiamine tetraacetic acid
EGTA	Ethylenglycol-bis(-β-aminoethylether) *N,N,N',N'* tetra acetic acid
ES cell	Embryonic stem cell
Em	Molar extinction coefficient
Erk	Extracellular signal-regulated kinases
eCFP	Enhanced cyan fluorescent protein
eGFP	Enhanced green fluorescent protein
FAAH	Fatty acid amide hydrolase

FIAU	2´-Deoxy-2´-fluoro-β-d-arabinofuranosyl-5-iodouracil
GM-CSF	Granulocyte monocyte colony stimulating factor
GPCR	G protein coupled receptor
HBSS	Hanks balanced salt solution
HEPES	*N*-2-Hydroxyethylpiperazin-*N'*-2-ethansulfonic acid
HSV-TK	Herpes simplex virus - thymidine-kinase
HU-210	(6aR,10aR)-3-(1,1'-dimethylheptyl)-6a,7,10,10a-tetrahydro-1-hydroxyl -6,6-dimethyl-6H-dibenzo[b,d]pyran-9-methanol
HU-308	4-[4-(1,1-diemethylheptyl)-2,6-dimethoxyphenyl]-6,6-dimethylbicyclo [3.1.1]hept-2-ene-2-methanol
i.p.	Intra peritoneal
JTE-907	[*N*-(benzo[1,3]dioxol-5ylmethyl)-7-methoxy-2-oxo-8-pentyloxy-1,2-dihydroquinoline-3-carboxamide]
LIF	Leukaemia inhibitory factor
loxP	*Locus of X-cross of P1*
MOPS	3-Morpholino propan sulfonic acid
NE	Noladine ether
MAPK	Mitogen-activated protein kinases
Sch.336	*N*-[1(*S*)-[4-[[4-methoxy-2-[(4-methoxyphenyl)sulfonyl]phenyl]-sulfonyl]phenyl]ethyl]methanesulfonamide
SDS	Sodium dodecyl sulfate
SSC	Saline sodium citrate solution
TAE	Tris-acetate EDTA
TEMED	*N,N,N´,N´* -Tetramethylethylendiamine
TPA	tetradecanoyl 13-acetate
Tris	2-amino-2-hydroxymethyl-1,3-propanediol
Tween	Tween 20, Polyoxyethylenesorbitan Monolaurate
U	Unit (s)
WIN	WIN 55,212-2 R(+)-[2,3-Dihydro-5-methyl-3-(4-morpholinylmethyl)pyrrolo-[1,2,3-de]-1,4-benzoxazin-6-yl]-1-naphtalenyl-methanonmesylate
WT	Wild type
Δ^9-THC	Delta-9-tetrahydrocannabinol, (R,R)-5,11-Diethyl-5,6,11,12-tetrahydro-2,8-chrysenediol

Index

1 Introduction

G protein coupled receptors (GPCR) are seven-transmembrane receptors, which constitute the largest, most ubiquitous and most versatile family of membrane receptors (Pierce, Premont et al. 2002). Analysis of the human genome reveals the possibility of 865 different GPCR sequences (Milligan 2006). Some estimate that the number could surpass 1000 (Brauner-Osborne, Wellendorph et al. 2007). GPCRs are membrane proteins that activate intracellular signaling cascades and undergo endocytosis, recycling, or degradation upon stimulation (Fig. 1.1) (Lee, Lynch et al. 2000).

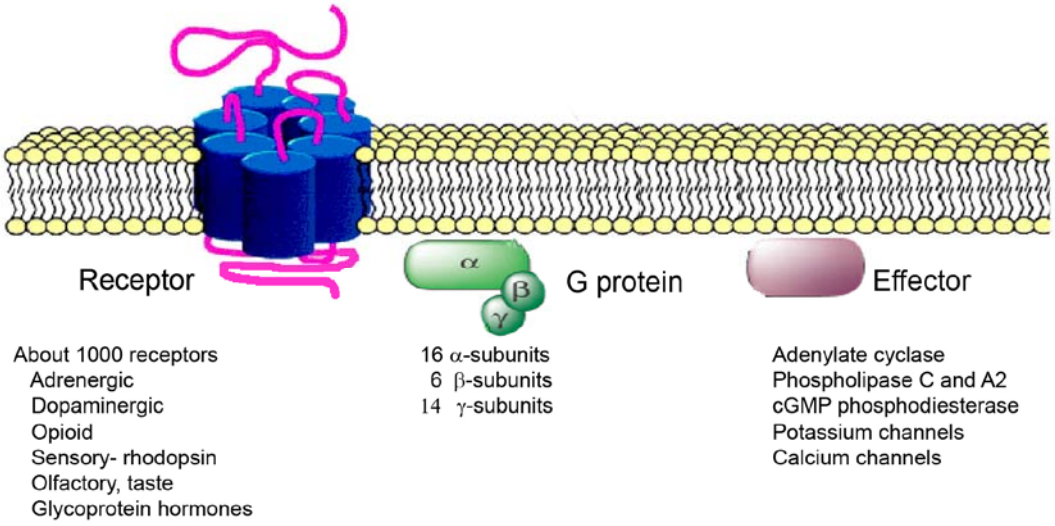

Fig. 1.1 General scheme of GPCR signaling. The GPCR signaling comprises three parts: a seven-transmembrane spanning receptor; a heterotrimeric G protein (figures next to each subunit indicate the number of variants that have been identified); and an effector, such as an enzyme or ion channel. (Adopted from Rockman and Kostenis et al.) (Rockman, Koch et al. 2002; Kostenis, Waelbroeck et al. 2005).

GPCRs are involved in the primary mechanism used by virtually all eukaryotic cells to receive, interprete and respond to a wide range of structurally and chemically diverse extracellular stimuli (Kostenis, Waelbroeck et al. 2005). Thus it is not surprising that they are also the most common (50 %) target of the therapeutic drugs (Pierce, Premont et al. 2002; Razvi 2005). They are studied using radioactively labeled receptor-specific-ligands, cell culture expression of these receptors (Richards and van Giersbergen 1995) or by analyzing downstream processes of receptor activation, such as reporter genes (Moro, Ideta et al. 1999; Liu and Wu 2004), GTP-γ-S (Moore, Xiao et al. 2000; Selley, Rorrer et al. 2001; Bidlack and Parkhill 2004), mitogen-activated protein kinase (MAPK) (Leroy, Missotten et al. 2007) and cyclic AMP (cAMP) assays (Howlett, Qualy et al. 1986; Childers and Deadwyler 1996;

Mukhopadhyay, Das et al. 2006). Transgenic knock-in (Mihara, Smit et al. 2005; Scherrer, Tryoen-Toth et al. 2006) as well as knock-out models (Zimmer, Zimmer et al. 1999; Buckley, McCoy et al. 2000) allowed an alternative approach to study the vital roles of these proteins in *in vivo* systems.

Cannabinoid receptors also belong to the family of GPCRs, defined as those that respond to cannabinoid drugs, such as Δ^9-tetrahydrocannabinol (Δ^9-THC) derived from plant *Cannabis sativa* and its biologically active synthetic analogues.

1.1 Cannabinoids and their receptors

The term cannabinoid was originally used to describe the family of approximately sixty, 21-carbon structures present within the preparations of plant *cannabis sativa* (Little, Compton et al. 1989; Howlett, Champion et al. 1990). Of these, the most significant in terms of both quantity and psychoactive efficacy is Δ^9-THC (Fig. 1.2).

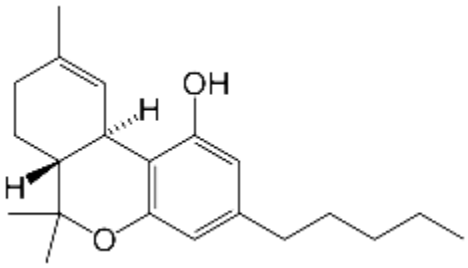

Fig. 1.2 Chemical structure of Δ^9-tetrahydrocannabinol: Structure of most studied psychoactive compound from plant *Cannabis sativa*, Δ^9-THC.

Recently the term ‘cannabinoid’ has been used to describe any compound that has activity at the cannabis receptors including synthetic and endogenous compounds (IUPHAR database). In 1992, the first endogenous compound was identified as arachidonoylethanolamide (AEA) and named anandamide, a name derived from the Sanskrit word ´anand´ for bliss and amide (Devane, Hanus et al. 1992) (Fig.1.3). It shows affinity for both centrally expressed cannabinoid receptor (CB1) and peripherally expressed (CB2) receptors and acts as a partial agonist for both. AEA shows Ki of 89 nM and 371 nM at CB1 and CB2 receptors respectively. Another endocannabinoid, 2-arachidonylglycerol (2-AG), binds also to both CB1 and CB2 receptors (Fig. 1.3). Unlike AEA, 2-AG acts as a full and potent agonist Ki values 472 nM and 1400 nM, respectively (Felder, Joyce et al. 1995; Mechoulam, Ben-Shabat et al. 1995; Showalter, Compton et al. 1996). Both endocannabinoids AEA and 2-AG are derived from the essential fatty acid arachidonic acid and are found in nearly all

tissues in a wide range of animals (Di Marzo 1998). For example, 2-AG levels (5.4 ± 0.6 nmol/g) in hippocampus of wild type male mice were found to be about 1000 fold higher than AEA (51.1± 10.2 pmol/g) (Di Marzo, Breivogel et al. 2000).

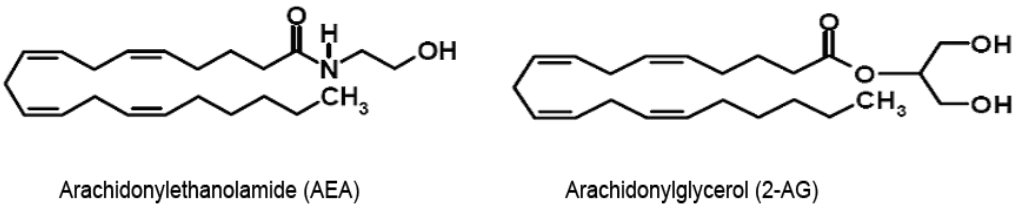

Arachidonylethanolamide (AEA) Arachidonylglycerol (2-AG)

Fig. 1.3 Chemical structure of endocannabinoids: Chemical structure of two endocannabinoids, arachidonylethanolamide (AEA) and arachidonylglycerol (2-AG).

Synthetic agonists that bind to cannabinoid receptors include cannabinoid compounds such as Δ^9-THC-like ABC tricyclic cannabinoid analogues, typified by HU-210 (Johnson 1986) and desacetyllevonantradol (Pacheco, Childers et al. 1991; D'Ambra, Estep et al. 1992); synthetic AC bicyclic and ACD tricyclic cannabinoid analogues, typified by CP55,940, and CP55,244 (Devane, Hanus et al. 1992; Fride and Mechoulam 1993), and aminoalkylindole compounds, typified by WIN 55,212-2 (Mechoulam, Ben-Shabat et al. 1995; Sugiura, Kondo et al. 1995).

Cannabinoid crude preparations were reported to be used since 2000 B.C. in China for medicinal purposes (Mathre 1997). However, recent clinical trials of cannabinoids for multiple sclerosis (Wade, Makela et al. 2006; Collin, Davies et al. 2007), pain (Pinsger, Schimetta et al. 2006) have been the subject of controversy. Primarily, this has been the result of an association with a ‘drug of abuse’, by moral, cultural beliefs as well as the lack of enough scientific evidence for their beneficial effects (Mandavilli 2003).

1.2 Cannabinoid receptors

1.2.1 Cannabinoid receptor 1

CB1 receptor has been first cloned from rat (Matsuda, Lolait et al. 1990), mouse (Chakrabarti, Onaivi et al. 1995) and human (Gerard, Mollereau et al. 1990) tissues. These receptors show 97-99% amino acid sequence identity across species. The CB1 receptor mRNA and protein are found primarily in central nervous system (CNS) (Herkenham, Lynn et al. 1990; Jansen, Haycock et al. 1992; Mailleux, Parmentier et al. 1992). It is particularly prevalent in basal ganglia, hippocampus, cerebellum and

cerebral cortex (Pettit, Harrison et al. 1998; Tsou, Brown et al. 1998). It is also shown to be present in some non-neuronal cells and tissues, for example leukocytes, testis (Mailleux, Parmentier et al. 1992; Pertwee 1997; Howlett, Barth et al. 2002) and bone cells (Idris, van 't Hof et al. 2005; Tam, Ofek et al. 2006).

Like most of the GPCRs, the coding sequence of the CB1 receptor is encoded by a single exon (for example, the human gene sequence Genebank accession U73304). However, an alternatively spliced form (CB1A) of the human receptor has been reported in which a 167 base portion of this exon is spliced out leading to the substitution of a different 28 residue sequence for the first 90 amino acids (Shire, Carillon et al. 1995).

Therapeutically beneficial effects of CB1 receptor in nervous system in responses to Δ^9-THC and other cannabinoid receptor agonists include analgesia (Ledent, Valverde et al. 1999; Zimmer, Zimmer et al. 1999), attenuation of nausea and vomiting in cancer chemotherapy (Niiranen and Mattson 1987; Grunberg 1989; Meiri, Jhangiani et al. 2007), appetite stimulation (Mattes, Engelman et al. 1994; Beal and Flynn 1995; Koch 2001), and decreased intestinal motility (Izzo and Coutts 2005; Carai, Colombo et al. 2006). Side effects also accompanying these therapeutic responses include alterations in cognition and memory (Bilkei-Gorzo, Racz et al. 2005; Rodriguez de Fonseca, Del Arco et al. 2005), dysphoria/euphoria and sedation (Purnell and Gregg 1975; Lukas, Mendelson et al. 1995).

CB1 receptors are coupled to pertussis toxin (PTX)-sensitive $G_{i/o}$ proteins to inhibit adenylate cyclase activity (Howlett, Qualy et al. 1986; Pacheco, Childers et al. 1991). They regulate L-, N- and P- or Q-type Ca^{2+} channels (Mackie and Hille 1992; Twitchell, Brown et al. 1997; Gebremedhin, Lange et al. 1999) and G protein-regulated, inwardly rectifying K^+ channels (Mackie, Lai et al. 1995). They are also shown to initiate intracellular Ca^{2+} transients (Sugiura, Kodaka et al. 1996), stimulate MAPK (Sugiura, Kodaka et al. 1996) and induce immediate early gene expression (Bouaboula, Bourrie et al. 1995).

1.2.2 Cannabinoid receptor 2

The second cannabinoid receptor, CB2, was cloned from a human leukemia HL60 library (Munro, Thomas et al. 1993). It exhibited 68% homology to the CB1 receptor. The mouse (Shire, Calandra et al. 1996) and rat CB2 (Griffin, Tao et al. 2000)

receptors exhibit 82% and 81% sequence identity to the human CB2 receptor respectively.

CB2 receptor mRNA was found primarily in immune tissue. It can be found in human spleen (Galiegue, Mary et al. 1995; Schatz, Lee et al. 1997), tonsils (Carayon, Marchand et al. 1998), bone marrow (Ponti, Rubino et al. 2001; Lu, Newton et al. 2006; Scutt and Williamson 2007), pancreas (Klein, Newton et al. 2001), splenic macrophage / monocyte preparations (Munro, Thomas et al. 1993; Carlisle, Marciano-Cabral et al. 2002; Carrier, Kearn et al. 2004), peripheral blood leukocytes (Bouaboula, Rinaldi et al. 1993), skin (Casanova, Blazquez et al. 2003; Stander, Schmelz et al. 2005) and in a variety of cultured immune cell models including the myeloid cell line U937 (Bari, Spagnuolo et al. 2006; Matsumoto, Hatanaka et al. 2006) and undifferentiated and differentiated granulocyte-like or macrophage-like HL60 cells (Das, Paria et al. 1995; Facci, Dal Toso et al. 1995; Gokoh, Kishimoto et al. 2005) and bone cells (Ofek, Karsak et al. 2006). Certain tumors, especially gliomas, express CB2 receptors (Galve-Roperh, Sanchez et al. 2000).

Signal transduction by the CB2 receptor includes PTX-sensitive inhibition of cAMP production in transfected host CHO cells (Felder, Joyce et al. 1995; Slipetz, O'Neill et al. 1995; Showalter, Compton et al. 1996; Griffin, Tao et al. 2000), MAP kinase activation and immediate early gene expression (Bouaboula, Poinot-Chazel et al. 1996). They modulate migration of several cell types (Sugiura, Kondo et al. 1995; Jorda, Lowenberg et al. 2003), proliferation of different type of cells for example immune cells like B cells (Derocq, Segui et al. 1995), T cells (Klein, Newton et al. 1985), splenocytes (Steffens, Veillard et al. 2005) and in bone cells like osteoblasts (Ofek, Karsak et al. 2006). Guzman and coworkers have shown that Δ^9-tetrahydrocannabinol and WIN-55,212-2, two non-selective cannabinoid agonists, induce the regression or eradication of malignant brain tumors in rats and mice (Juan-Pico, Fuentes et al. 2006). The rat glioma C6 expresses the CB2 receptor and, on the basis of studies with CB1 and CB2 selective antagonists, it has been proposed that activation of either of the two receptors may trigger apoptosis (Galve-Roperh, Sanchez et al. 2000; Sanchez, de Ceballos et al. 2001). Intially, no modulation of ion channels or alterations of intracellular Ca^{2+} were observed in host cells expressing CB2 receptors (Felder, Joyce et al. 1995; Slipetz, O'Neill et al. 1995). However, recently the endocannabinoid 2-arachidonylglycerol is shown to regulate Ca^{2+} signals in β-cells and as a consequence, it is shown to decrease insulin

secretion through CB2 receptors (Zoratti, Kipmen-Korgun et al. 2003; Juan-Pico, Fuentes et al. 2006) as well as in calf pulmonary endothelial cells CB2 receptors are shown to initiate Ca^{2+} signaling linked with phospholipase C (Zoratti, Kipmen-Korgun et al. 2003).

1.2.3 Novel cannabinoid receptor, GPR55

Recent studies indicate that the human orphan GPCR, GPR55 (Sawzdargo, Nguyen et al. 1999) which is extensively expressed in brain, is the novel cannabinoid receptor (Johns, Behm et al. 2007; Ryberg, Larsson et al. 2007). Cannabinoid ligand CP55,940 as well as endocannabinoids such as anandamide and virodhamine activate GTP-γ-S binding via this receptor (Baker, Pryce et al. 2006). It also binds to ligands such as cannabidiol and abnormal cannabidiol, which exhibit no CB1 or CB2 activity and are believed to function at a novel cannabinoid receptor (Johns, Behm et al. 2007; Ryberg, Larsson et al. 2007). GPR55 couples to Gα-13 and can mediate activation of *rhoA*, *cdc42* and *rac1*. Lysophosphatidic acid and sphingosine 1-phosphate also induced phosphorylation of the MAPK in GPR55-expressing cells, thus it is also termed as a lysophosphatidylinositol receptor (Oka, Nakajima et al. 2007). Various types of other lysolipids as well as the cannabinoid receptor ligands did not induce phosphorylation of the extracellular signal-regulated kinase.

The development of selective agonists or antagonists for this novel receptor will further aid to understand the functional relevance of this receptor.

1.2.4 Non cannabinoid receptor mediated effects

Endocannabinoid compounds have also demonstrated a number of biological activities (Bouaboula, Poinot-Chazel et al. 1996) that are not considered to be mediated via CB1 or CB2 receptors. For example, vasodilation by AEA in the endothelial cell (Nazzaro, Manzari et al. 1999) and nervous tissue (Zygmunt, Petersson et al. 1999). This might be due to the metabolized products of arachidonic acid such as prostacyclin, epoxyeicosatrienoic acids, or due to the action of AEA on vanilloid VR1 receptors. Studies with atypical agonists have also shown non CB1 or CB2 dependent change in blood pressure (Adams, Earnhardt et al. 1977) and vasodialation (Jarai, Wagner et al. 1999; Wagner, Varga et al. 1999; Offertaler, Mo et al. 2003; Begg, Pacher et al. 2005). These effects were thought to be mediated by an unknown cannabinoid receptor. However, recent study with novel GPR55 receptor

knock-out mice, showed no significant difference in blood pressure and vasodialation compared to the wild type mice (Johns, Behm et al. 2007).

Studies suggest that in spleen, brain and gut, 2-AG is accompanied by several 2-acyl-glycerol esters, mainly 2-linoleoylglycerol (2-LinoG) and 2-palmitoylglycerol (2-PalmG) (Ben-Shabat, Fride et al. 1998; De Petrocellis, Bisogno et al. 2002). These two esters do not bind to the cannabinoid receptors, nor do they inhibit adenylate cyclase (Di Marzo 1998; Lambert and Di Marzo 1999); however, they significantly potentiate the apparent binding of 2-AG to cannabinoid receptors and their ability to inhibit adenylate cyclase. In mice these esters have been shown to significantly potentiate 2-AG induced motor behavior inhibition, ring immobility, hot plate analgesia and hypothermia. Thus indicating that the biological activity of 2-AG can be increased by related endogenous 2-acyl-glycerols, which alone do not show any significant activity. This effect is termed as 'Entourage effect'. These 2-acylglycerol derivatives also bind to vanilloid receptor and exert entourage effects (Smart, Jonsson et al. 2002).

1.3 The endocannabinoid system

The endocannabinoid system consists of enzymes involved in cannabinoid biosynthesis (Bradley 1987; Di Marzo, Fontana et al. 1994), degradation (Cravatt, Giang et al. 1996) and release (Di Marzo, Fontana et al. 1994; Cadas, Gaillet et al. 1996), as well as specific endocannabinoid transporters (Brozoski, Dean et al. 2005) (Fig 1.4) (Di Marzo 1998; Rodriguez de Fonseca, Del Arco et al. 2005; Bermudez-Siva, Serrano et al. 2006). For example, AEA is synthesized by *N*-arachidonylphosphatidylethanolamine (N-ArPE), which is believed to originate from the transfer of arachidonic acid from the sn-1 position of 1,2–sn–di-arachidonylphosphatidylcholine to phosphatidylethanolamine catalyzed by a Ca^{2+}-dependent N-acyltransacylase (NAT) (Basavarajappa 2007). N-ArPE is then cleaved by an N-acylphosphatidylethanolamine (NAPE)-specific phospholipase D (PLD) (NAPE-PLD) (Natarajan, Reddy et al. 1981; Schmid, Reddy et al. 1983; Bradley 1987; Di Marzo, Fontana et al. 1994), which releases AEA and phosphatidic acid. AEA is degraded by a well-characterized enzyme, the fatty acid amide hydrolase (FAAH)(Cravatt, Giang et al. 1996). Phospholipase C (PLC)-mediated hydrolysis of membrane phospholipids may produce diacylglycerol (DAG), which may be subsequently converted to 2-AG by diacylglcerol lipase (DAGL) activity (Prescott and

Majerus 1983; Sugiura, Kondo et al. 1995). Alternatively, the formation of DAG involves the hydrolysis of phosphatidic acid through Mg^{2+} and Ca^{2+}-dependent phosphohydrolase activity (Bisogno, Melck et al. 1999; Carrier, Kearn et al. 2004). 2-AG is degraded by the monoacylglycerol lipase (Dinh, Carpenter et al. 2002).

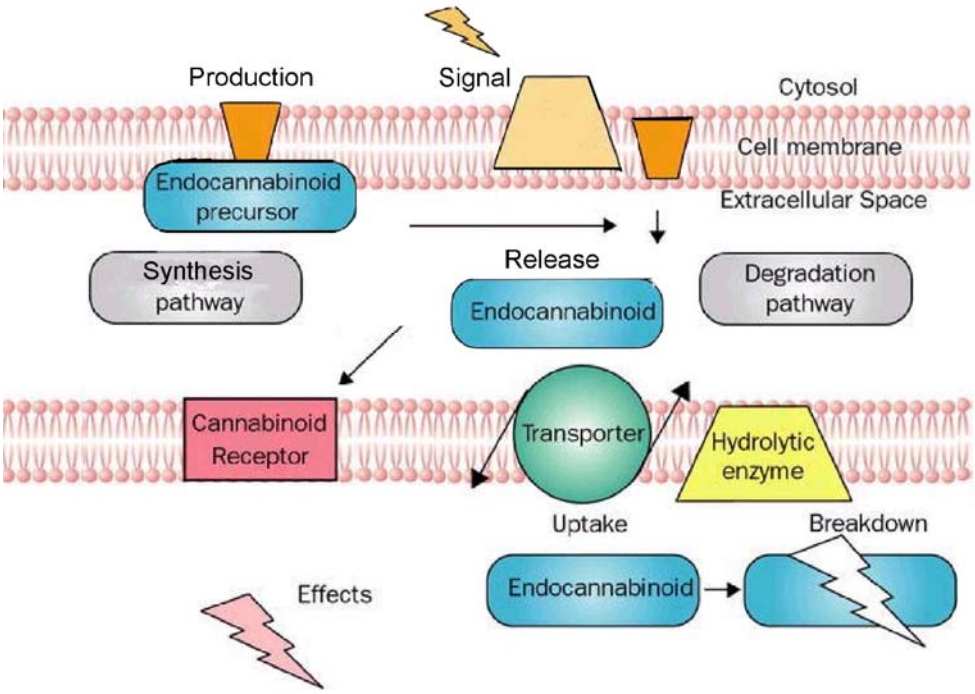

Fig. 1.4 Schematic diagram of endocannabinoid system: Scheme above represents the endocannabinoid system, consisting of enzymes involved in synthesis, degradation and release as well as specific endocannabinoid transporters. Adopted from Baker et al. (Baker, Pryce et al. 2003).

1.3.1 Transgenic approach to study the endocannabinoid system

To study this system transgenic approaches have been undertaken, where specific enzymes or receptors have been knocked out. We and other researchers have used a genetic approach and generated mice with the targeted deletions in the cannabinoid receptor genes CB1 (Ledent, Valverde et al. 1999; Zimmer, Zimmer et al. 1999; Marsicano, Wotjak et al. 2002; Robbe, Kopf et al. 2002), CB2 (Buckley, McCoy et al. 2000) and GPR55 (Johns, Behm et al. 2007). Studies using CB1 knock-out mice have demonstrated that this receptor participates in the control of several behavioral responses including locomotion, and anxiety like states (Zimmer, Zimmer et al. 1999), cognitive functions such as memory and learning processes (Bilkei-Gorzo, Racz et al. 2005), cardiovascular responses (Jarai, Wagner et al. 2000), modulator of the rewarding and addictive properties of other drugs of abuse (Ledent, Valverde et al. 1999; Martin, Ledent et al. 2000; Cossu, Ledent et al. 2001) and feeding (Wiley, Burston et al. 2005).

The CB2 knock-out model has been successfully used to reveal cannabinoid-induced inhibition of helper T cell activation in macrophages (Buckley, McCoy et al. 2000), the antifibrogenic role of the CB2 receptor in the liver injury (Julien, Grenard et al. 2005), in formation of B and T cell subsets (Ziring, Wei et al. 2006), in regulation of bone mass (Ofek, Karsak et al. 2006), in lymphocyte proliferation and cytokine secretion and macrophage phagocytic activity (Buckley, Burbridge et al. 2006). Activation of the CB2 receptor has been also shown to have anti-artherosclerotic properties in mouse model (Steffens, Veillard et al. 2005).
We have also generated the cannabinoid receptor double knock-out mice. This model had helped to understand residual cannabinoid effects of cannabinoids like 2-AG, on interferon-gamma suppression in phorbol ester/ionomycin activated splenocytes (Kaplan, Ouyang et al. 2005), Δ^9- THC and cannabinol on induction of calcitonin gene-related peptide (Zygmunt, Andersson et al. 2002), and of cannabinol on induction of hypotension in mice (Jarai, Wagner et al. 1999).

1.4 Aim

I wanted to investigate severe ulcerations phenotype of CB1-CB2 receptors deficient mice. I also aimed to generate a novel knock-in mouse line, with functional fluorescent tagged CB2 receptors. This will help to study the exact localization and dynamics of the receptors in an *in vivo* system. For this I wanted to intially establish an *in vitro* overexpression system to characterize the functionality of fused CB2 receptors.

In context of this work the following aims were set:

- To study wound healing in the CB1-CB2 knock-out mice
- Generation of Knock-in mice, with fluorescent tagged receptor, GFP- coupled (and CFP coupled) CB2-receptor
- Generation of an *in vitro* system having CB2 fusion protein

2 Materials

All chemicals used had the quality p.a. (per analysis) from Invitrogen (Karlsruhe), Sigma (Taufkirchen) or AppliChem (Darmstadt) unless mentioned otherwise.

2.1 Instruments

-80 °C Freezer	Heraeus Instruments GmbH (Hanau)
Autoclave	Varioclave 25T, HP Labortechnic AG (Oberschleißheim)
Bacterial shaker	Innova 4200 Incubator shaker, New Brunswick Scientific (USA)
BD LSR II FACS	BD LSR II Flowcytometer BD (USA)
Bioanalyzer	Agilent 2100 Bioanlyzer, Agilent (Waltbronn)
CCD camera	KY-F75U, JVC (Japan)
Cell incubator	CB 210, Binder GmbH (Tuttlingen)
Centrifuge	Biofuge pico, Heraeus Instruments GmbH (Hanau)
Centrifuge	Biofuge stratos, Heraeus Instruments GmbH (Hanau)
Centrifuge	Biofuge fresco, Heraeus Instruments GmbH (Hanau)
Chemical balance	BP 121 S, Sartorius AG (Goettingen)
Confocal microscope	Olympus (USA)
Cryopreservator	Linde systems (Muenchen)
Cryostat	CM 3050 S, Leica GmbH (Nussloch)
Developing machine	X-OMAT 1000, Kodak GmbH (Stuttgart)
Digital gel documentation	ChemiDoc System, Bio-Rad Laboratories GmbH (Muenchen)
Electroporator	Gene pulser II, Bio-Rad Laboratories GmbH (Muenchen)
Electrophoresis chamber	Bio-Rad Laboratories GmbH (Muenchen)
Engineer's micrometer	Oditest, Fa. Kroeplin (Schluechtern)
Fluorescence macroscope	Leica MZ16F, Leica microsystems (Nussloch)
Fluorescence microscope	Axiovert 40 CFL, Carl Zeiss AG (Jena)
Fluorescence microscope	Axioplan 2, Carl Zeiss AG (Jena)

Heating block	HLC (Bovenden)
Homogenizer	T8 Ultra-turrax, IKA GmbH (Staufen)
Hybridization incubator	HB 1000, UVP Laboratory (USA)
Magnetic stirrer	MR 3001 K, Heidolph, Fischer (Duesseldorf)
Microplate reader	DYNEX Technologies GmbH (Berlin)
Millipore unit	Millipak express 20, Millipore (USA)
Mini-Protean® 3 Cell	Bio-Rad Laboratories GmbH (Muenchen)
Neubauer cell chamber	Bright–Line, Hausser Scientific (USA)
PCR iCycler	iCycler, Bio-Rad Laboratories GmbH (Muenchen)
pH meter	inoLab, WTW GmbH (Weilheim)
Powerpac 300	Bio-Rad Laboratories GmbH (Muenchen)
Shaker	Combi shaker KL2, Edmund Buehler GmbH (Hechingen)
Spectro photometer	91-ND-1000 UV/Vis, Nanodrop (USA)
Sterile bank	Herasafe KS15, Heraeus Instruments GmbH (Hanau)
Ultracentrifuge	Sorvall Evolution RC, Kendro (USA).
Ultrasonic homogenizer	Sonoplus, Bandelin (Berlin)
UV crosslinker	UV Stratalinker 2400, Stratagene (USA)
UV handlamp	UVM-57, Upland (USA)
Vacuume blotter	Basic Unit (1655003), Bio-Rad Laboratories GmbH (Muenchen)
Vacuume pump	Bio-Rad Laboratories GmbH (Muenchen)
Vortexer	Vortex-Genie 2, Scientific Industries (USA)

2.2 Reagents and Chemicals

Agarose	Invitrogen GmbH (Karlsruhe)
AM 630	Biotrend GmbH (Koeln)
Aqua/polymount	Polyscience Europe GmbH (Eppelheim)
Blocking reagent	Roche Diagnostics GmbH (Mannheim)
Bovine serum albumin (fraction V)	Sigma GmbH (Taufkirchen)
CDP–Star	New England BioLabs GmbH (Frankfurt)
Complete mini protease inhibitor cocktail	Roche Diagnostics GmbH (Mannheim)
Dulbecco´s MEM	Gibco / Invitrogen GmbH (Karlsruhe)

ECL reagent	Perbio GmbH (Bonn)
F12 + glutamax-I (Hams)	Gibco / Invitrogen GmbH (Karlsruhe)
Fetal calf serum	Gibco / Invitrogen GmbH (Karlsruhe)
G418™	Gibco / Invitrogen GmbH (Karlsruhe)
HBSS	Gibco / Invitrogen GmbH (Karlsruhe)
Lipofectamine 2000	Invitrogen GmbH (Karlsruhe)
MOPS	AppliChem GmbH (Darmstadt)
Non essential aminoacids	Invitrogen GmbH (Karlsruhe)
Penicillin/Streptomycin	Gibco / Invitrogen GmbH (Karlsruhe)
RNase-Off	AppliChem GmbH (Karlsruhe)
RPMI 1640	PAA GmbH (Pasching)
Salmon sperm DNA	Invitrogen GmbH (Karlsruhe)
Sodium pyruvate (100mM)	Invitrogen GmbH (Karlsruhe)
Transferrin conjugate (Texasred)	Molecular probes, Invitrogen GmbH (Karlsruhe)
TRIzol®reagent	Invitrogen GmbH (Karlsruhe)
Trypsin EDTA (0.25% / 0.02%)	Gibco / Invitrogen GmbH (Karlsruhe)
Ultrapure distilled water	Gibco / Invitrogen GmbH (Karlsruhe)
Win 55,212-2 mesylate	Tocris Bioscience (USA)

2.3 Enzymes

Accutaq LA polymerase	Sigma Chemicals GmbH (Deisenhofen)
Alkaline phosphatase	New England BioLabs GmbH (Frankfurt)
DNase I	Applera GmbH (Darmstadt)
Hotstart DNA polymerase	Qiagen GmbH (Hilden)
Proteinase K	Invitrogen GmbH (Karlsruhe)
Recombinant *Pfx* DNA polymerase	Invitrogen GmbH (Karlsruhe)
Restriction endonucleases	New England BioLabs GmbH (Frankfurt)
Superscript II RT (200 U)	Invitrogen GmbH (Karlsruhe)
T4 DNA Ligase	Invitrogen GmbH (Karlsruhe)

2.4 Consumables

Bacterial culture tubes	Sarstedt (Nuembrecht)
24 and 96 well plates	Greiner Labortechnik (Solingen)
Autoradiography film	GE Healthcare Europe GmbH (Muenchen)
Cell culture plates	Greiner Labortechnik (Solingen)
Cryo Tube™	Nunc (Wiesbaden)
Eppendorf reaction tubes	Eppendorf–Netheler-Hinz GmbH (Hamburg)
Falcon 2052	Becton & Dickinson (Aalst, Belgien)
Needle (sterile)	Microlance 3 (Fraga, Spanien)
Nylon Transfer membrane	Schleicher & Schuell (Dassel)
PCR tubes	Sarstedt (Nuembrecht)
Petri dish (bacterial)	Greiner Labortechnik (Solingen)
pH strips	Merck (Darmstadt)
Protran Cellulose nitrate	Schleicher & Schuell (Dassel)
SuperFrost®Plus slides	Menzel GmbH & Co. KG (Braunschweig)
Whatman paper	Schleicher & Schuell GmbH (Dassel)

2.5 Molecular weight standards

The following molecular weight standards were used for agarose gels and Southern blots.

Tab. 2.1: Molecular weight standards for Southern blot

Molecular weight standard	**Fragment sizes [bp]**
DNA 100bp ladder (Invitrogen GmbH, Karlsruhe)	2,072; 1,500; 1,400; 1,300; 1,200; 1,100; 1,000; 900; 800; 700; 600; 500; 400; 300; 200; 100
DNA 1kb ladder (Invitrogen GmbH, Karlsruhe)	12,216; 11,198; 10,180; 9,162; 8,144; 7,126; 6,108; 5,090; 4,072; 3,054; 2,036; 1,636; 1,018; 506; 496; 344; 298; 220; 201; 154; 134; 75
DNA–Marker II, DIG–coupled (Roche Diagnostics GmbH Mannheim)	23,130; 9,416; 6,557; 4,361; 2,322; 2,027; 564; 125

The following molecular weight standards were used on polyacrylamide gels in Western blots.

Tab. 2.2: Molecular weight standards for Western blot

Molecular weight standard	**Calibrated molecular weight [kD]**
Prestained SDS- PAGE standards (Bio-Rad, Karlsruhe)	220; 120; 100; 80; 60; 50; 40; 30; 20
Magic mark™ Western standard (Invitrogen GmbH, Karlsruhe)	201; 115; 96; 52; 38; 29; 20; 7

2.6 Oligonucleotides

All oligonucleotide primers were synthesized by Metabion (Martinsried) or Invitrogen (Karlsruhe).

Tab. 2.3: Sequencing primers

Name	**Sense + antisense -**	**Primer sequence 5' - 3'**
CFP KI Geno1F	+	TCGGACCTGAGGGGAAAGAAGA
BGH rev	-	TAGAAGGCACAGTCGAGG
Dsred Mono F	+	ATGGTGCGCTCCTCCAAGAA
Dsred Mono R	-	CTACAGGAACAGGTGGTGGC
Dsred1-N	+	GTACTGGAACTGGGGGGACAG
EGFP-N	-	CGTCGCCGTCCAGCTCGACCAG
EGFP-N 1 rück	+	GTAATACGACTCACTATAGGGC
EXFP-1 hin	+	CAGCACGACTTCTTCAAGTC
EXFP-1 rück	-	CAGCTCGATGCGGTTCACCAG
CFP KI Geno WT 3R	-	CTACAGCCACAGAGGATGAAG
CFP KI GFP 1R	-	CCTCGGCGCGGGTCTTGTA
mCB2 2 hin	+	CACCGGCATGTAGCCACCTTGG
mCB2 2 rück	-	AGCGTGATCTTCGCCTGCAACTTTG
mCB2 4 rück	-	CCAAGGTGGCTACATGCCGGTG
mCB2 5 hin	+	AGCCGTGATCTTCGCCTGCAACTTTG

Name	Sense + antisense -	Primer sequence 5' - 3'
mCB2-1 rück	-	CAAAGTTGCAGGCGAAGATCACGCT
Neo 1 rück	-	GATATTCGGCAAGCAGGCATC
Neo 1hin	+	GAGGCTATTCGGCTATGACTG
New LOX P2	+	ATATTGCTGAAGCTTGGCGGC
PPNT-loxP1 hin	+	GCGGCCGCTCGAAGTTAACG
PPNT-neo 1 hin	+	CAGCTGTGCTCGACGTTGTCAC
PPNT-neo 1 rück	-	GAGTACGTGCTGGCTCGATGC
SP6-Primer	+	ATTTAGGTGACACTATAG
T7-Primer	+	TAATACGACTCACTATAGGG

Tab. 2.4 Knock-in construct cloning primers

Name	Sense + antisense -	Primer sequence 5' - 3'
Short arm		
mCB2-exon 3 hin Pac	+	TTAATTAAGGTGCTGTGCTTGAGCTACG
mCB2-exon rück Gly,AgeI	-	ACCGGTCCGGTGGTTTTCACATCAGCCTC
Long arm		
mCB2-3'UTR 1rück KpnI	-	GGTACCCTCGACCACAGCGTGTGCATG
mCB2-3'UTR hin Xma	+	CCCGGGTAGGAGCCAGGATCCAGAACTC

Tab. 2.5: DIG probe primers

Name	Sense + antisense -	Primer sequence 5' - 3'
mCB2-5'sonde 5hin	+	CAGGAGCAGCAGTCTGCAGA
mCB2-5'sonde 5rück	-	GTGTATTTCCACATCCCTATG
eGFP hin	+	CAGCACGACTTCTTCAAGTC
eGFP rück	-	CTGCTTGTCGGCCATGATA
Neo hin	+	GAGGCTATTCGGCTATGACTG
Neo rück	-	GATATTCGGCAAGCAGGCATC

Tab. 2.6: Expression vectors cloning primers

Name	**Sense + antisense -**	**Primer sequence 5' - 3'**
Fusion construct		
D_mCB2_KZ_F	+	CACCATGGAGGGATGCCGGGAGAC
GFP Stop Not1 R	-	GCGGCCGCTTTACTTGTACATGT
Control construct		
mCB2-exon stop rück	-	CTAGGTGGTTTTCACATCAGCCTC

Tab. 2.7: RT–PCR Primer

Name	**Sense + antisense -**	**Primer sequence 5' - 3'**
CFP KI Geno1F	+	TCGGACCTGAGGGGAAAGAAGA
CFP KI Geno WT 3R	-	CTACAGCCACAGAGGATGAAG
CFP KI Geno GFP 1R	-	CCTCGGCGCGGGTCTTGTA
ß actin F	+	AGAGGGAAATCGTGCGTGAC
ß actin R	-	CAATAGTGATGACCTGGCCGT

2.7 Antibody and Antiserum

The following antibodies were used. The source and the used dilutions are indicated.

Tab. 2.8: Antibodies

Antibody	**Description**	**Source**
Primary Antibody		
p44/42 MAP Kinase Antibody #9102	Detects total p44/42 MAP-Kinase Cell Signaling Technology, WB 1:1,000 dilution	Rabbit
Phospho-p44/42 MAP Kinase (Thr202/Tyr204) Antibody #9101	Detects phospho-p44/42 MAP-Kinase forms, Cell Signaling Technology, WB 1:1,000 dilution	Rabbit

Antibody	**Description**	**Source**
AntiGFP antibody # Ab290	Detects GFP protein Abcam, WB 1:5,000 dilution	Rabbit
Anti-GFP Obtained from Prof. Magin (University of Bonn)	Detects GFP protein Hybridoma generated by Prof. Noegel (Inst. for Biochem. I, Cologne), WB 1:5,000 dilution	Mouse
Anti ß-actin # A1978	Detects ß-actin, SigmaAldrich, WB 1:12,000 dilution	Mouse
∝- Giantin Obtained from Prof. Walter (University of Bonn)	Detects Giantin protein. Generated by Linstedt et. al ICC 1:500 dilution	Rabbit
LAMP I # 121603	Detects LAMP I protein, BioLegends, ICC 1:500 dilution	Mouse
LIMP II # sc25869	Detects LIMPII protein, Santacruz Biotechnology Inc., ICC 1:500 dilution	Goat
Calnexin # sc11397	Detects Calnexin protein, Santacruz Biotechnology Inc., ICC 1:500 dilution	Rabbit
CB2 antibody # 101550	Detects Cannabinoid receptor 2 Cayman chemicals, ICC 1:500 dilution, WB 1:2,000	Rabbit
Secondary antibody		
Anti-Rabbit Cy 3 # 111-165-003	Detects Rabbit IgG, Cy3 coupled; red emission; Dianova, ICC dilution 1:500	Goat
Anti-Goat Cy 3 # 305-165-003	Detects Goat IgG, Cy3 coupled; red emission; Dianova, ICC dilution 1:500	Rabbit

Antibody	Description	Source
Anti-Mouse Cy 3 # 715-165-150	Detects Mouse IgG, Cy3 coupled; red emission; Dianova, ICC dilution 1:500	Donkey
Anti-Rabbit HRP # 111-035-144	Detects Rabbit IgG, Horseradish peroxidase coupled; Jackson ImmunoResearch Laboratories	Goat
Anti-Mouse HRP # 315-035-006	Detects Mouse IgG, Horseradish peroxidase coupled; Jackson ImmunoResearch Laboratories	Rabbit

2.8 Kits

The following kits were used:

- BCA™ Protein assay kit, Perbio GmbH (Bonn)
- Expand high fidelity PCR system, Roche Diagnostics GmbH (Mannheim)
- Nucleotide removal kit, Qiagen GmbH (Hilden)
- PCR DIG labeling mix, Roche Diagnostics GmbH (Mannheim)
- Peqlab gel extraction kit, Peqlab GmbH (Erlangen)
- PureLink™ HiPure midi plasmid purification kit, Invitrogen GmbH (Karlsruhe)
- PureLink™ HQ mini plasmid purification kit, Invitrogen GmbH (Karlsruhe)
- RNeasy mini kit, Nr.79654, Qiagen GmbH (Hilden)
- SYBR® Green JumpStart™ *Taq* ReadyMix™, Sigma Chemie GmbH (Deisenhofen)
- TOPO TA cloning®, Invitrogen GmbH (Karlsruhe)
- Zero Blunt® TOPO® PCR cloning, Invitrogen GmbH (Karlsruhe)

2.9 Plasmids

Tab. 2.9: Description and origin of all plasmids used in this work

Vector	Description	Source
Knock-in constructs		
2.5 kb-mCB2 exon- gly/AgeI PCR-blunt II -TOPO	2.5 kb short arm for homologous recombination	Generated by Andrea Oster
2.5 kb-mCB2 exon-gly/AgeI-eCFP-N1	2.5 kb short arm fused with eCFP protein for homologous recombination	Generated by Andrea Oster
2.5 kb-mCB2 exon-gly/AgeI-eGFP-N1	2.5 kb short arm fused with eGFP protein for homologous recombination	Generated during this work
pPNT-M2	pPNT-M2 vector used for homologous recombination	Lab stock
6.4 kb-mCB2-3'UTR kpnI-PCR XL-TOPO®	6.4 kb long arm used for homologous recombination	Generated by Andrea Oster
2.5 kb-mCB2 exon-eCFP-pPNT-M2	Plasmid containing short arm of CB2-eCFP and pPNT-M2 vector	Generated during this work
2.5 kb-mCB2 exon-eGFP-pPNT-M2	Plasmid containing short arm CB2-eCFP and pPNT-M2 vector	Generated during this work
mCB2-eCFP short+long arm-pPNT-M2	CB2-eCFP, targeting construct containing short and long arms	Generated by Andrea Oster
mCB2-eGFP short+long arm-pPNT-M2	CB2-eCFP, targeting construct containing short and long arms	Generated during this work
pCR®-Blunt II-TOPO®	LacZa, ccdB lethal, MCS, KanR	Invitrogen

Vector	Description	Source
EGFP-N1	MCS, NeoR; vector for expression of C-terminal eGFP fusion (CMV promotor)	Clontech
ECFP-N1	MCS, NeoR; vector for expression of C-terminal eCFP fusion (CMV promotor)	Clontech
Expression constructs		
pcDNA™3.1D/V5-His-TOPO®	MCS, AmpR, NeoR, V5–Epitope, 6x His-Tag; expression vector (CMV promotor)	Invitrogen
pCR®II-TOPO®	*lac*Za, MCS, Amp^R, Kan^R; cloning, sequencing vector	Invitrogen
mCB2 exon- gly/AgeI PCR-blunt II -TOPO	CB2 coding exon where stop signal was mutated	Generated during this work
mCB2-eCFP pcDNA™3.1 D/V5-His-TOPO®	CB2-eCFP construct used for expression analysis	Generated during this work
mCB2-eGFP-pcDNA™ 3.1D/V5-His-TOPO®	CB2-eGFP construct used for expression analysis	Generated during this work
mCB2 * pcDNA™ 3.1 D/V5-His-TOPO®	CB2 control construct used for expression analysis	Generated during this work
DsRed-monomer-N1	Vector containing dsRed fluorescent protein	Clontech
mCB2-DsRed-monomer-N1	CB2-dsRed construct used for expression analysis	Generated during this work

2.10 DIG labeled probes

Tab. 2.10: Description of the DIG labeled PCR probes

Probe	Primers used	Blot
GFP DIG	eGFP hin (+) and eGFP rück (-)	Southern blot
5' UTR DIG	mCB2-5' sonde 5hin (+) and mCB2-5' sonde 5rück (-)	Southern blot
Neo DIG	Neo hin (+) and Neo rück (-)	Southern blot

2.11 *Escherichia coli (E. coli)* stock

These bacteria were used for the transformation of recombinant plasmids.

DH5α (Invitrogen GmbH, Karlsruhe) F-, φ80*lac*ZΔM15, Δ(*lac*ZYA-*arg*F)U169, *rec*A1, *end*A1, *hsd*R17(rk^-, mk^+), *pho*A, *sup*E44, *thi*-1, *gyr*A96, *rel*A1 and *ton*A

TOP10 (Invitrogen GmbH, Karlsruhe) F-, *mcr*A, Δ(*mrr-hsd*RMS-*mcr*BC), Φ80*lac*ZΔM15, Δ*lac*X74, *rec*A1, *ara*D139, Δ(*araleu*)7697, *gal*U, *gal*K, *rps*L, (Str^R), *end*A1 and *nup*G.

2.12 Eukaryotic cell lines

Tab. 2.11: Description and origin of cell lines used in this work

Cell line	Description	Origin /Reference
CHO-K1	Chinese hamsters ovary cell line	American Type Culture Collection (ATCC)
HEK-293	Human embryonic kidney cell line	American Type Culture Collection (ATCC)
HeLa	Human cervical cancer cell line	American Type Culture Collection (ATCC)

2.13 Mouse strains

The Rheinische Friedrich Wilhelms University of Bonn and the Government of NRW, Germany, or the local veternary authorities of Zurich, Switzerland approved all animal experiments. The institutional and national guidelines for the care and use of laboratory animals were followed.

Tab. 2.12: Description and origin of all mouse strains used in this work

Mouse strain	**Origin**
C57BL/6J	Charles River GmbH, Sulzfeld
CD1	Charles River GmbH, Sulzfeld
$Cnr1^{-/-}$	House of experimental therapy, Bonn
$Cnr2^{-/-}$	House of experimental therapy, Bonn
$Cnr1^{-/-}/Cnr2^{-/-}$	House of experimental therapy, Bonn

2.14 ES cells

Tab. 2.13: Description and origin of all mouse ES cell lines used in this work

ES cell	**Origin**
R1	Embryonic stem cell line from F1 crossing between 129/Sv and 129/J mice
MPI 2	Embryonic stem cell line from blastocytes from 129/Sv mice

2.15 Growth Mediums

2.15.1 Growth medium for *E. coli*

All growth mediums were made in ultrapure milli Q water.

Luria Bertani (LB) medium

Bactotryptone	1% (w/v)
Yeast extract	0.5% (w/v)
NaCl	0.5% (w/v)

pH was adjusted to 7.5 with NaOH and then solution was autoclaved.

Luria Bertani (LB) 1.5% agar

Bactotryptone	1% (w/v)
Yeast extract	0.5% (w/v)
NaCl	0.5% (w/v)
Agar	1.5% (w/v)

The pH was adjusted to 7.5 with NaOH. The solution was autoclaved, cooled to 50°C and the corresponding antibiotics (30 μg/ml Kanamycin, 30 μg/ml Ampicillin) were added. Approximately 25 ml medium were poured per petridish and allowed to solidify. Plates were then packed under sterile conditions and stored at 4 °C until use.

2.15.2 Growth medium for ES cells

ES cell growth medium:

DMEM (high glucose)	
FCS (ES-cell tested)	26%
Non essential amino acids	1.2%
Penicillin	3 U/l
Streptomycin	3 U/l
Sodium pyruvate solution	0.6%
ß-Mercaptoethanol	0.2%
LIF	2 ng/ml

Fibroblast growth medium:

DMEM (high glucose)	
FCS	10%
Penicillin streptomycin mix	0.6%
Sodium pyruvate solution	0.5%

ES cell selection medium:

DMEM (high glucose)	
FCS (ES cell tested)	26%

Non essential amino acids	1.2%
Penicillin streptomycin mix	0.6%
Sodium pyruvate solution	0.6%
ß-Mercaptoethanol	0.2%
LIF	2 ng/ml
G418	170 ng/ml
FIAU	130 nM

ES cell freezing medium:

DMEM (high glucose)	
FCS	50%
DMSO	10%

2.16 Solutions

Unless otherwise mentioned, all solutions were made in ultrapure milli Q water at room temperature.

DEPC water: 1ml DEPC solution was added to 1 l ultrapure milli Q water. The solution was shaked and kept in the dark overnight and next day solution was autoclaved.

Gelatine solution:

Gelatine	1% (w/v)

The solution was autoclaved and then used for cell culture experiments.

1x Phosphate buffered saline (PBS) Ca^{2+}/Mg^{2+} free, pH 7.4:

NaCl	140 mM
KCl	10 mM
Na_2HPO_4	6.4 mM
KH_2PO_4	2 mM

The solution was autoclaved and then used for cell culture experiments.

4% Paraformaldehyde (PFA)/PBS (w/v):

10 g PFA were dissolved in 250 ml 1x PBS and heated to 60°C and 3 - 4 drops of 2 M NaOH was added to clear the solution. PFA solution was cooled to 4°C before use.

Mitomycin solution:

Mitomycin C in fibroblast medium	10 µg/ml

Lysis buffer for ES cells:

Tris HCl, pH 8.0	20 mM
NaCl	10 mM
EDTA	10 mM
SDS	0.5%
Proteinase K	1 mg/ml

Colchicin solution:

Cholchicin in HBSS buffer	10 µg/ml

TE buffer, pH 8:

Tris HCl	10 mM
EDTA	100 mM

Alkaline lysis reagent for genomic DNA isolation:

NaOH	25 mM
EDTA	0.2 mM

Neutralization reagent for genomic DNA isolation:

Tris HCl, pH 5	40 mM

Lysis buffer for protein isolations:

$MgCl_2$	30 mM
NaCl	100 mM
NP-40	5%

Tris HCl, pH 8	100 mM

Lysis buffer for protein isolations (Erk-MAPK):

Tris HCl	50 mM
Triton X-100	1%
NaCl	150 mM
EGTA	1 mM
β-glycerol phosphate	50 mM
NaF	1 mM
Leupeptin	10 µg/ml
Aprotinin	10 µg/ml
PMSF	0.5 mM
Sodium orthovanadate	1 mM

2.16.1 DNA gel electrophoresis

6x Sample buffer:

Glycerol	50% (v/v)
EDTA	0.002 mM
Bromo phenol blue	0.0025% (w/v)
Xylene cyanol	0.0025% (w/v)

6x Sample buffer:

Glycerol	50% (v/v)
EDTA	0.002 mM
Orange G	0.0025% (w/v)

TAE gel electrophoresis buffer:

EDTA	0.5 mM
Tris acetate	40 mM

2.16.2 RNA gel electrophoresis

10x Formaldehyde (FA) buffer:

EDTA	10 mM
Sodium acetate	50 mM
MOPS	200 mM

Chemicals were dissolved in DEPC milli Q water and pH was adjusted to 7 with NaOH.

1x Formaldehyde (FA) gel running buffer:

10x Formaldehyde buffer	10% (v/v)
Formaldehyde, 37%	2% (v/v)

Chemicals were dissolved in DEPC milli Q water.

5x RNA sample buffer:

Bromophenol blue	0.0025% (w/v)
EDTA	4 mM
Formaldehyde, 37%	7.2% (v/v)
Formamide	30.84% (v/v)
10x Formaldehyde buffer	40% (v/v)
Glycerol	20% (v/v)

Chemicals were dissolved in DEPC milli Q water.

2.16.3 Solutions for *Southern* blot

Depurination solution:

HCl	250 mM

Denaturation solution:

NaOH	500 mM
NaCl	1.5 M

Neutralization solution, pH 7:

Tris HCl	500 mM
NaCl	1.5 M

Maleic acid buffer, pH 7.5:

Maleic acid	100 mM
NaCl	150 mM

20x SSC buffer, pH 7:

NaCl	3 M
Sodium citrate	300 mM

Standard hybridization buffer for Southern blot:

Blocking reagent	1% (w/v)
20x SSC buffer	25% (v/v)
N-Lauroyl sarcosine	0.1% (w/v)
SDS	0.02% (w/v)

Wash buffer 1:

20x SSC buffer	10% (v/v)
SDS	1% (w/v)

Wash buffer 2:

20x SSC buffer	1% (v/v)
SDS	0.1% (w/v)

Stock solution for blocking:

Blocking reagent	10% (w/v)

Reagent was dissolved in maleic acid buffer, autoclaved and stored at -20°C.

Blocking solution:

Stock solution for blocking	10% (v/v)
Maleic acid buffer	90% (v/v)

The solution was filtered with Whatman filters (Schleicher & Schuell).

Wash buffer 3:

0.3% Tween 20 in maleic acid buffer.

Assay buffer pH 9.5:

Tris HCl	100 mM
NaCl	100 mM
$MgCl_2$	50 mM

The pH was set with NaOH to 9.5

2.16.4 Solutions for protein gel electrophoresis and *Western* blot

12% Separation gel buffer:

Tris HCl, pH 8.8	375 mM
SDS	0.1% (w/v)
Acrylamide	12% (w/v)
Bisacrylamide	0.24% (w/v)
Ammonium persulphate	0.1% (w/v)
TEMED	0.1% (v/v)

5% Stacking gel buffer:

Tris HCl, pH 6.8	187.5 mM
SDS	0.1% (w/v)
Acrylamide	5% (w/v)
Bisacrylamide	0.1% (w/v)
Ammonium persulphate	0.1% (w/v)
TEMED	0.1% (v/v)

4x Protein Sample buffer:

Tris HCl, pH 6.8	200 mM
SDS	8% (w/v)
Glycerol	40% (v/v)
Bromophenol blue	0.01% (w/v)
1 M DTT	40% (v/v)

Laemmeli gel electrophoresis buffer:

Tris HCl	25 mM
SDS	0.1% (w/v)
Glycine	192 mM

Transfer buffer:

Tris HCl	25 mM
Glycine	192 mM
Methanol	10% (v/v)

Ponceau red solution:

Acetic acid	5% (v/v)
Ponceau red	0.1% (w/v)

Wash buffer:

Tris HCl	20 mM
NaCl	140 mM
Tween 20	0.1% (v/v)

Immunoprecipitation buffers:

STEN buffer:

Tris, pH 7.6	150 mM
NaCl	500 nM
EDTA	2 mM
Igepal	0.2%

STEN lysis buffer:

Triton X-100	1% (v/v)
Igepal	1% (v/v)
BSA	2% (v/v)

Chemicals were dissolved in STEN buffer.

STEN NaCl:

Tris pH 7.6	50 mM
NaCl	500 mM
EDTA	2 mM
Igepal	0.2% (v/v)

Protein A/G sepharose suspension (Zymed):

100 mg/ml protein-A bound sepharose beads were washed with STEN buffer and resuspended in STEN buffer. Beads were blocked with 2 mg/ml BSA to avoid non-

3 Methods

3.1 Molecular biological methods

3.1.1 DNA restriction digestion

Digestions of DNA with restriction endonucleases were performed according to the instructions given by the manufacturer (New England BioLabs).

3.1.2 Dephosphorylation of DNA fragments

Vectors that were digested with restriction endonucleases and have two compatible ends can self ligate. In order to minimize such ligations and to increase the cloning efficiency, the 5'-phosphate group of the linearized vectors was removed by an alkaline phosphatase from the Garnele *P. borealis* (New England BioLabs). Linearized vectors (1 µg) were treated with 1 U of *shrimp alkaline phosphatase* SAP (New England BioLabs) for 15 min at 37°C. Prior to addition of insert DNA for ligation, dephosphorylation reactions were terminated by heat inactivation at 65°C for 30 min.

3.1.3 Ligation of digested DNA fragments

75 ng of purified linearized vector and PCR product were used in a molar ratio of 1:2 or 1:3 respectively. Using T4 ligase (5U/µl, Invitrogen), the ligation reaction was carried out according to the instructions supplied by the manufacturer. The ligation reaction volume (5-10 µl) was used for transformation of competent *E. coli*.

3.1.4 Ligation of PCR products

PCR products were ligated with the TOPO® TA cloning kit (Invitrogen). To avoid auto degradation of adenosine overhangs upon longer storage intervals, freshly prepared PCR products were used. If blunt end producing (3´-5´ exonuclease activity, proof reading activity) polymerase was used, the ligation was carried out using the Zero Blunt® TOPO® PCR cloning kit (Invitrogen). The ligation was done according to the manufacturer's directions.

3.1.5 Transformation and culture of *E. coli*

The ligation product (10 µl) was mixed with 100 µl of competent *E. coli* (*DH5 α* or *Top 10*) and incubated on ice for 30 min. Next the cells were heat shocked at 42°C for 40

s and were quickly placed on ice for 2 min. 1 ml LB or SOC medium was added and cells were incubated in a bacterial shaker at 37°C with for 1 h. Tubes were then centrifuged for 1 min at 12,000 rpm. The pellet was resuspended in 50- 200 µl of respective medium and cells were streaked on LB-plates with respective antibiotic. After 14-20 h of incubation at 37°C, colonies were chosen and kept for overnight cultures in 5 ml LB-growth medium with the respective antibiotic.

3.1.6 Preparation of plasmid DNA

3.1.6.1 Plasmid DNA isolation (mini preparation)

For analytical purposes, 2 ml of overnight bacterial culture was used. The plasmids were isolated using silica columns according to manufacturer's instructions (mini kit, Invitrogen).

3.1.6.2 Preparative Plasmid DNA isolation (midi/maxi preparations)

For preparative purposes, 100 ml - 500 ml of overnight bacterial culture was used. The plasmids were isolated with silica columns according to manufacturer's instructions (Midi/Maxi kit, Invitrogen).

3.1.7 Agarose gel electrophoresis

Agarose gel electrophoresis was used to resolve DNA constructs. Agarose gels were casted in TAE Buffer. DNA samples were diluted in 5x loading dye before loading on agarose gels. One kb and 100 bp molecular weight ladders (Invitrogen) were used to analyze the molecular size of the DNA. Gels were run at 80-120 V in TAE buffer. After a run, gels were soaked in 0.5 µg/ml ethidium bromide containing TAE buffer for 15 min. The run was documented using the Chemi Doc system (Bio-Rad).

3.1.8 Isolation of DNA fragments from agarose gel

Under UV-light desired bands were cut out from the gel using a sterile scalpel. DNA was extracted from the agarose using the Peqlab gel extraction kit.

3.1.9 DNA precipitation in ethanol / isopropanol

Ethanol and isopropanol precipitation was used for the purification of DNA and RNA. Ionic concentration of the aqueous DNA and/or RNA solution was increased by addition of 1/10 volume 3 M sodium acetate solution (pH 5.2). About 2.5 times

volumes of ethanol/isopropanol were added. The DNA and/or RNA was incubated at -20°C for 30-60 min. Afterwards the sample was centrifuged at 13,000 rpm, the pellet was washed with 70% ethanol and dried for 10 min at 60°C. Then the DNA and/or RNA pellet was dissolved in the desired quantity of milli Q water or buffer.

3.1.10 Concentration determination of nucleic acids

To determine the concentration of DNA or RNA in a solution the optical density (OD) was measured. Nucleic acids have an absorption maximum at 260 nm and proteins absorb UV light maximally at a wavelength of 280 nm. Pure DNA exhibits an OD 260/OD 280 ratio of up to 2. This ratio is inversely proportional to the amount of proteins present in the solution.

For pure nucleic acids: 1 OD 260 corresponds to a concentration:
dsDNA:
Oligonucleotide: 20 - 30 µg/ml
ssDNA: 33 µg/ml
RNA: 40 µg/ml

A nanodrop spectrophotometer was used for quantification of DNA and RNA.

3.1.11 Polymerase chain reaction (PCR)

DNA sequence for the respective gene was obtained from the NCBI web site. Primers for PCR were designed based on the following general considerations: the length of the primer should be around 19 bp, the melting temperature (Tm) of the primer should be close to 60°C, and the nucleotide at the 3' end should be either G or C. Primers used in the same PCR reaction were checked carefully to avoid formation of primer-primer dimers.
The melting temperature of the primer was calculated according to the following formula:
Tm = 4 (G+C) + 2 (A+T)

3.1.12 PCR-setup

Unless specified differently, PCR reactions were performed in a total volume of 50 µl. To avoid nonspecific annealing of the primers and undesired PCR amplification, all the constituents (Tab. 3.1) were pipetted on ice and transferred to a cycler (iCycler, BioRad) immediately. The PCR was performed along with corresponding positive and negative controls. For multiple PCR reactions, a master mix was made and respective templates were added in appropriate aliquots of master mix.

Tab. 3.1: PCR reaction setup

Detail	**End concentration**
DNA template (cDNA, plasmid DNA)	2 ng/µl
Primer sense	0.3 µM
Primer antisense	0.3 µM
Taq DNA polymerase 10x buffer	1x
$MgCl_2$	2 mM
DNTPs	25 nM
Taq DNA polymerase	1 U
Made upto 50 µl with milli Q water	

The reaction parameters (temperature, cycle) were adapted to the respective PCR setup.

The standard PCR program consists of the following steps:

Initial denaturation	94°C	5 min	
Denaturation	94°C	45 s	} 30-35 Cycles
Annealing	50–60°C	45 s	
DNA synthesis	72°C	2 min	
Terminal DNA-Synthesis	72°C	10 min	
Cooled at 4°C.			

3.1.13 Generation of DIG probes

Denatured PCR fragments can be used as probes in hybridizing experiments. For this purpose it is necessary to label a probe in order to make later detection possible. The incorporation of digoxigenin labeled nucleotides (DIG dNTPs, Roche

diagnostics) during the PCR amplification of DNA instead of dNTPs gives a non-radioactive labelling alternative.

The DIG PCR was setup as mentioned in Tab. 3.2. The labelling of the probe was always examined on the basis of slight gel retardation in agarose migration compared with similar nonlabelled PCR product. PCR products were cleaned by the Nucleotide Removal Kit (Qiagen).

Tab. 3.2: Reaction setup for the synthesis of Probes

Detail	**Volume**
Plasmid DNA 100 ng	X µl
Primer sense 20 µM	2 µl
Primer antisense 20 µM	2 µl
Taq DNA Polymerase 10x buffer	5 µl
$MgCl_2$ 2mM	4 µl
10x PCR DIG probe labelling mix (Roche)	5 µl
Taq DNA polymerase 1 U	1 µl
Made up to 50 µl with milli Q water	

3.1.14 Sequencing of DNA

The sequencing of plasmids was performed by the Macrogen Incorporations in Seoul (South Korea).

3.1.15 Purification of PCR-Products

PCR products were cleaned up over spin columns (Qiagen) in accordance to the manufacturer data.

3.1.16 Reverse Transcription

cDNA synthesis

About 5 µg of RNA were used for cDNA synthesis and volume was adjusted to 10 µl with DEPC water. One µl of oligo (dT) primer was added to RNA and mixture was incubated at 60°C for 5 min. In the meantime, master mix was prepared as follows:

1 µl DEPC water, 1 µl 10 mM dNTPs, 4 µl 5x first strand buffer, 2 µl 0.1 M DTT and 1 µl reverse transcriptase.

Nine µl of master mix was added to each tube and tubes were incubated at 42°C for 1 h followed by 15 min incubation at 70°C for cDNA synthesis.

PCR amplification

A maximum of 1/10th volume of the reverse transcribed cDNA was used as template for the PCR reaction setup.

3.1.17 Topo cloning

Topo blunt (Invitrogen) or TA cloning (Invitrogen) was performed according to the instructions given by the manufacturer.

3.1.18 Generation of Expression vector

The pcDNA^{TM} 3.1 Directional TOPO® Vector (Invitrogen) was used as expression vector due to its rapid directional cloning of blunt end PCR products for expression in mammalian cells. This vector allows for high-level expression of proteins in most mammalian cells.

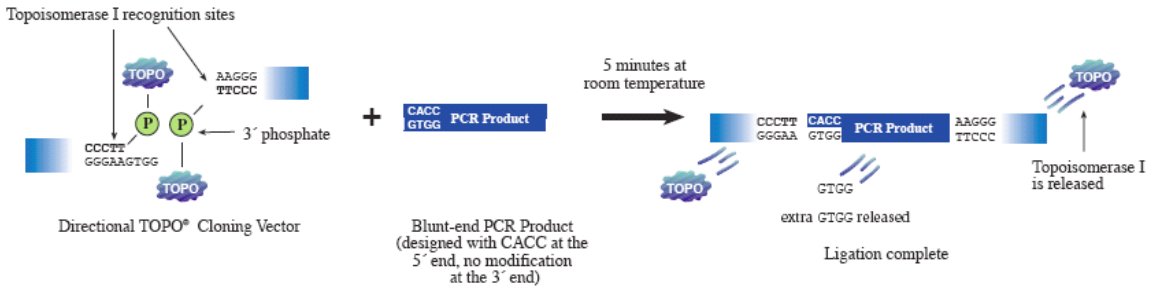

Fig. 3.1 Directional blunt end cloning strategy: Directional blunt end cloning strategy using the pcDNA^{TM} 3.1 Directional TOPO® vector is shown. (Taken from Invitrogen catalog K4900-01).

As shown in Fig. 3.1, a KOZAK sequence (CACC) which is complementary to a pcDNA^{TM} 3.1 Directional TOPO® vector end sequence, was added to the 5' end of the CB2 coding signal.

3.1.19 Isolation of genomic DNA from mouse tail biopsy

3.1.19.1 For Southern blot application

For the isolation of genomic DNA from mouse tail biopsy, approximately 0.5 cm long tail pieces were lysed overnight in lysis buffer containing proteinase K at 55°C and centrifuged at 13,000 rpm for 5 min. The supernatant was carefully removed and mixed with an equal volume of 100% isopropanol. The genomic DNA (white thread-like precipitate) was then fished with a sterile pipette tip, transferred into 1 ml of 70% ethanol solution and centrifuged at 13,000 rpm. The pellet was washed with 70%

ethanol and dried at 50°C for 10 min. Afterwards the DNA pellet was dissolved in 100 µl of milli Q water.

3.1.19.2 For genotyping application

For the quick isolation of genomic DNA from mouse tail biopsy (Truett, Heeger et al. 2000), approximately 0.2 cm long tail pieces were incubated with alkaline lysis reagent at 95°C for 1h in PCR cycler. After cooling to 4°C, 75 µl of neutralization reagent was added, quickly vortexed, and then centrifuged at 5,000 rpm for 5 min. 1-2 µl of supernatant was used for the genotyping PCR.

3.1.20 Southern blot

The restriction digestion and the agarose gel electrophoretic separation of DNA were performed as previously explained. About 20 µl (10-15 µg) of the genomic mouse DNA obtained from tail biopsy were digested overnight with 30 U of the restriction enzyme using the optimal temperature and buffer conditions indicated by the manufacturer. After electrophoresis the gel was gently shaken for 10 min in 0.25 N HCl to achieve DNA depurination. The agarose gel was then transferred to the alkaline denaturing solution and gently shaken for 30 min before transferring into neutralization solution for 30 min. After the neutralization step, using a Vacuum blotter (BioRad) DNA was transferred on a nylon membrane at a pressure of 5 bars for approximately 90 min in 10x SSC solution. DNA was then crosslinked to the membrane by UV irradiation (150 mJ, UVCROSS-left, Stratagene). The DIG probes used for screening were manufactured by PCR as described in 3.1.13.

3.1.21 Isolation of RNA

For the isolation and the analysis of RNA some precautionary measures were followed. For all buffers and solutions DEPC treated milli Q water was used. All used glassware was baked for at least 4 h at 180°C before use. Metallic parts such as spatulas, pincets or the homogenizer were washed thoroughly with RNase off and followed by sterile DEPC treated milli Q water. The RNA was isolated with TRIzol reagent (Invitrogen). A 100 mg tissue or $5x10^6$ cells were treated in each case with 1.6 ml TRIzol reagent. The tissue was homogenized in TRIzol reagent with a homogenizator (T8 ultra turrax, IKA) and passed through a 21 G needle at least 10 times. Homogenized samples were left at room temperature for 5 min in 2 ml

eppendorf tubes to allow complete dissociation of nucleoprotein complexes. The homogenate was centrifuged at 5,000 rpm at 4°C for 5 min. The supernatant was then mixed with 1/10 volume 1-Bromo-3-chloro-propane by vortexing. The mixture was incubated for 3 min and centrifuged at 4°C at 11,400 rpm. The aqueous phase was carefully transferred into a fresh tube and mixed with an equal volume isopropanol and incubated for 10 min. Afterwards the sample was centrifuged at 4°C at 11,400 rpm. The resulting RNA pellet was washed with 75% ethanol. The pellet was dried in air for 10-15 min and dissolved in DEPC milli Q water by incubating 15 min at 55°C. The RNA concentration was estimated by reading O.D. using the Nanodrop.

3.1.22 RNA Electrophoresis

To determine the quality of isolated RNA, denaturating formaldehyde gels were used. All apparatus were cleaned with milli Q water followed by RNAse off solution and DEPC milli Q water.

For 1.2% agarose gel, 0.6 g RNase free agarose was dissolved in 45 ml DEPC milli Q water by boiling in a microwave. A 5 ml 10x FA buffer was added to the agarose solution. Then it was cooled down to 50-60°C with constant stirring. Before casting, 900 µl of 37% formaldehyde and 1 µl ethidium bromide (5 mg/ml) were added. About 5-10 µg of the isolated RNA diluted in 4 µl 5x RNA sample buffer were heated up for 3 min to 65°C, then were cooled immediately on ice for 10 min. Samples were loaded on the gel and separated at 70 V in 1x FA gel buffer. The quality of the isolated RNA was judged under UV light on the basis of the ribosomal RNA bands or by the Bioanalyzer instrument (Agilent).

3.1.23 Tissue preparation

Isopentane was precooled on dry ice before the preparation. The tissue was removed and rinsed with PBS. Organ was quickly frozen with help of precooled isopentane in Tissuetek molds or for PFA fixation, it was transferred to a 50 ml 4% PFA containing solution. After overnight shaking at 4°C, it was transferred to 30% sucrose solution till the organs sink at the bottom of the tube at 4°C. Tissuetek cryomold plastic cassette bottom and corners were immersed in dry ice precooled with isopentane. Removed organs were kept in plastic mold until it solidified and were immediately stored at -80°C until further use.

3.1.23.1 Cryosectioning

The prepared organs were sectioned in the cryostat (cm 3050 S, Leica) at a temperature of -18 to -24°C to a thickness of 12-20 µm. After cutting, the sections were dried for 10-15 min on a 42°C warm plate and fixed or stored at -80°C.

3.1.23.2 Fixation of sections

Dried sections were fixed with aqua poly/mount mounting medium (Polysciences) and allowed to dry at 4°C overnight in the dark prior to visualization with fluorescence under confocal microscope or fluorescent microscope.

3.2 Protein biochemical and immunological methods

3.2.1 Protein isolation from tissues

100-600 mg tissue were homogenized with a homogenizer (T8 ultra turrax, IKA) in 1 ml of lysis buffer in the presence of the complete mini protease inhibitor cocktails (Roche) for 3 X 20 s long pulses and then kept in an ultrasonicator bath (Sonoplus, Bandelin) for 30 s over 5 cycles. Following 15-30 min incubation on ice, the homogenate was centrifuged for 30 min at 13,000 rpm at 4°C. The supernatant was transferred to a new tube and one aliquot was used for protein measurement.

3.2.2 Protein isolation from cells

Cells were washed and scrapped off in ice cold PBS. Cells were pelleted by centrifugation at 1,000 rpm/ 5 min/ 4°C and lysed with STEN lysis buffer (200 µl for 6 cm dish and 400 µl for 10 cm dish) or lysis buffer on ice for 30 min in the presence of protease inhibitor mix. The lysates were cleared by centrifugation at 12,000 rpm. Protein estimation was performed and 20 µg of protein were aliquoted from each sample. The samples were then boiled with loading dye.

3.2.3 Estimation of protein concentration (BCA method)

Samples were diluted appropriately and the BCA kit (Perbio) was used to analyze the protein concentrations in triplicates.

3.2.4 Immunoblotting

After electrophoresis, proteins from a polyacrylamide gel were transferred to a nitrocellulose membrane using blotting chamber (BioRad). The transfer was confirmed by Ponceau S staining. The stain was removed by washing in PBS-T solution 10-15 min. Membrane was blocked with 5% Rotiblock reagent for 1 h. The blot was then incubated with appropriately diluted primary antibody solution for 2 h at room temperature or overnight at 4°C. The blots were washed 5 times each for 5 min with PBS-T and later incubated with appropriate secondary antibody conjugated to HRP (Horseradish peroxidase) for 1 h at RT. The blots were again washed with PBS-T and chemiluminescent peroxidase substrate was used to visualize protein bands. Signals were measured and analyzed using an ECL imager (ChemiDoc^{TM} XRS, BioRad) or by using Hyperfilm (Amersham biosciences) and the Quantity One software package (BioRad).

3.2.5 Immunoprecipitation

Approximately 80-90% confluent 15 cm cell plate or tissue were lysed in 700 µl STEN-lysis buffer on ice for 10 min in presence of complete mini protease inhibitor cocktail (Roche). Lysates were cleared by centrifugation for 10 min at 14,000 rpm. An appropriate amount of primary antibody and 40 µl of protein-A sepharose beads were incubated overnight with cleared protein lysates at 4°C. The antigen-antibody complex bound to beads was separated by centrifugation for 5 min at 5,000 rpm and washed with STEN buffers. Beads were boiled with loading sample buffer, and loaded on polyacrylamide-SDS gel.

3.2.6 Immunocytochemistry

Cells were cultured on poly-L-lysine-coated glass coverslips to 50-80% confluence. Cells were fixed in 4% paraformaldehyde for 10 min followed by permeabilization with 0.1% Triton X-100 for 10 min and blocking with 5% BSA for 1 h. Cells were incubated with desired primary antibody/antibodies, for example α-Giantin (golgi marker), Calnexin (endoplasmic reticulum marker) and LAMP I, II (lysosomal markers) at appropriate concentrations for 2 h in 1% BSA. Primary antibodies were detected by using Cy3 conjugated secondary antibodies (Dinova) diluted at 1:1000. Coverslips were mounted on glass slides using 15% Mowiol containing 50 mg/ml DABCO or

aqua poly/mount mounting medium. Images were acquired on a fluorescence-inverted microscope (Zeiss).

3.2.7 Hematoxylin and Eosin (H&E) staining

Parafin embedded sections of wounds were deparaffinized by incubating slides in Xylol bath 2X5 min under the hood. This was followed by short 1 min incubations with decreasing ethanol gradient (100% to 50%). Slides were then icubated with milli Q water for 2-3 min followed by 45 sec incubation in 1% Hematoxylin solution. Slides were then washed 5X10 s with milli Q water. Followed by 10 s 70% ethanol wash. Further, slides were incubated 10 s in 0.1% Eosin solution. Slides were then incubated with increasing gradient of ethanol (80%-100%) prior to incubating 2X10 min with Xylol solution. Excessive xylol was removed with clean tissue paper and slides were covered with Roti Histo-Kit II (Roth) mounting medium. Slides were allowed to dry prior to the microscopic visualization.

3.3 Cell culture methods

3.3.1 Common cell culture methods

All cell lines were cultivated at 37°C in an incubator with 5% CO_2 and humid atmosphere. Adherent growing cells were grown in tissue culture dishes on 6, 10 or 15 cm diameter dishes. The growth medium was renewed twice a week. Antibiotic mixtures of penicillin and streptomycin (Pen/Strep) were used to minimize bacterial contamination.

3.3.2 Passage of mammalian cells

Almost confluent (80-90%) grown cells were passaged into a new culture dish. First the medium was removed and cells were washed with 10 ml PBS. Approximately 2 ml of a trypsin/EDTA solution (Invitrogen) were added and the plate was incubated at 37°C for 3-5 min to dislodge the cells. Trypsinization was inhibited by addition of 10 ml growth medium. Cells were mixed well by pipetting up and down with a 10 ml glass pipette and transferred into a Falcon tube. The cells were pelleted by centrifugation (1,200 rpm, 2 min), resuspended in growth medium and seeded at suitable density.

3.3.3 Freezing and storage of cells

A 15 cm confluent culture dish was passaged as above. Cells were resuspended in 5 ml freezing medium with 10% DMSO and transferred with a sterile 1 ml pipette in cryotubes. The cells were stored overnight at –20°C prior to -80°C long term storage.

3.3.4 Thawing of cells

Cells were thawed in a 37°C waterbath as quickly as possible. In order to minimize the toxic effect of the DMSO, 5 ml fresh growth medium were added and cells were pelleted by centrifugation at 1,200 rpm for 2 min. The cell pellet was resuspended in the appropriate cell culture medium and seeded depending upon desired cell density in tissue culture dishes and cultivated under standard conditions.

3.3.5 Culturing of HEK 293 and HeLa cells

HEK and HeLa cells were grown in DMEM + 10% FCS + 1 mM sodium pyruvate + non-essential amino acids in an incubator at 37°C, 5% CO_2 concentration and a humid atmosphere.

3.3.6 Culture of CHO-K1-Cells

CHO-K1 cells were grown in HAM´s F12 (*Coon´s Modification*) + 10% FCS + 1 mM sodium pyruvate in an incubator at 37°C, 5% CO_2 concentration and a humid atmosphere.

3.3.7 Culture of L929 cells

L929 cells were grown in RPMI 1640 medium + 5% FCS + 1 mM sodium pyruvate in an incubator at 37°C, 5% CO_2 concentration and humid atmosphere.

3.3.8 Cell counting

The cell number was determined using a Neubauer modified cell chamber. The cell number per ml was calculated by determining the average number of cells in the 4 large squares and multiplying by 10^4.

3.3.9 Mycoplasma test

Mycoplasma detection test was performed once a month on the mostly used and newly coming cell lines. Minera Biolabs, Venor Ge® M Kit was used for this purpose.

3.3.10 Transient and stable transfection of fluorescent tagged eukaryotic cells

Cells were grown to 60-80% confluence before transient transfection. Transfection was performed using Lipofectamine reagent (Invitogen) according to the manufacturer's instructions. To generate stable cell lines expressing a fluorescent tagged CB2 plasmid, two days after transfection, cells were seeded/diluted and maintained in selection medium, containing 400 µg/ml G418. Medium was replaced every third day with fresh selection medium. Clonal expression was examined initially by fluorescent microscopy and clones for further study were selected and expanded.

3.3.11 eCFP and eGFP visualization

GFP excitation variant eGFP, enhanced green fluorescent protein (GFPmut1; (Cormack, Valdivia et al. 1996)) and GFP emission variants ECFP (enhanced cyan fluorescent protein) contains six amino acid substitutions, one of which shifts the emission spectrum from green to cyan (Heim and Tsien 1996; Miyawaki, Llopis et al. 1997) were used in this work.

Tab 3.3: Excitation and emission maxima of eCFP and eGFP fluorescent proteins.

Protein	**Excitation maxima** (nm)	**Emission maxima** (nm)	**Em** (cm–1 M–1)	**Quantum yield**
EGFP	488	507	55,000	~60
ECFP	433 (453)	475 (501)	26,000	~40

Appropriate filter set no. 424920 (Zeiss) were used to screen fluorescence proteins. For cyan filter with band pass of 390-440 nm and for green filter with 450-490 nm was used.

3.3.12 Confocal laser scanning microscopy

Cells were observed using a laser scanning confocal microscope (Olympus) 40X1.40 NA water immersion objective, pinhole of 35, and electronic zoom of 1 or 3. The GFP or CFP was excited using 458 nm Argon/Crypton laser and detected with a 515-540 nm band pass filter. The Texas red-conjugated transferrin (TR) was exited at 543 nm and detected with a long pass band filter 570 nm.

3.3.13 Co-localization of CB2 with transferrin

Cells stably expressing fluorescent tagged CB2 receptor were grown on coverslips treated with poly-L-lysine to ~50% confluency and serum-starved for 60 min prior to 30 min incubation with Alexa red conjugated TR. Cells were washed with PBS and fixed for 20 min with 4% PFA in PBS. The cells were washed twice with PBS and fixed with Mowiol prior to confocal visualization.

3.3.14 Erk phosphorylation

Erk-MAPK Assay. Cells grown to 80% confluence in 24-well plates were placed in medium containing 0.5% FCS for 24 h before assay. After treatment, cells were washed twice in buffer A (50 mM HEPES, pH 7.4, 150 mM NaCl, 10 mM $Na_4P_2O_7$, 50 mM NaF, 1 mM EDTA, 20 mM ß-glycerophosphate, 1 mM EGTA, 2 mM Na_3VO_4) and lysed for 15 min in 100 µl of buffer A containing 1% (v/v) Triton X-100, 100 U/ml aprotinin, 20 mM leupeptin, 0.2 mg/ml phenylmethylsulfonyl fluoride and 2 mM dithiothreitol (Bouaboula, Bourrie et al. 1995). Solubilized cell extracts were centrifuged at 14,000 rpm for 15 min. The protein content in the supernatant was determined using a micro BCA protein assay kit (Pierce Chemical Co., Rockford, IL) and 20 µg of proteins were analyzed for Erk-MAPK activity using Western blot technique. The extent of phosporylated p42/p44 Erk-MAPK proteins were detected by using phosphorylated p42/p44 Erk-MAPK specific antibody and total Erk-MAPK protein were detected using total p42/p44 Erk-MAPK specific antibody (Cell Signaling).

3.3.15 Effect of agonist and antagonist on internalization

Agonists or antagonists were dissolved in HymaxDMSO (Sigma). Only DMSO was used as vehicle control. Cells were grown on a poly-L-lysine coated coverslips. Prior to the experiment, cells were serum starved overnight and then were incubated for different time intervals with corresponding agonist and/or antagonist. The cells were fixed with 4% PFA prior to fluorescent visualization.

3.3.16 Bone marrow culture

3.3.16.1 Bone marrow cell isolation

After removing all muscle tissues with gauze from the femurs and tibias of mouse, the bones were placed in a 10 cm dish with ice cold PBS, washed twice with PBS and transferred into a fresh dish. Both ends of the bones were cut with scissors and

the marrow was flushed out using 2 ml of PBS with a syringe and a 25 G needle. The tissue was suspended and passed through a 30 µm nylon mesh (Miltenyi Biotec) to remove small pieces of bone and debris. Cells were centrifuged at 1,200 rpm for 5 min, resuspened in RPMI medium and then counted.

3.3.16.2 Bone marrow cell differentiation (macrophages and dendritic cells)

Bone marrow cells (3-5 x 10^6) were suspended in 10 ml RPMI medium containing 70% fresh RPMI medium with 5% FCS, Pen/Step, ß-mercaptoethanol (50 µM end concentration), L-glutamine and 30% of the L929 supernatant (containing rGM-CSF) on a non-treated Petri dish. Cells were split on day 3 by dislodging in PBS containing 2 mM EDTA. To remove nonadherent granulocytes without dislodging clusters of developing dendritic cells that were loosely attached to firmly adherent macrophages, the cultures were fed every second day by gently swirling the plates, aspirating 75% of the medium, and adding back fresh medium with GM-CSF. At day 7, adherent cells (mostly macrophages) or suspension cells (mostly dendritic cells) were used for FACS analysis or for RNA isolation.

3.3.17 Isolation of peritoneal macrophages

Macrophages were collected by peritoneal lavage from Cnr2-eCFP mice and wild type sibling mice by intraperitoneal injection of 2 ml 30% sucrose in PBS. The cells were separated by centrifugation and washed and resuspended in RPMI 1640 medium containing 5% FCS. Cells were counted and used for FACS analysis.

3.3.18 Isolation of splenocytes, lymph node and thymus cells

For FACS analysis, mRNA and immunoprecipitation (IP) analysis, mice were sacrificed by cervical dislocation. Organs were removed, washed quickly with sterile PBS/HBSS buffer to remove the blood and adhering material. For mRNA analysis, organs were and quickly crushed with help of liquid nitrogen in presence of Trizol and processed further. For FACS analysis, organs were gently pressed with a Nylon mesh (Milteyi) of pore size 30 µm. Cells were centrifuged and the pellet was resuspended with fresh buffer prior to FACS analysis. For IP, organs were lysed as explained in 3.2.5.

3.3.19 FACS analysis

Flow cytometry data files were collected on an LSR-II flow cytometer (Becton Dickinson), equipped with standard violet, blue, and red lasers and standard filter sets. Flow cytometry data were analyzed with the FlowJo© software (TreeStar, Ashland, Oregon).

3.4 ES cells

3.4.1 Preparation of feeder cells

Female CD1 mice were paired with transgenic male mice, containing a Neomycin resistance gene. Next day, female mice were observed for the appearance of a plug (vaginal deposits), which is an indicator for pairing. Plug-positive female mice were sacrificed 12-14 days by cervical dislocation. An uterus containing mouse embryos was washed twice with HBSS. Embryos were seperated of from the placentas by opening uterus. Attached remaining organs were removed. The embryos were cut into small pieces and incubated in 30 ml Trypsin/EDTA for 15-20 min (37°C, 5% CO_2), shaked every three min. Centrifuged for 2 min at 1,200 rpm. The remaining pellet was resuspended in 25 ml fibroblast medium and plated in 15 cm cell culture plates. The cells were subcultured 2-3 days and stored further for use.

3.4.2 ES cell culture

ES cells of MPI2 and R1 origin were grown on ES cell culture medium on growth arrested embryonic feeder cells in an incubator at 37°C, 5% CO_2-concentration and humid atmosphere. Culture medium was changed every 24 h and cells were trypsinated every second day.

3.4.3 ES cell electroporation

Approximately 3X15 cm plates of ES cells were used for two electroporations of the constructs. Prior to trypsinization, about 1-2 h medium was changed. To trypsinize ES cells, culture medium was removed and 8-10 ml trypsin per plate was added. Plate was incubated 3-5 min to obtain single cell suspensions. Trypsin was inactivated by addition of 5 ml ES cell medium. The cell suspension was transferred into a 50 ml tube. Cells were counted with a hematocytometer. Aliquots were made to obtain 2 x 10^7 cells per 15 ml tube. Cells were pelleted by low-speed 2,000 rpm centrifugation. The cells were resuspened in 10 ml PBS. The cells were pelleted and resuspended in 700 µl of PBS such that the final volume was 800 µl.

The electroporation cuvette was prepared by addition of linearised plasmid 20-25 µl (1 mg/ml) and the ES cells. For electroporation, the suspension was mixed well and electroporated at 250 V and 500 µF. ES Cells were left at RT for 10 min and then transferred into 10 ml ES medium. ES cells were platted into 4 x 15 ml dishes, pre-plated with G418 resistant embryonic fibroblast cells and cultured in selection medium containing G418 (170 ng/ml) for 7-9 days with fresh medium change everyday. The ES cell colonies were harvested.

3.4.4 Isolation and identification of recombinant ES cell clones

The growth medium was removed from ES cell plates and 25 ml PBS were added. The colonies were picked with a glass micropipette and transferred to the 24 well plates containing a drop of trypsin. A fresh 500 µl ES medium was added to each well and mixed with a pipette to obtain single cell suspensions. Embryonic fibroblast cells were added and ES cells were further cultured for 48 h with medium change after 24 h. The cells were trypsinized by adding 2-3 drops of trypsin and incubating plate at 37°C for 5-8 min. The cells were resuspended in 1 ml per well in freezing medium and 750 µl aliquots were frozen. The remaining cell suspension was kept in culture in the 24 well plates. After 4-7 days, the colonies were lysed in 300 µl lysis buffer for DNA isolation and incubated for 2 h at 52^{o}C. To precipitate DNA 150 µl saturated NaCl and 900 µl absolute ethanol was added and mixed well. The DNA precipitate was transferred with a disposable micropipette tip into a 1.5 ml tube filled with 70% ethanol. The tube was centrifuged for 5 min at 12,000 rpm. The supernatant was removed and the pellet was air dried for 20-30 min. Pellet was resuspended in 100 µl milli Q water. Recombinant clones were identified by Southern blot or PCR analysis.

3.4.5 Preparation of recombinant ES cell clones

Positive clones were thawed and plated on 6 cm dishes pre-plated with embryonic fibroblast cells. The ES cell medium was changed every 24 h. When colonies were grown large enough (usually after 3-5 days) cells were split into 6 x 6 cm dishes preplated with embryonic fibroblast cells. 5 dishes were frozen as described above for further use. The remaining cells were again subcultured into 6 x 6 cm dishes and immediately used for chimera generation.

3.5 Generation of knock-in chimeric mice

3.5.1 Generation of injection chimera

Blastocyts were harvested from super ovulated C57BL/6J or CD1 female mice by flushing the uteri with M2 medium. Blastocytes were washed in M16 medium and stored in a CO_2 incubator.

ES cell medium was removed and 2 ml trypsin was added per plate. The plates were incubated 3–5 min to obtain single cell suspensions. Trypsin was inactivated by addition of 5 ml ES medium. The cells were pelleted by low speed centrifugation at 2,000 rpm for 2 min. The pelleted cells were resuspended in 3 ml ES medium and replated into the same 6 cm dish. About 15 blastocysts and approximately 400 ES cells were added into the injection chamber with M2 medium and the blastocysts were microinjected. The injected blastocysts were transferred into a fresh drop of M16 medium and stored in a CO_2 incubator until all blastocysts were injected. Blastocyts were transferred into pseudo pregnant foster mice. This was done by the microinjection service of the House for Experimental Therapy (HET, Bonn).

The 8 - 24 weeks old pseudo pregnant fosters were paired with vasectomized males overnight. After 20-25 days chimeras were obtained. Germ line transmission was evaluated by coat colour and the genotypes of the transgenic mice were further determined using Southern blot as well as PCR.

3.5.2 Deletion of the neomycin gene

Germ line chimeras were further bred with wild type mice to obtain the F1 generation. Mice carrying the Cnr2-CFP-neo gene were bred to PGK-Cre transgenic mice (Lallemand, Luria et al. 1998) to delete the neomycin gene. The elimination of the neomycin gene was confirmed by an allele specific PCR analysis as well as by Southern blot analysis.

3.5.3 Breeding and animal facility

For the described experiments Cnr2-eCFP and Cnr2-eGFP animals were bred in the HET facility. The animals were held in artificial day-night cycle: Lighting from 7:00 to 19:00 clock, darkness from 19:00 to 7:00 clock. The animals were housed in groups and received water and food *ad libitum*.

3.6 Wound healing experiments

Mice were anaesthetized by intraperitoneal (i.p.) injection of ketamine (75 mg/kg) / xylazine (5 mg/kg). Two full-thickness 4 mm diameter excisional wounds were made on both sides of the dorsal midline by excising skin and panniculus carnous as described (Werner, Smola et al. 1994). Wounds were left uncovered and harvested at different time points after injury. Mice were kept separately in cages to prevent fighting and no self-induced trauma was observed in control or mutant mice. Littermates of the same sex were used for the analysis of wound closure. Wound closure was determined as the percentage of distance covered by the epidermis between the wound edges. For histological analysis, dissected wounds were fixed overnight in 4% formaldehyde or in 95% ethanol/1% acetic acid, followed by dehydratation through a graded ethanol series and embedding in paraffin. Sections from the middle of the wound were stained with HE (3.2.7). Histological sections were used to determine the epithelial length and area of wound by using the measure and area function of the Image J or Openlab 4 program. The percentage of the wound closure for open wound is calculated by 100 X (the the sum of the left and right epithelial wound length / the total wound length).

3.7 Contact hypersensitivity

DNFB (1-fluoro-2,4 dinitrobenzene, Merck) was diluted in acetone/olive oil (4:1) immediately before use. Mice were sensitized by painting 50 µl of 0.2% DNFB on the shaved abdomen on two consecutive days. Controls were treated with 50 µl acetone: olive oil. For elicitation of CHS, ears of mice were painted with 10 µl of 0.3% DNFB on day 5. Ear thickness was measured 48 h after the challenge using an engineer's micrometer (Oditest, Fa. Kroeplin, Schluechtern, Germany) and ear swelling was calculated in each mouse as the difference in ear thickness between the unchallenged (left) and the challenged (right) ear.

3.8 Neuropathy pain model

Under 2% isoflurane anaesthesia and aseptic conditions the right sciatic nerve was exposed at mid-thigh level. Approximately one-third to one-half the diameter of the nerve was tightly ligated with 9-0 silk sutures. The wound was closed. After 4 days the mice were sacrificed, spinal cord was removed and fixed in 4% PFA overnight followed by transfer into the 30% sucrose solution till it sank. The tissue was fixed

with tissuetek and cryosections were made. The sections were then visualized under fluorescent microscope after fixation with aqua poly/mount mounting medium.

3.9 Statistical Methods

The descriptive statistics were performed on the basis from average values and their standard errors (S.E.M.). All raw data were listed with the spreadsheet program EXCEL® (Microsoft) and evaluated with the statistics program Prism 4 (graph PAD software). Depending upon the conditions parametric or non-parametric test was used. Average value comparisons in pairs were examined with Students t-test or the man Whitney U-test for statistical significance. Differences were termed as significant if the probability (p), $p < 0.05$ and were called as very significant with $p < 0.01$.

3.10 Used databases and programs

The human and murine genome sequences can be searched on the Golden Path browser of the University of Santa Cruz (the USA) under http://genome.ucsc.edu, the Ensembl Browser under http://www.ensembl.org, and with the NCBI under http://www.ncbi.nlm.nih.gov/genome/guide/.

NCBI Homepage (http://www.ncbi.nlm.nih.gov/)

On the homepage "National Centres for of the Biology and Information" (NCBI) are numerous links to programs and databases. Frequently used are mentioned below:

NCBI *mouse genome resources*:

http://www.ncbi.nlm.nih.gov/genome/guide/M_musculus.html

Under mouse genome resources, data from Mouse genome sequencing project was accessed.

BLAST (*Basic Local Alignment Search Tool*, [Altschul et al., 1990]):

http://www.ncbi.nlm.nih.gov/cgi-bin/BLAST/

The Blast algorithm was primarily used for similarity searches in sequence databases.

DNAStar and Vector NTI 7:

With help of DNAstar 6 (Dnastar Inc.) and Vector NTI 7 (Invitrogen) programs restriction maps from DNA sequences and vector maps for cloning of plasmids were made.

4 Results

Our group have been using metallic ear tags for the management of mouse colonies for more than 10 years and tagged well over 50,000 animals from numerous mice strains, including many different knock-outs. These tags are generally well tolerated. However, severe ulcerations were observed in the head and neck regions of cannabinoid receptor double knock-out mice as a result of frequent scratching around ear tags (Karsak, Gaffal et al. 2007). These necrotic lesions initially developed around the ear tag as shown in Fig. 4.1.

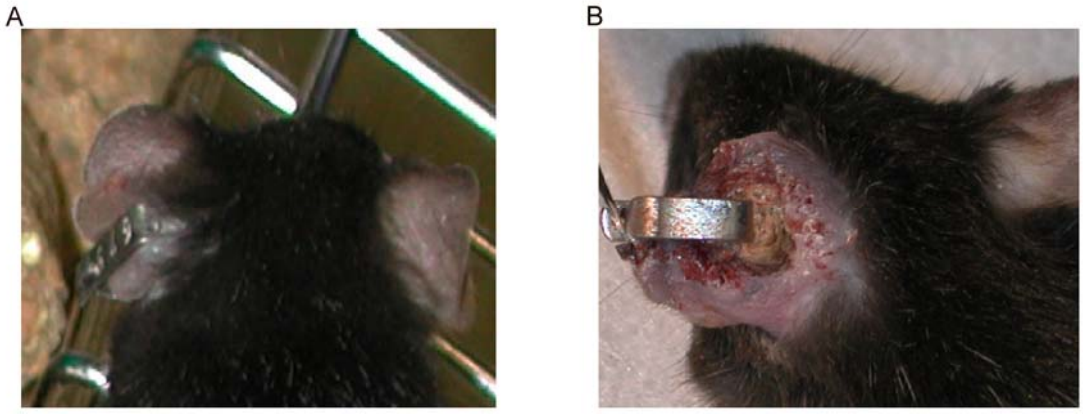

Fig. 4.1 Macroscopic views of ear-tagged double knock-out mice: Ears of animals with (B) or without (A) allergic response towards clips with high nickel content leading to chronic ulceration (B).

4.1 Wound healing of cannabinoid double knock-out animals

Since localized necrotic lesions initially developed around the ear tag, impairment of wound healing process can possibly potentiate the formation of observed skin lesions. In order to investigate this possibility, full-thickness excision wounds were inflicted on animals by removing skin and panniculus carnosus on either side of the dorsal midline. Wounds were left uncovered and excised 3, 5 or 13 days after injury (Werner, Smola et al. 1994; Werner and Grose 2003; Bamberger, Scharer et al. 2005).

For histological analysis bisected wounds were fixed and sections were analyzed visually (day 3 and day 13) for wound healing impairments. Sections (6 µm) from the middle of the 5-day wounds of (A) $Cnr1^{+/+}/Cnr2^{+/+}$ and (B) $Cnr1^{-/-}/Cnr2^{-/-}$ mice were stained with haematoxylin/eosin and used for morphometric analysis. Only littermates of the same sex were used for direct histological comparison. Morphometric analysis

resulted in no genotypic differences. For example ethanol fixed morphological analysis for 5 day wound experiment is shown here percentage of closure ($Cnr1^{-/-}$ /$Cnr2^{-/-}$, 72.07 ± 21.23% vs. $Cnr1^{+/+}$/$Cnr2^{+/+}$, 63.18 ± 24.65; p<0.26) (Fig. 4.2 C), epithelial length ($Cnr1^{-/-}$/$Cnr2^{-/-}$, 2.41 ± 1.21 mm vs. $Cnr1^{+/+}$/$Cnr2^{+/+}$, 2.60 ± 0.55 mm; p<0.92) (Fig. 4.2 D) and total area ($Cnr1^{-/-}$/$Cnr2^{-/-}$, 0.18 ± 0.06 mm^2 vs. $Cnr1^{+/+}$/$Cnr2^{+/+}$, 0.24 ± 0.09 mm^2; p<0.06) (Fig. 4.3 E).

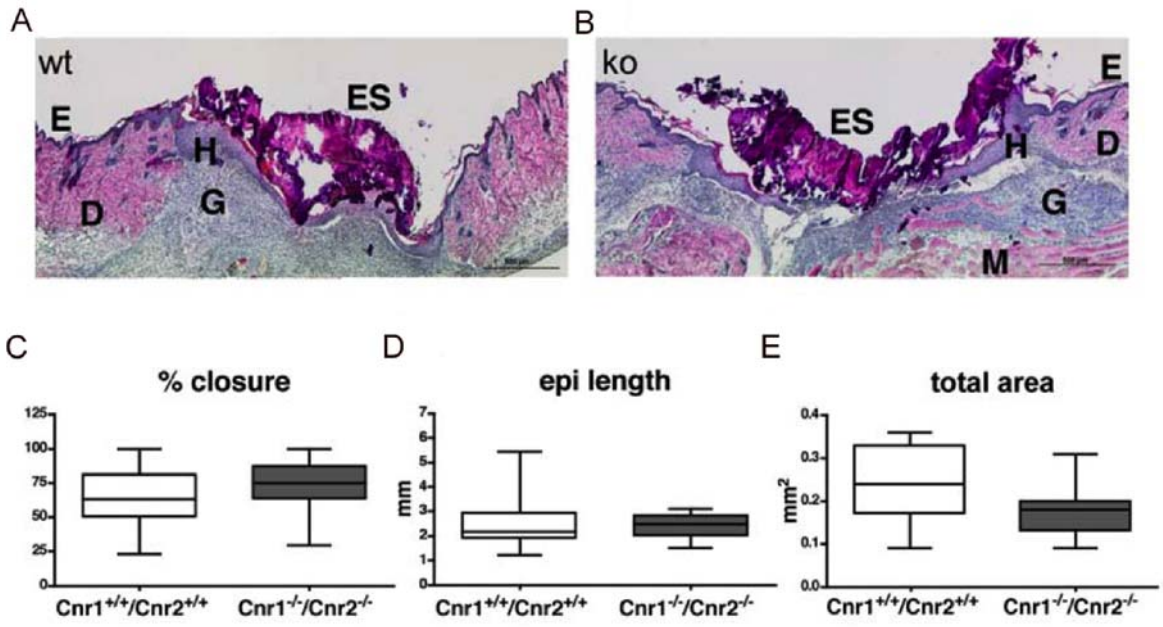

Fig. 4.2 Wound healing experiment: Ten to 12-week-old mice were anaesthetized with ketamine/xylazine. Four full-thickness excisional wounds (5 mm diameter) were generated on the shaved back, two on each side of the vertebral column, by excising skin and panniculus carnosus. For histological analysis bisected wounds were fixed overnight in 4% PFA in PBS or in 95% ethanol/1% acetic acid, followed by paraffin embedding. Sections (6 µm) from the middle of the 5-day wounds of (**A**) $Cnr1^{+/+}$/$Cnr2^{+/+}$ and (**B**) $Cnr1^{-/-}$/$Cnr2^{-/-}$ mice were stained with haematoxylin/eosin and used for morphometric analysis. Only littermates of the same sex were used for direct histological comparison. Morphometric analysis resulted in no genotypic differences in (**C**) percentage of closure (**D**) epithelial length(epi length) and (**E**) total area.
D: dermis, E: epidermis, G: granulation tissue, H: hyperproliferative wound epidermis, ES: eschar, M: muscle (Panniculus carnosus)

Cannabinoid double knock-out mice were of mixed genetic background of C57BL/6J and 129/Sv strains whereas CB1 and CB2 knock-out animals were of C57BL/6J background. Thus control animals of C57BL/6J background were also included in the experiments (Tab. 4.1).

Expt No.	Study group	Control group	Sex	Remark
1	$Cnr1^{-/-}/Cnr2^{-/-}$	$Cnr1^{+/+}/Cnr2^{+/+}$	M	Slight tendency was seen. 5 day wound
2	$Cnr1^{-/-}$, $Cnr2^{-/-}$, $Cnr1^{-/-}/Cnr2^{-/-}$	C57BL/6J, $Cnr1^{+/+}/Cnr2^{+/+}$	F	No strong tendency 5 day wound
3	$Cnr1^{-/-}/Cnr2^{-/-}$	$Cnr1^{+/+}/Cnr2^{+/+}$	M	No tendency was observed. 5 day wound
4	$Cnr1^{-/-}/Cnr2^{-/-}$	$Cnr1^{+/+}/Cnr2^{+/+}$	M	No tendency was observed. 13 day wound

Tab 4.1 Summary of wound healing experiments: Indicating that wound healing impairment is not the cause for the lesions seen in the $Cnr1^{-/-}/Cnr2^{-/-}$ knock-out animals. N=4 animals per group.

Both PFA and ethanol fixed wound slides were initially analyzed for the wound healing parameters like percentage of wound closure, epithelial length and total area. In the initial 5 day wound experiment, PFA fixed wound samples showed no significant difference in the percentage wound closure of $Cnr1^{-/-}/Cnr2^{-/-}$ mice compared to wild type mice ($Cnr1^{-/-}/Cnr2^{-/-}$, 95.0 ± 10 vs. $Cnr1^{+/+}/Cnr2^{+/+}$,86.7 ± 11.94 %; $p<0.31$) but in parameters like epithelial length ($Cnr1^{-/-}/Cnr2^{-/-}$, 1.73 ± 0.32 mm vs. $Cnr1^{+/+}/Cnr2^{+/+}$, 2.75 ± 0.59 mm; $p<0.03$) and total area ($Cnr1^{-/-}/Cnr2^{-/-}$, 0.18 ± 0.05 mm^2 vs. $Cnr1^{+/+}/Cnr2^{+/+}$, 0.38 ± 0.13 mm^2; $p<0.01$) significant difference was observed. However, from the same wound samples when fixed with ethanol showed no difference in any of the wound healing parameters, percentage of closure ($Cnr1^{-/-}/Cnr2^{-/-}$, 96 ± 7.3% vs. $Cnr1^{+/+}/Cnr2^{+/+}$, 79.14 ± 17.87; $p<0.14$), epithelial length ($Cnr1^{-/-}/Cnr2^{-/-}$, 1.9 ± 0.52 mm vs. $Cnr1^{+/+}/Cnr2^{+/+}$, 1.96 ± 0.52 mm; $p<0.95$) and total area ($Cnr1^{-/-}/Cnr2^{-/-}$, 0.19 ± 0.03 mm^2 vs. $Cnr1^{+/+}/Cnr2^{+/+}$, 0.23 ± 0.08 mm^2; $p<0.53$). Thus, I termed this result as tendency (Tab. 4.1, Expt. 1).

Upon further experiments with 5 day wound and 13 day wound, I found no significant difference in the wound healing parameters of $Cnr1^{-/-}/Cnr2^{-/-}$ mice compared to wild type mice. The results for 5 day wounds are summerized in Tab. 4.1. The results for 13 days wounds showed no significant difference (% of closure ($Cnr1^{-/-}/Cnr2^{-/-}$, 96.0 ± 7.2 vs. $Cnr1^{+/+}/Cnr2^{+/+}$,79.15 ± 17.86 %; $p<0.14$), epithelial length ($Cnr1^{-/-}/Cnr2^{-/-}$, 1.9

± 0.52 mm vs. $Cnr1^{+/+}/Cnr2^{+/+}$, 1.96 ± 0.52 mm; p<0.14) and total area ($Cnr1^{-/-}/Cnr2^{-/-}$, 0.23 ± 0.1 mm^2 vs. $Cnr1^{+/+}/Cnr2^{+/+}$, 0.19 ± 0.03 mm^2; p<0.95)).

Thus, it can be concluded that wound healing impairment did not cause the lesions seen in the knock-out animals.

The aforementioned wound healing experiments were carried out in collaboration with Prof. Sabine Werner (Zurich). The following work of contact hypersensitivity model was done with collaboration with Dr. Meliha Karsak, Jennifer Rehnelt and Dr. Evelyn Gaffal (Bonn).

4.2 Contact hypersensitivity model in cannabinoid receptor knock-out animals

As we observed no skin ulcerations in single $Cnr1^{-/-}$ or $Cnr2^{-/-}$ knock-outs or in any other mouse strain but in $Cnr1^{-/-}/Cnr2^{-/-}$ double knock-out mice, the skin ulcerations appeared to be prominent with ear tags containing high nickel content (65 to 70%). In these cases, skin ulcerations were observed in 88 out of 304 (29%) animals, possibly due to an increased allergic response in the $Cnr1^{-/-}/Cnr2^{-/-}$ mice. To verify this hypothesis the cutaneous contact hypersensitivity model (Knop, Stremmer et al. 1982; Schwarz, Beissert et al. 2000) was evaluated in these mice.

In this well-established experimental model, mice without any skin lesions and ear tags were exposed to repeated obligate contact with the DNFB allergen to trigger a specific cutaneous T-cell mediated allergic response. To sensitize the mice, DNFB was repeatedly administered to the abdominal skin and subsequently challenged by DNFB application to the ear. Allergic ear swelling was measured over a time course of 24 days. As shown in Fig. 4.3, a strikingly increased allergic response in knock-out $Cnr1^{-/-}/Cnr2^{-/-}$ mice was observed as compared to wild type $Cnr1^{+/+}/Cnr2^{+/+}$ mice. The genotype difference was particularly greater 48 h after the second ($Cnr1^{-/-}/Cnr2^{-/-}$, 1.89 ± 0.16 mm vs. $Cnr1^{+/+}/Cnr2^{+/+}$, 0.71 ± 0.05 mm; p<0.01) and third DNFB challenge ($Cnr1^{-/-}/Cnr2^{-/-}$, 3.83 ± 0.29 mm vs. $Cnr1^{+/+}/Cnr2^{+/+}$, 1.64 ± 0.09 mm; p<0.01).

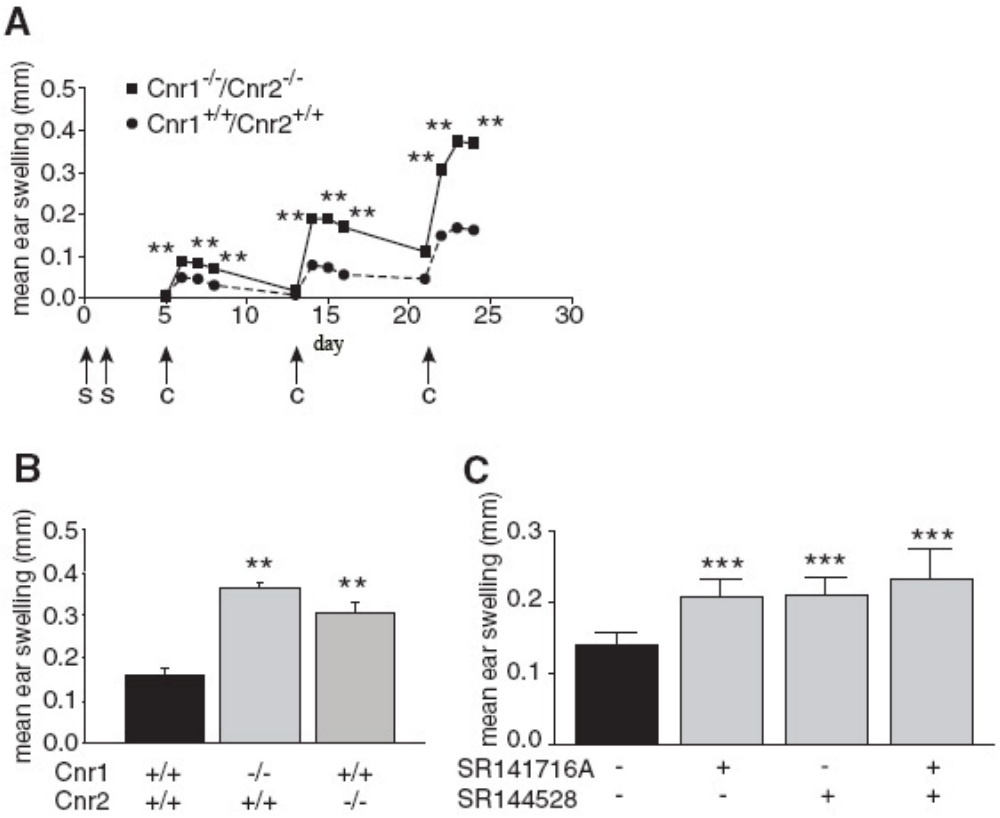

Fig. 4.3 Contact allergy in cannabinoid receptor deficient mice: (A) $Cnr1^{-/-}/Cnr2^{-/-}$ and $Cnr1^{+/+}/Cnr2^{+/+}$ mice were sensitized (indicated by "s") with DNFB on the shaved abdomen. On day 5, mice were challenged (indicated by "c") with DNFB on the right ear. A second and third challenge was performed on day 13 and 21. Shown is the mean ear swelling over time ± SEM of a representative experiment with nine mice per group. Statistical significance was evaluated with the Wilcoxon-Mann-Whitney two-sample test (**P<0.01). This experiment was independently repeated four times with similar results. (B) $Cnr1^{-/-}/Cnr2^{+/+}$, $Cnr1^{+/+}/Cnr2^{-/-}$, and $Cnr1^{+/+}/Cnr2^{+/+}$ mice were sensitized as described in (A). Ear swelling 48 h after the third challenge of a representative experiment with eight mice per group is shown. Similar results were obtained in four independent experiments with a total of 23 mice (**P < 0.01). (C) Contact allergic response in C57BL/6J mice after treatment with the indicated CB receptor antagonists. Ear swelling 48 h after the second challenge of a representative experiment with 10 mice per group is shown. Similar results were obtained in four independent experiments with a total of 25 mice (***P < 0.001). Errors bars in (B) and (C) indicate SEM. (Karsak, Gaffal et al. 2007)

To further examine the allergic response of DNFB in animals with a single deletion in CB1 or CB2 receptors, we performed a similar experiment on these animals. As shown in Fig. 4.3 B, $Cnr1^{-/-}$ and $Cnr2^{-/-}$ mice show a similarly pronounced increase of allergic ear swelling.

To obtain independent evidence for the role of CB1 and CB2 receptors in the regulation of CHS, the CB1 receptor antagonist SR141716A (Rimonabant) and the CB2 receptor antagonist SR144528 were administered in wild type mice. After the induction of CHS, animals received three injections of the corresponding antagonist, 30 min before and after each challenge. In these cases, ear swelling was significantly

increased in treated mice as compared with control mice (Fig. 4.3 C), further supporting the role of both receptors in CHS.

Due to the possibility that administration of cannabinoids such as Δ^9-THC might attenuate CHS in wild type animals, after CHS was induced, mice were injected with Δ^9-THC (5 mg per kilogram of body weight, administered subcutaneously) 30 min before, as well as 24 and 48 h after DNFB challenge. Ear swelling was measured in these animals over a course of 21 days (Fig. 4.4).

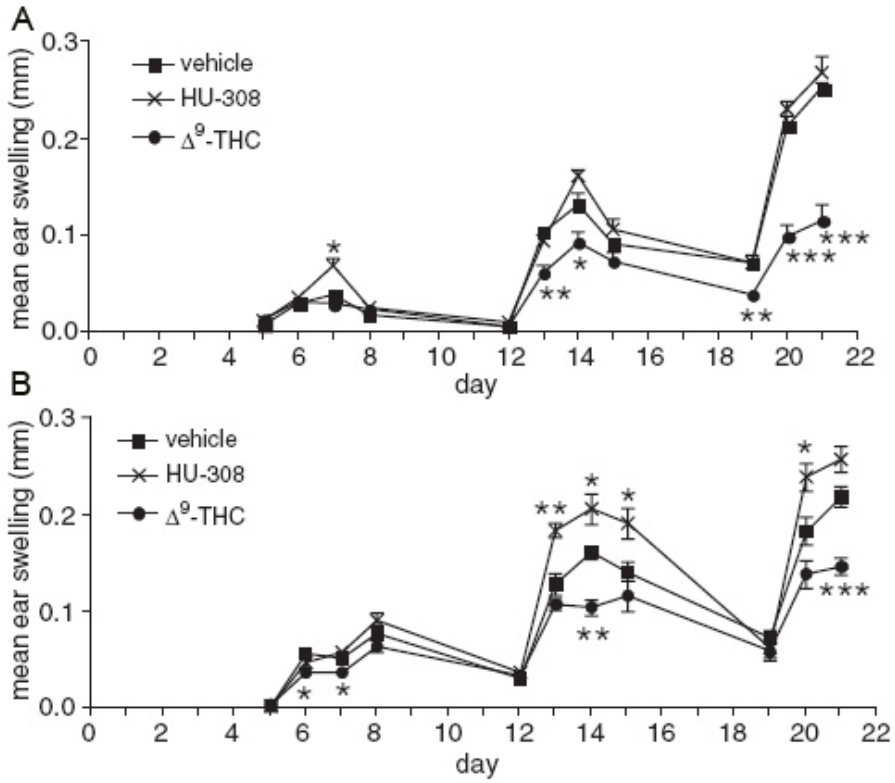

Fig. 4.4 Effect of cannabinoid receptor agonist on contact allergic response: Contact allergic responses in C57BL/6J mice after subcutaneous (A) or topical (B) treatment with the agonist's Δ^9-THC and HU-308 or with vehicle alone. Error bars indicate SEM. (Karsak, Gaffal et al. 2007)

Δ^9-THC significantly decreased ear swelling (Fig. 4.4 A). A similar therapeutic effect of Δ^9-THC was observed after topical application of 30 µg of Δ^9-THC 30 min before, as well as 24 and 48 h after DNFB administration (Fig. 4.4 B). The CB2-specific agonist HU-308 either showed no efficacy or even an increased allergic response was observed in contrast after subcutaneous or topical application (Fig. 4.4, A and B).

As the CB2 receptor seems to play an important role in the cutaneous hypersensitivity, the cutaneous expression of CB2 receptors at protein levels should

be further investigated. Unfortunately, we and other labs often observe non specific CB2 staining in tissues of knock-out animals with commercially available CB2 receptors antibodies, despite many efforts by competent labs. Therefore one of the aims of the following work was to generate fluorescent tagged CB2 receptors using a knock-in approach. CB2 receptor is denoted as Cnr2 receptor, but henceforth in my work I use more common denotation CB2, instead of Cnr2.

4.3 Expression vectors for the CB2 receptor

In order to determine if tagging of a fluorescent protein to the CB2 receptor interferes with its subcellular localization and its function, two versions of fusion proteins, one using GFP and the other using CFP were generated. A vector system commonly used for expression of GPCRs in tissue culture cells was used.

4.3.1 Generation of fluorescent tagged CB2 receptors

The CB2 receptor was modified at the C-terminus by in frame addition of the eCFP or eGFP sequence to generate CB2-eCFP-N1 and CB2-eGFP-N1 vectors. Initially the CB2 receptor sequence containing an additional 1.5 kb fragment homologous to 5 ´ UTR upstream of the CB2 coding sequence was amplified by PCR from 129/Sv ES cell genomic DNA. By using appropriate primers, a *Pac I* restriction site (TTAATTAA) was added to the 5´ end of the genomic CB2 sequence (NM_009924) and the CB2 stop codon sequence (TAG) was replaced by the glycine coding sequence (GGA) yielding a fragment of 2.5 kb.

Additionally, *Age I* restriction site (ACCGGT) was cloned in at the 3´end. This modified CB2 fragment was cloned in a pCR®blunt II TOPO vector (Invitrogen), referred as 2.5 kb-CB2 PCR blunt-TOPO. This vector was digested with the restriction enzymes *Xho I* and *Age I.* The fluorescent protein containing vectors pEGFP-N1 or pEGFP-N1, were also digested with the same enzymes. The resulting fragments were separated by gel electrophoresis and recovered from the gel using an agarose gel extraction kit (Qiagen). An insert containing the CB2 coding region was then ligated to the eGFP or eGFP containing vector (Fig. 4.5).

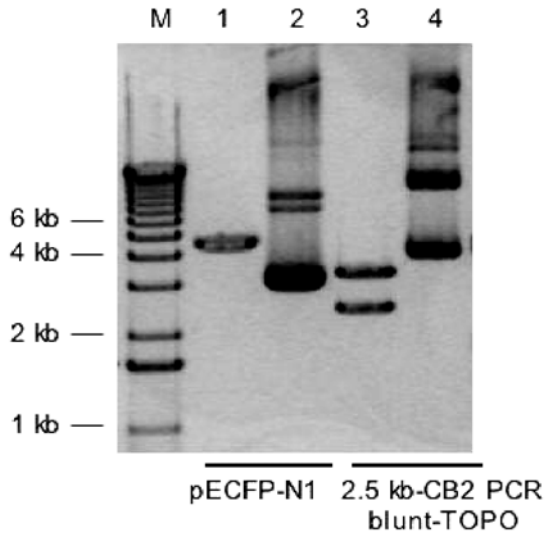

Fig. 4.5 Restriction digestion of pECFP-N1 vector and 2.5 kb-CB2 PCR blunt TOPO vectors: eCFP and CB2 short arm containing vectors were digested with *XhoI* and *Age I* restriction enzymes and fragments were analyzed by agarose electrophoresis (lanes 1 and 3 respectively), lanes 2- 4 show undigested vectors. M: 1 kb Invitrogen molecular ladder.

This resulted in the C-terminal CB2 fusion with the linker sequence of the six amino acids GPVAT (Fig. 4.6). This vector was used as template for the generation of expression vectors for cell culture experiments and the generation of knock-in mice.

…….. T E A D V K T T G P V A T M V S K G……..

…….. CAGAGGCTGATGTGAAAACCACC GGACCGGTCGCCACC ATGGTGAGCAAGGGC……..

C-terminal CB2 sequence Linker sequence N-terminal GFP/CFP sequence

Fig. 4.6 Sequence of the C-terminal GFP/CFP fusion: Primers were selected such that the stop codon sequence was modified to the amino acid sequence of glycine. Black: C-terminal sequence of the murine CB2 receptor, red: linker sequence, green: GFP/CFP N-terminal sequence.

For the CB2-eCFP or CB2-eGFP sequence amplification D_mCB2_KZ_F and GFP Stop Not1 R primers were used for the generation of expression vectors. This resulted into amplification of a 1776 bp PCR fragment (lane 3 and 4, Fig. 4.7). For the amplification of the control CB2 vector D_mCB2_KZ_F primer and mCB2-exon stop rück primer were used. This resulted into amplification of a 1041 bp fragment (lane 2, Fig. 4.7).

The PCR products were verified by agarose gel electrophoresis and by sequencing.

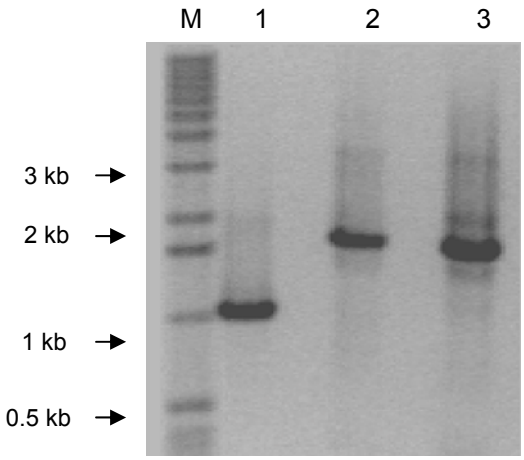

Fig. 4.7 Gel electrophoresis of PCR products CB2-eCFP, CB2-eGFP and CB2: In each lane 3 µl of the PCR product of the appropriate vector was loaded and separated on a 1% agarose gel at 120 V. Lane M show 1 kb ladder (Invitrogen), lane 1 show CB2 and lane 2,3 shows CB2-eCFP and CB2-eGFP PCR fragments.

In Fig. 4.7, the expected amplified products of 1.8 kb for CB2-eCFP (lane 2) as well as CB2-eGFP (lane 3) and 1 kb for CB2 (lane 1) are shown. These PCR products were ligated in the pcDNA^{TM}3.1 Directional TOPO$^{®}$ vector according to the protocol supplied by the manufacturer. After transformation in chemical competent *E. coli.* cells, positive clones were selected by restriction analysis and verified by sequencing.

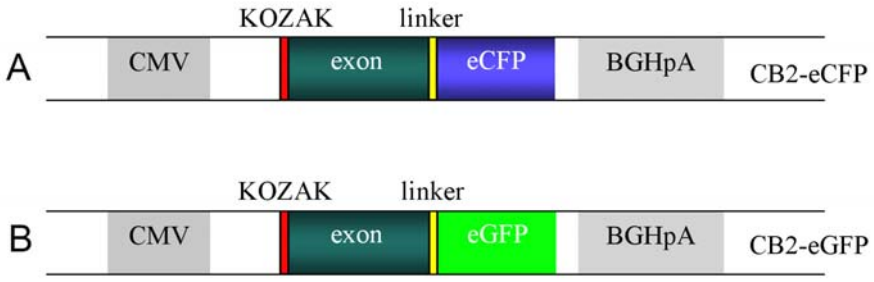

Fig. 4.8 Schematic representation of CB2-eCFP and CB2-eGFP expression constructs: Two essentially similar expression vectors under the control of a CMV promoter were generated. The CB2 coding exon was fused with either eCFP (A) or eGFP (B). In order to optimize the expression efficacy, a Kozak sequence was added upstream of the CB2 start codon and a BGHpA - bovine growth hormone at the 3'-UTR.

The CB2-eCFP and CB2-eGFP expression vectors contain a human cytomegalovirus virus (CMV) immediate early enhancer/promoter for high-level constitutive expression of the gene of interest in a wide range of heterologous proteins in most mammalian cells (Boshart, Weber et al. 1985; Nelson, Reynolds-Kohler et al. 1987; Andersson,

Davis et al. 1989). Additionally, they have a neomycin resistance gene for the selection of stable cell lines using Geneticin®, G418 (Fig. 4.8).
The control plasmid, pcDNA™3.1 Directional TOPO® served as a negative control and the pECFP-N1 or pEGFP-N1 plasmids, served as positive controls for transfection and expression in the mammalian cell line of choice.

4.3.2 Western blot analysis of the CB2-eCFP fusion protein

The CB2-eCFP and CB2-eGFP expression constructs were transfected in CHO-K1, HEK-293 and HeLa cell lines, that are commonly used for the functional analysis of GPCRs. Cells were selected for 3-4 weeks using the antibiotic G418. At the end of the selection process, single colonies were chosen and further cultured using G418 containing cell culture medium.
To verify the presence of the intact CB2-eCFP fusion protein, immunoprecipitation using an anti-GFP antibody (Abcam) was performed. About 2 mg of the total protein extract of CB2-eCFP cells was used.

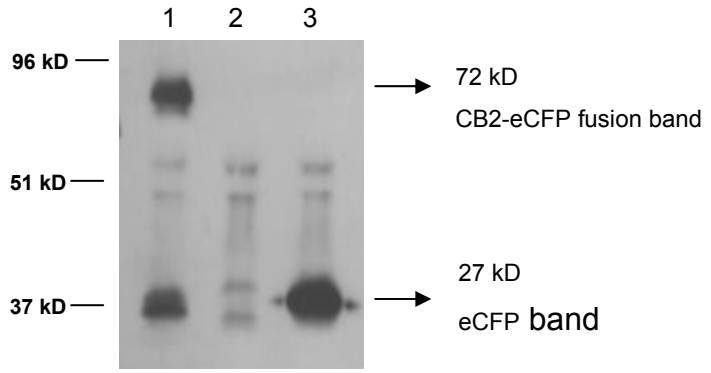

Fig. 4.9 Western blot analysis using a CHO cell extract: 2 mg of lysates from CHO cells, CB2, CB2-eCFP and eGFP expressing cells were used for immunoprecipitation with anti-GFP (ab290, abcam) antibody. The blot shows labeling of a 72 kD protein which is the expected molecular weight of CB2-eCFP fusion proteins (lane 1) and 27 kD for eCFP transfected cells (lane 3 - positive control). The CB2 control cell lysate shows no specific band (lane 2 - negative control).

The theoretical calculated weight of murine CB2 receptor is 45 kD and for the eCFP protein 27 kD. Thus CB2-eCFP fusion will result in a 72 kD band (45 kD +27 kD). As expected, a major fusion band of 72 kD (Fig. 4.9) was observed, indicating that the full-length fusion protein was expressed in the CHO-K1 cells. Additionally a band corresponding to eCFP (27 kD) was also observed.

4.3 3 Cellular expression of CB2-eCFP in different cell lines

Since the CB2 receptor fusion resulted in a full-length expression of the fusion protein, I further wanted to analyze the cellular expression of this fusion receptor in cell lines. I had used 3 different cell lines, CHO-K1, HEK-293 and HeLa cell lines for this purpose. Expression resulting from fluorescent analysis of the stably selected cell lines is shown in Fig. 4.10.

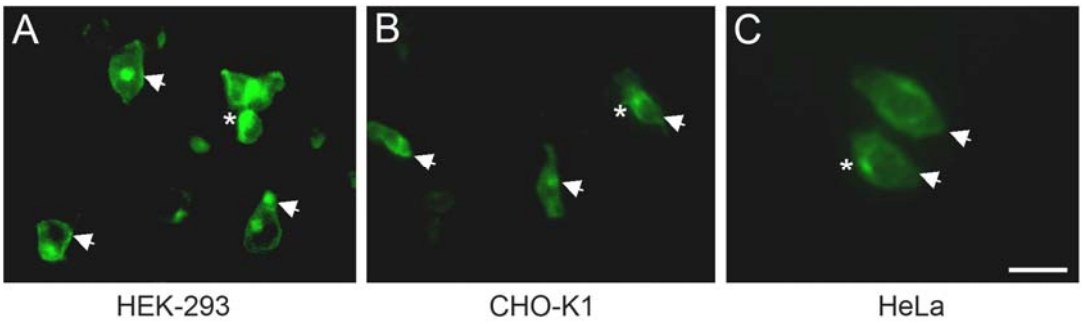

Fig. 4.10 Cellular expression of CB2-eCFP: HEK-293 (A), CHO-K1 (B) and HeLa cells (C) transfected with CB2-eCFP show a localization of the fusion protein on the cell membrane (indicated by arrow) and intracellular (indicated by star). Scale bar = 20 µm.

As shown above (Fig. 4.10), a strong fluorescence signal with CB2-eCFP fusion construct was obtained in HEK-293, HeLa and CHO-K1 cells. The fusion proteins CB2-eGFP and CB2-eCFP showed a similar subcellular expression pattern with a pronounced labelling of cell membranes. In most cells, an additional intracellular signal was obtained, suggesting a vesicular localization of CB2 receptors.

4.3.4 Co-localization of CB2-eGFP with transferrin and ∝-giantin

To verify the vesicular localization of fluorescent labelled CB2 receptors, CB2-eGFP expressing HEK-293 cells were incubated with Alexa-red-conjugated transferrin (TR). These cells were incubated with the cannabinoid receptor agonist HU-308 [100 nM] to stimulate the internalization of TR receptors (Xia, Kjaer et al. 2004). As shown in Fig. 4.11, a Co-localization of CB2-eGFP with the internalized TR receptors was observed, indicating an endosomal origin of the intracellular CB2-eGFP receptor fraction. To further determine the intracellular fluorescence origin, different markers such as Lamp I, Lim II (lysosomal markers), Calnexin (endoplasmic reticulum marker) and ∝-giantin (golgi marker) were used. Interestingly, the intracellular fluorescence signal was mainly colocalized with the golgi marker ∝-giantin.

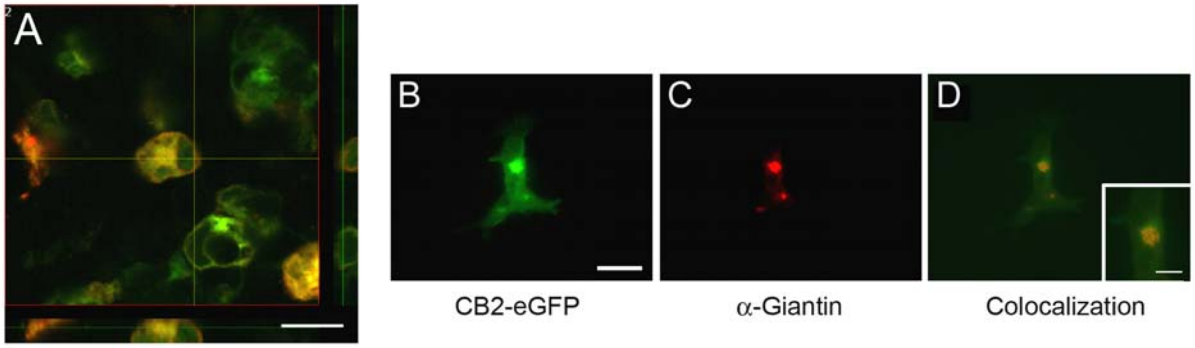

Fig. 4.11 Co-localization of CB2-eGFP with transferrin and ∝-giantin: A) Cells were incubated for 30 min with cannabinoid agonist HU-308 [100 nM] and Alexa red conjugated TR at 37°C. Cells were then fixed with 4% paraformaldehyde. The yellow fluorescence indicates a Co-localization of CB2-eGFP (green) with internalized transferrin receptors (red) in endosomes. B) Cells were fixed, permeabilized and incubated with golgi marker, ∝-Giantin. Co-localization was observed as indicated by yellow fluorescence (D). Inlet: magnified view of the colocalisaton. Scale bar = 20 µm

These data indicate that the CB2-eGFP protein was colocalized with transferrin and that the intracellular signal of the CB2-eGFP protein was largely restricted to a Golgi network.

4.4 Functional investigation of the CB2-eCFP fusion protein

To determine whether the CB2-eCFP fused receptor is still functional with respect to the downstream signaling pathway and agonist or antagonist mediated internalization, Erk-MAPK assays and internalization experiments were performed.

4.4.1 MAPK assay in CB2 and CB2-eCFP expressing cells

The ability of cannabinoids to regulate Erk-MAPK activity in the present cellular model was examined. A standard Western blot technique was used for studies. Serum starved cells were exposed to cannabinoid receptor agonists or antagonists and immediately proteins were isolated. The cellular proteins were seperated by SDS polyacrylamide gel electrophoresis. The relative amounts of active (phosphorylated) and total forms of Erk-MAPK in a given sample were analyzed by immunoblots performed with selective antibodies and quantified using an ImageJ software.

No additional increase in the activation of Erk-MAPK in native CHO-K1 or HEK-293 cells with or without the cannabinoid receptor agonist HU-308 or vehicle control DMSO under described experimental conditions was observed (data not shown).

4.4.2 MAPK activation in CB2-eCFP expressing HEK-293 cells

As shown by Bouaboula et al. CB2 receptor transfected cells showed time-dependent increase in levels of Erk-MAPK (Bouaboula, Dussossoy et al. 1999). I wanted to observe whether similar effects were seen in the CB2-eCFP cells. Thus, serum starved CB2-eCFP expressing HEK-293 cells were incubated with the cannabinoid receptor 2 agonist [10^{-8}M] HU-308 for different time intervals. The levels of activated MAPK (phosphorylated form) and total MAPK were monitored after 5, 10, 15, 20 and 30 min. The levels of active Erk-MAPK increased significantly within 15-20 min of agonist incubation. After 30 min of incubation, the levels of the active Erk-MAPK form began to decrease to basal levels (at 0^{th} min) (Fig. 4.12).

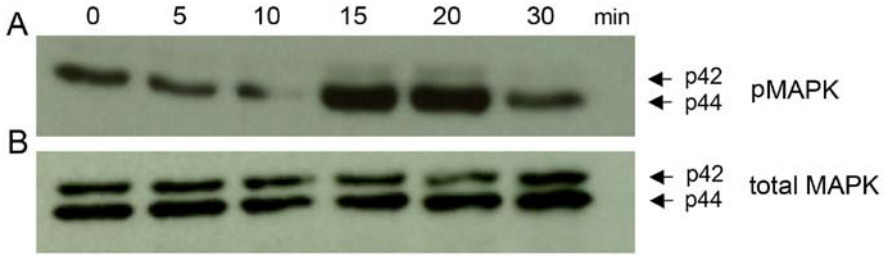

Fig. 4.12 Activation of Erk-MAPK in CB2-eCFP expressing HEK-293 cells: CB2-eCFP expressing HEK-293 cells were incubated with the CB2 agonist HU-308 [100 nM], for different time intervals. The level of activated Erk-MAPK was monitored in cells by using a pMAPK antibody (A). Total MAPK was detected by using an antibody directed against both activated and non-activated forms of MAPK (B).

A time-dependent change of the phosphorylated Erk-MAPK form was observed in CB2-eCFP expressing HEK-293 cells incubated with the cannabinoid receptor 2 agonist, HU 308, whereas the levels of total MAPK remained unaltered. Both HEK-293 and CHO-K1 cells showed the Erk-MAPK activation in the presence of the cannabinoid receptor 2 agonist. HEK-293 cells under the experimental conditions used were easily detached from the surface. This resulted into a less number of cells available for assay and hence the less protein for the assay. Thus henceforth, I had used CHO-K1 cells for further Erk-MAPK assay.

4.4.3 Direct comparison of CB2 and CB2-eCFP expressing CHO-K1 cell lines

Similar to that of HEK-293 cells, I compared the downstream Erk-MAPK signaling activation in CB2 and CB2-eCFP expressing CHO-K1 cells.

Both cell lines were incubated for 15 min with increasing concentrations of the CB2 receptor agonist, HU-308, and the level of Erk-MAPK was measured. In CB2 and CB2-eCFP expressing CHO-K1 cells, a concentration-dependent increase of phosphorylated Erk-MAPK levels was observed (Fig. 4.13).

The level of activated Erk-MAPK was increased with 10^{-7} M HU-308 and reached the maximum at 10^{-5} M. However, the level of total Erk-MAPK remained unchanged. A difference in Erk-MAPK activation in CB2 and CB2-eCFP expressing cells was not observed (Fig. 4.13). I further wanted to examine the effect of CB2 antagonist on Erk-MAPK activation in CB2 and CB2-eCFP cell lines. The antagonist treatment should result in the decrease of the Erk-MAPK phosphorylation upon treatment with the cannabiniod receptor agonist.

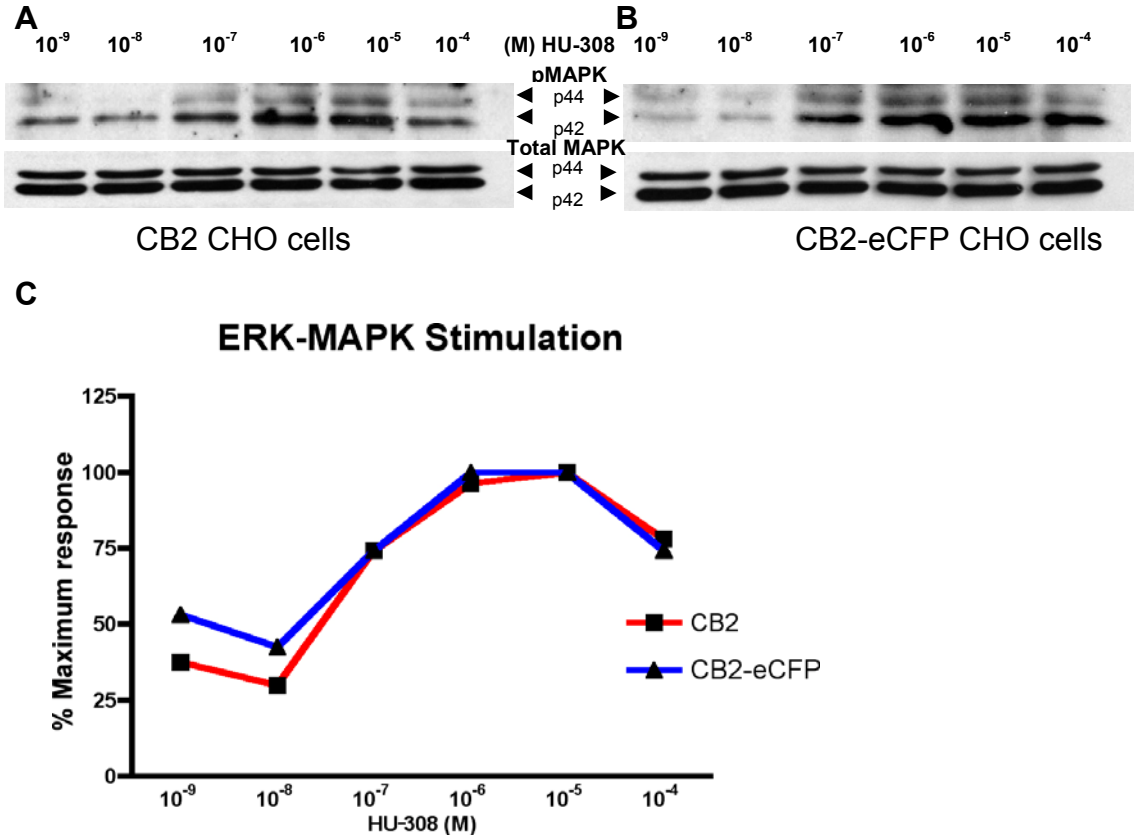

Fig. 4.13 Erk-MAPK stimulation after HU-308 treatment: Activation of Erk-MAPK in CHO cells expressing CB2 (A) and CB2-eCFP (B) by incubation of CB2 agonist HU-308 for 15 min. The level of activated Erk-MAPK was monitored in cells using a pMAPK antibody. Total MAPK levels were measured by antibody detecting both activated and non-activated forms of MAPK. (C): Data obtained after densitometric analysis of signals for both CB2 and CB2-CFP cells is shown. MAPK-Erk phosphorylation is shown as the percentage of the maximal response occurring in the presence of increasing concentrations of the cannabinoid receptor agonist HU-308.

CB2 and CB2-eCFP cells were treated with the cannabinoid receptor antagonist AM-630 in presence or absence of HU-308 for 15 min. The level of MAPK-Erk activation was determined. As shown in Fig. 4.14, the level of Erk-MAPK was reduced by co-

incubation with AM-630. No activation of Erk-MAPK in CB2 or CB2-eCFP cells treated with the cannabinoid receptor antagonist AM-630 or the vehicle control DMSO under the described experimental conditions was observed (data not shown).

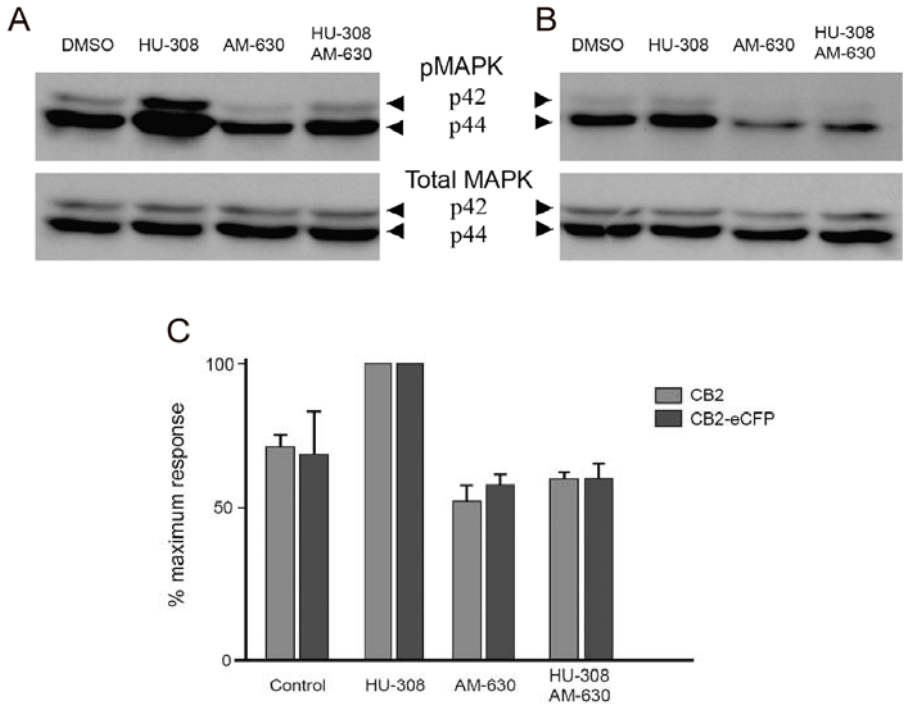

Fig. 4.14 Effect of cannabinoid receptor antagonist treatment on MAPK-Erk phosphorylation: CHO cells expressing (A) CB2-eCFP and (B) CB2 were incubated with CB2 agonist, HU-308 (HU) [100nM], with or without CB2 antagonist, AM-630 (AM) [1µM] for 15 min. The level of activated Erk-MAPK was monitored in cells by using a pMAPK antibody. Total MAPK was detected by using antibody detecting both activated and non-activated forms of MAPK. C) Effect of antagonist: Data obtained after densitometric analysis of immuno-signals for both CB2 and CB2-eCFP in CHO-K1 cells is shown. MAPK-Erk phosphorylation was expressed in the percentage, taking the maximal response by the cannabinoid receptor agonist HU-308 (HU) as 100%.

The extent of MAPK-Erk phosphorylation was equally observed in both CB2 and CB2-eCFP tagged CHO-K1 cells (Fig. 4.14). I could not detect any difference in the extent of MAPK-Erk phosphorylation after treatment with cannabinoid receptor 2 agonist and antagonist in CB2 and CB2-eCFP cells. This led to the conclusion that the CB2-eCFP fusion protein exhibited no change in Erk-MAPK activation as compared to that of CB2 expressing CHO cells.

4.5 Internalization of fluorescent tagged CB2 receptors

Various G protein coupled receptors are shown to undergo receptor internalization after stimulation with the agonist. Cannabinoid receptor 1 also undergoes internalization after the stimulation with the agonists. Thus, I wanted to analyze the receptor mediated internalization in the stably transfected CB2-eCFP cell lines.

4.5.1 Effects of cannabinoid receptor agonists on internalization of CB2-eCFP in CHO-K1 cells

In untreated CB2-eCFP CHO-K1 cells stably expressing murine CB2 receptors, the receptors were primarily localized on the cell membrane (Fig. 4.15 a). In many cells, a faint blush of intracellular staining was also observed; this represented staining of CB2 receptors in the Golgi network shown in Fig. 4.11. CHO-K1 cells were incubated with CB2 agonist HU-308 [100 nM] for 1 h with (D) or without CB2 antagonist AM-630 [1µM] (B).

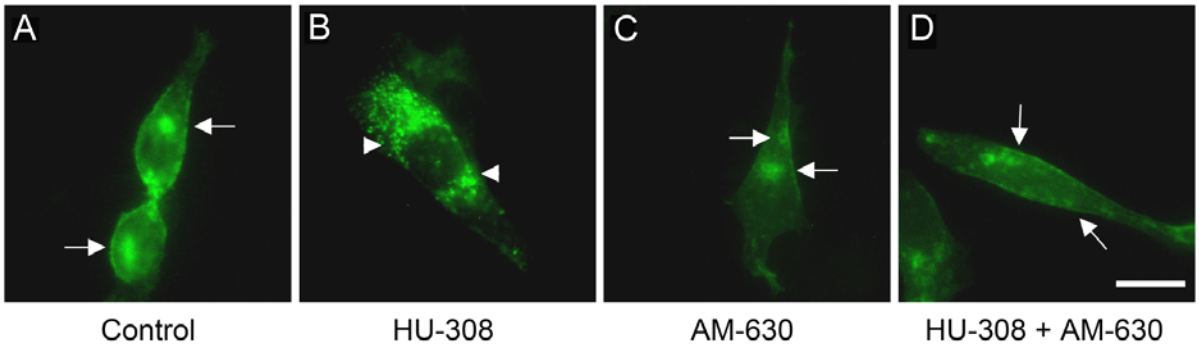

Fig. 4.15 Internalization of fluorescent tagged CB2-eCFP receptors in CHO-K1 cells: CHO-K1 cells were incubated with CB2 agonist HU-308 [100 nM] for 1 h with **(D)** or without CB2 antagonist AM-630 [1µM] **(B)**. The cannabinoid receptor agonist HU-308 caused CB2 receptor internalization, which is blocked by the CB2 antagonist AM-630. (**A**) In unstimulated CB2-eCFP CHO-K1 cells stably expressing CB2 receptors, receptors were predominantly found on the plasma membrane (arrows). **(B)** After a 1 h treatment with the cannabimimetic [100 nM] HU-308 receptors internalized (arrowheads). **(C)** AM-630 alone did not caused any change in internalization. **(D)** Cotreatment with HU-308 and the CB2 receptor antagonist AM-630 blocked internalization with CB2 receptors remaining at the cell surface (arrows). Cells were stimulated with agonist alone or with antagonist for 1 h in Hams F-12 medium containing 0.2 mg/ml bovine serum albumin at 37°C. Bar = 20 µm

Following the treatment with the cannabinoid receptor agonist HU-308 [100 nM] for 1 h at 37°C, most receptors were found inside the cell with a punctuated distribution (Fig. 4.15 b). Consistent with the CB2 receptor involvement, co-incubation of the CB2 antagonist AM-630 [1µM] with HU-308 prevented receptor internalization (Fig. 4.15 c). AM-630 treatment alone did not cause CB2 receptor internalization (Fig. 4.15 d). Cannabinoid agonists caused CB2-eCFP receptor internalization, which was blocked by the CB2 antagonist AM-630.

4.5.2 Effects of cannabinoid receptor agonists on internalization of CB2-eCFP in HEK-293 cells

After establishing the internalization effects in CHO-K1 cells, I wanted to observe the internalization of the CB2-eCFP receptors after the treatment with different agonists in HEK-293 cells. HEK-293 cells expressing CB2-eCFP were incubated with [100 nM] of the agonists HU-308, WIN 55,212-2 (Wotherspoon, Fox et al.) and HU-210 for 5 min, 30 min and 1 h. The cannabinoid receptor agonists caused CB2 receptor internalization. As shown in Fig. 4.16, the cannabinoid receptor agonists HU-308, HU-210 caused more internalization as compared to the cannabinoid receptor agonist WIN.
However, these cells show weak internalization effect after incubation with agonists in comparison with the reported internalization effects with CB1 receptor. With increase in time the CB2-eCFP receptors are internalized in HEK-293 cells (Fig. 4.16). However, even without agonist treatment, some of the tagged cannabinoid receptors were internalized.

Taken together, these observations with agonist treatment indicated that the CB2 receptors do undergo internalization. Upon the treatment with the antagonist, CB2 receptors appeared more prominently on the membrane.
I had observed that eCFP fused cannabinoid receptor undergo internalization upon treatment with agonist and this is prevented by the antagonist treatment. These receptors also display unaltered downstream Erk-MAPK signaling. Thus C-terminal fusion of these receptors seems to unalter the functionality of these receptors. Based on this information I wanted to generate two similar constructs of CB2 protein namely CB2-eCFP and CB2-eGFP knock-in for the generation of fluorescent tagged mouse strains.

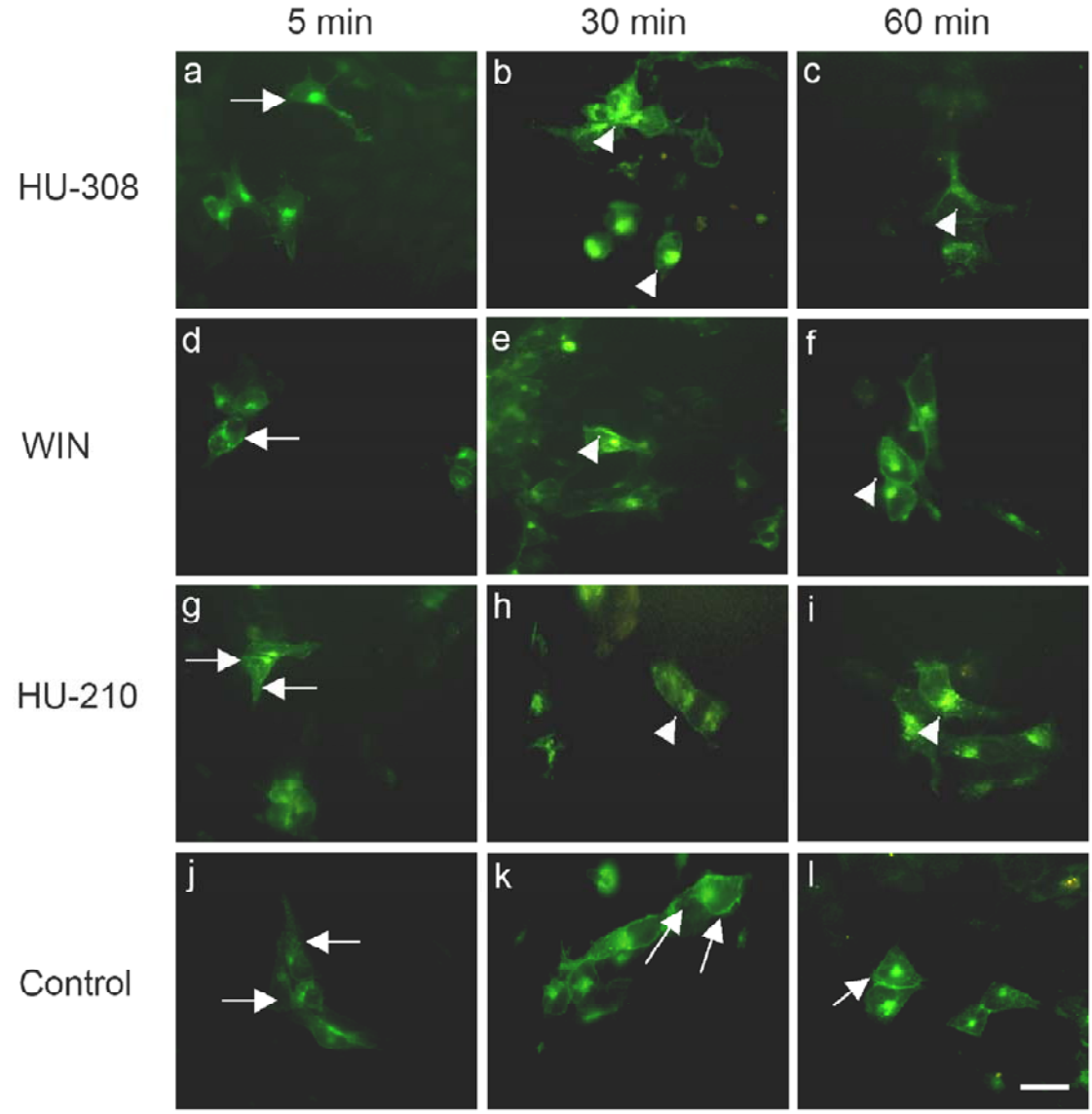

Fig. 4.16 Internalization of fluorescent tagged CB2-eCFP receptors in HEK-293 cells: HEK-293 cells expressing CB2-eCFP were incubated with the cannabinoid receptor agonists HU 308, WIN and HU-210 at [100 nM] concentration for 5 min, 30 min and 1 h. The cannabinoid receptor agonists caused CB2 receptor internalization. (**a**) In unstimulated CB2-eCFP CHO cells stably expressing CB2 receptors, receptors were predominantly found on the plasma membrane (arrows). After a 60 min treatment with the cannabinoid receptor agonists, receptors internalized (arrowheads). Cells were stimulated with agonists for 5 min, 30 min and 60 min in DMEM medium containing 0.2 mg/ml bovine serum albumin at 37°C. Bar=20 µm

4.6 Generation of CB2-eCFP and CB2-eGFP knock-in mouse strains

4.6.1 Targeting strategy of the CB2-eCFP knock-in mice

The knock-in construct was designed such that it contains two homologous regions of *CB2* sequence, termed as short arm and long arm. The short arm has a 1.5 kb homologous 5' UTR region followed by the coding sequence of cannabinoid receptor gene fused with eCFP or eGFP sequence by a linker of six amino acids (GPVAT).

The fusion proteins generated from the corresponding knock-in alleles are essentially identical to those analyzed in the tissue cultures, except for the 5'-Kozak sequence which was not introduced.

This was followed by a floxed neomycin gene and a 6.4 kb homologous 3´ UTR termed as long arm. Long arm sequence was followed by the HSV-TK cassette as shown in Fig. 4.17.

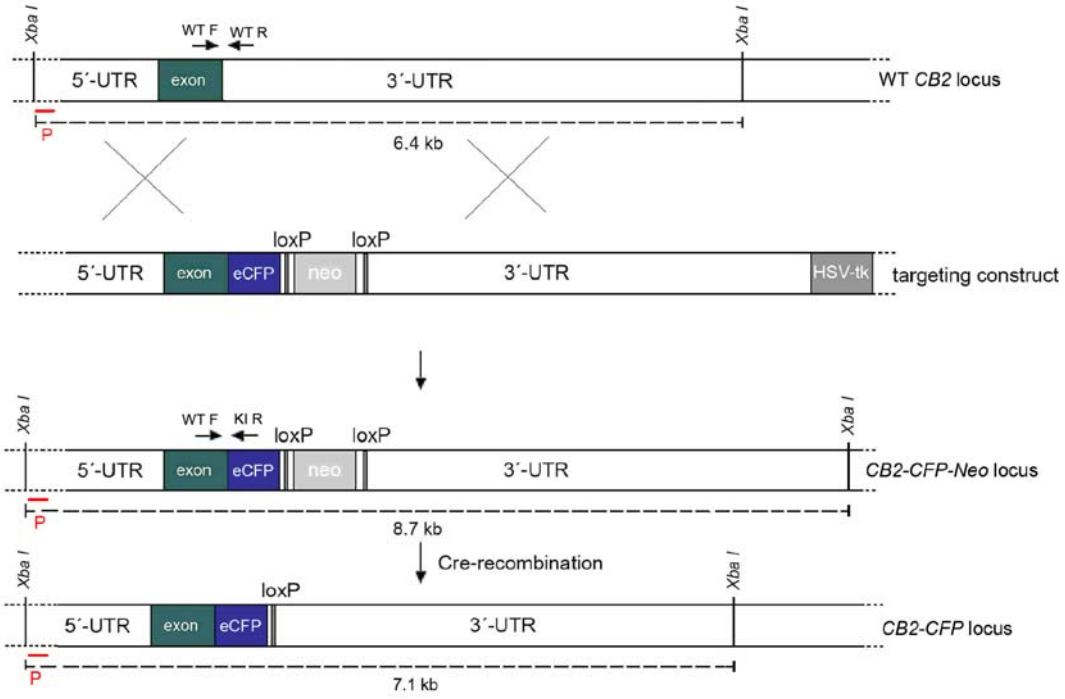

Fig. 4.17 Targeting strategy for generation of CB2-eCFP knock-in mice: The *CB2* exon, *eGFP* and the floxed neomycin cassettes are displayed as green, cyan, and grey boxes respectively. Upon homologous recombination, the resulting CB2-CFP-neo mice are bred to *PGK-Cre* transgenic animals in order to delete the floxed neo gene, thus resulting in the final *CB2-CFP* locus. P (red)- Southern probe, WT F and WT R - forward and reverse primers for the amplification of the wild type *CB2* locus, KI R - reverse primer for the amplification of the *CB2-CFP* locus.

4.6.2 Amplification of the 3´ and 5´ homology

For the generation of the 3' homology (long arm), a fragment of 6.4 kb in 3´ UTR of the murine CB2 gene was amplified from 129/Sv genomic DNA by PCR. Apart from the genomic sequence additional *Kpn I* at 5´end, and *Xma I* restriction sites at 3´ end, were incorporated for further cloning procedures. The PCR product was purified by agarose gel extraction (Fig. 4.18). The amplified sequence was verified by sequencing reactions. This fragment was cloned into the pCR XL-TOPO vector, termed as 6.4 kb-CB*2* pCR XL-TOPO vector. Clones with an insertion of the

sequence in 3´-5´ orientation were screened by restriction analysis, sequenced and used for further cloning steps.

For the amplification of the 5' homology (short arm), a 2.5 kb region was amplified using ES cell genomic DNA of the 129/Sv mouse strain. Apart from the genomic sequence the primers contained additional *Pac I* and *Age I* restriction sites which were incorporated. The *Pac I* restriction site was incorporated for the linearization of the knock-in construct since it does not digest the short arm or the long arm. The PCR product was purified by agarose gel extraction and verified by sequencing reactions (Fig. 4.18). The amplified sequence was cloned into the pCR blunt II TOPO vector and termed as 2.5 kb-CB2 PCR blunt TOPO vector. Clones in 3´-5´ orientations were screened by restriction analysis and used further for cloning steps.

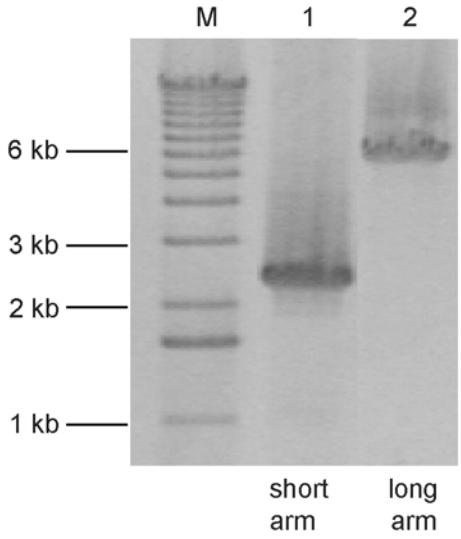

Fig. 4.18 Gel electrophoresis of PCR products short and long arm: In each lane 3 µl of the appropriate PCR product was loaded and separated on a 1% agarose gel at 120 V. Lane M show 1 kb ladder (Invitrogen), lane 1 shows 2.5 kb CB2 short arm and lane 2 shows 6.4 kb long arm PCR fragments.

Fusion step for CB2-eCFP fusion was described earlier in section 4.3.1. Resulting CB2-eCFP-N1 vector was digested with restriction enzyme *Not I*. A fragment containing 2.5 kb short arm was cloned into an exit vector, pPNT-M2 resulting vector was termed as CB2-short arm pPNT-M2 vector.

A 6.4 kb long arm fragment from the 6.4kb-CB2 pCR XL-TOPO vector was cloned in by using *Kpn I* restriction site into CB2-short arm pPNT-M2 vector. The orientation was checked by the restriction analysis and then sequenced to verify the same. This resulted into a knock-in CB2-eCFP construct.

A similar targeting construct for the CB2-eGFP was generated using the pEGFP-N1 vector in CB2 receptor fusion step. Fig. 4.18 represents two knock-in constructs used for the generation of knock-in mice.

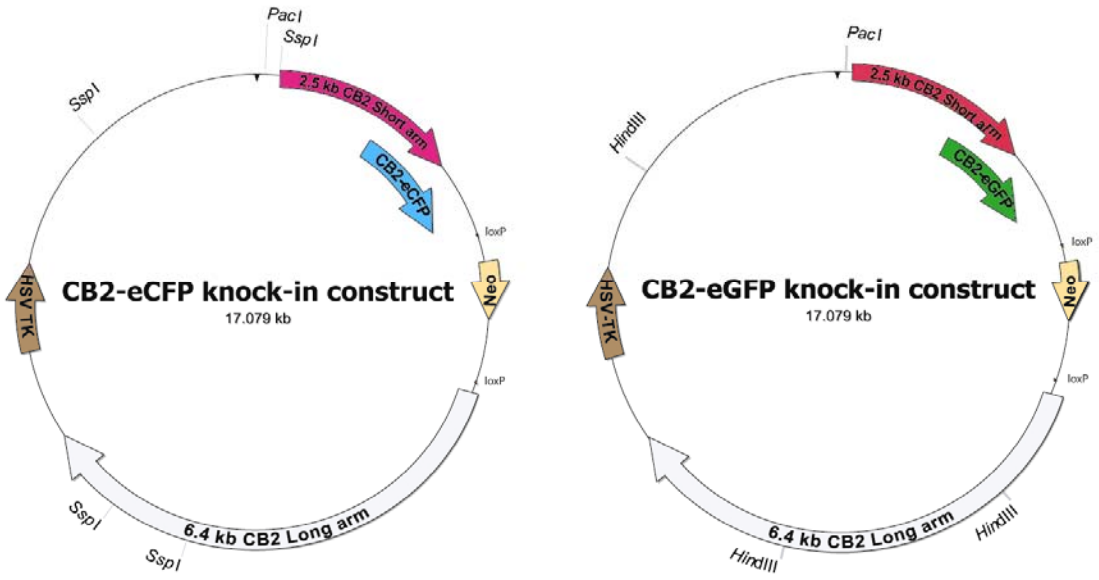

Fig. 4.19 Vector diagram for CB2-CFP and CB2-GFP knock-in constructs: Two similar constructs were generated containing CB2-eCFP or CB2-eGFP fusion proteins. These constructs contained 2.5 kb of short arm followed by the eCFP or eGFP. Neomycin gene was floxed by loxP sites followed by a 6.4 kb long arm. The vectors were lineralized with *Pac I*. The *Ssp I* and *Hind III* restriction sites were used for restriction analysis.

4.6.3 Restriction analysis of the CB2-eCFP knock-in construct

For the electroporations with knock-in constructs, clones were analyzed by restriction digestion with *SspI* and *Hind III* enzymes. The knock-in clone should result in fragments of 9.1, 4.8, 2.3 and 0.9 kb upon *Ssp I* digestion (Fig. 4.19). Similarly upon *Hind III* digestion knock-in clone should result in 9.3, 5.3, and 2.6 kb fragments.

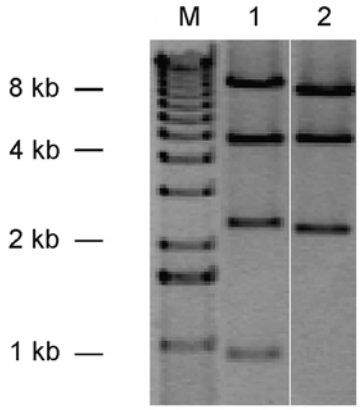

Fig. 4.20 Restriction analysis of CB2-eCFP knock-in construct: Knock-in construct was digested with *SspI* and *Hind III* restriction enzymes and fragments were analyzed by agarose electrophoresis. Lane 1 shows *SspI*, lane 2 show *Hind III* digested clone.

As seen in above Fig. 4.20, lanes 1 show fragments of 9.1, 4.8, 2.3 and 0.9 kb with *Ssp I* digestion. With *Hind III* digestion this clone showed 10.4, 4.2 and 2.6 kb fragments (lanes 2). This clone was further cultured, verified by sequencing, and used for the electroporations.

4.7 Transfection of ES cells

The targeting vectors were linearized with *Pac I* restriction enzyme and electroporated in ES cells. In total 11 electroporations were carried out in ES cells of R1 or MPI 2 origin. ES cells with a passage number between 15-18 were used for the electroporations.

Construct	ES cell origin	No. of screened clones	No. of positive clones
CB2-CFP-neo	MPI2	613	70
CB2-CFP-neo	R1	192	3
CB2-GFP-neo	MPI2	168	23
CB2-GFP-neo	R1	96	1

Tab. 4.2 Screening of knock-in ES cell clones: CB2-CFP-neo or CB2-GFP-neo knock-in constructs were electroporated in MPI2 or R1 ES cells. All together 1069 ES cells were screened with Southern blot analysis and 97 clones were tested positive for the homologous recombination (9%).

As shown in Tab. 4.2, approximately 10-fold higher recombination frequency was observed with the MPI 2 ES cell line (11.9%) to that with R1 ES cell line (1.3%).

4.8 Southern analysis of ES cells

As shown in Tab. 4.3, a total of 1069 ES cells were screened by Southern blots for the homologous recombination. The Southern blot DIG probe of 406 bp was generated by PCR (Section 3.1.13). The probe binds to a sequence in the 3'-region of the CB2 gene (Fig. 4.17).

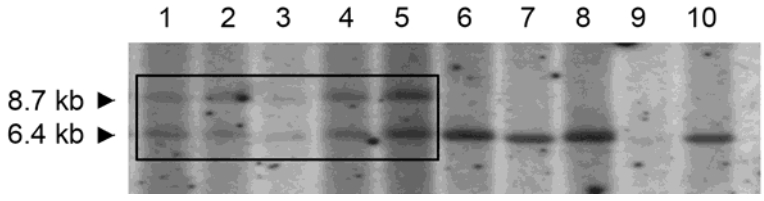

Fig. 4.21 Southern blot analysis of ES cell clones: Lanes 1-5, marked with a box, represent the homologous recombinated ES cell clones. ES cell genomic DNA was digested with restriction enzyme *XbaI*. The DIG probe was used for the Southern screening. Lanes 6 -10 represents wild type ES cell clones. Recombinated clones show 2 bands of size 8.7 kb and 6.4 kb whereas wild type clones show a band of 6.4 kb.

ES cell genomic DNA was digested with restriction enzyme *XbaI.* As shown in Fig. 4.21, the homologously recombinant locus yielded two fragments of size 8.7 kb and 6.4 kb whereas the wild type locus yielded only 6.4 kb fragment.

4.9 Karyotypic evaluation of positively recombinant ES cells

To determine the quality of homologous recombinated ES cells, karyotypic evaluation was performed. About 100 independent counts of homologous recombinated ES cell chromosomes were counted. In Fig. 4.22, a representative analysis used for counting is shown.

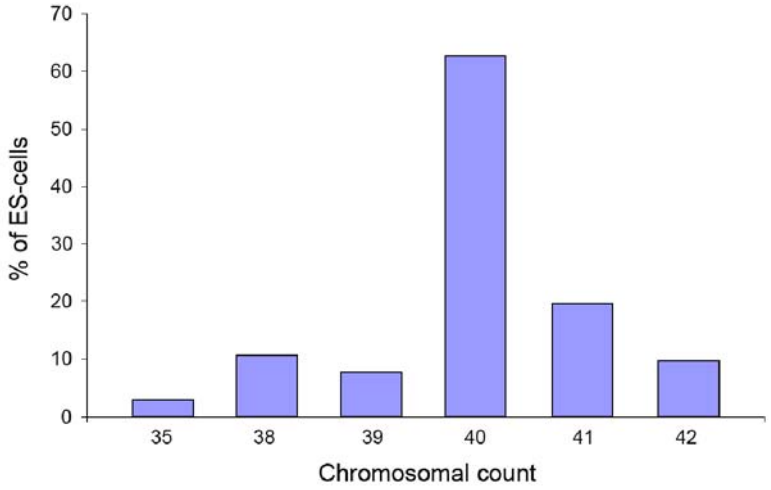

Fig. 4.22 Representative graph for chromosomal number analysis of homologous recombinated ES cell clone: The karyotype measurement showing 65% of the ES cells showed 40 chromosomal count.

The karyogram analysis showed of 60-70% euploid cells, which indicated the recombinated ES cells were in good condition and could be used for the microinjection (Longo, Bygrave et al. 1997; Suzuki, Kamada et al. 1997).

4.10 Generation of chimeric animals

For the generation of CB2-eCFP chimeras, ten homologous recombinant ES cell clones were microinjected all together 26 times in blastocyts obtained from CD1 or C57BL/6J mice. The microinjections were performed by Juergen Schmidt and Charlotte Schick in the house of experimental therapy in Bonn (Tab. 4.3).

Construct	ES cell origin	Clones / No of injections	Germline transmission
CB2-eCFP	R1	3/6	1
CB2-eGFP	R1	-----	----
CB2-eCFP	MPI	4/8	
CB2-eGFP	MPI	3/12	----
		∑10/26	1

Tab. 4.3 Microinjections of the CB2-eCFP and CB2-eGFP knock-in constructs: CB2-eCFP or CB2-eGFP clones were microinjected in ES cells of MPI 2 or R1 origins. In all 10, different ES cell clones were microinjected 26 times. The expected CB2-eCFP germ line transmission was seen in only one animal.

After microinjection of CB2-eCFP and CB2-eGFP ES cell clones, different chimeric animals were born. Only one expected CB2-eCFP germ line transmission was obtained from the CB2-eCFP knock-in construct (Tab. 4.3). With the very similar CB2-eGFP knock-in construct, no germ line transmission was observed.

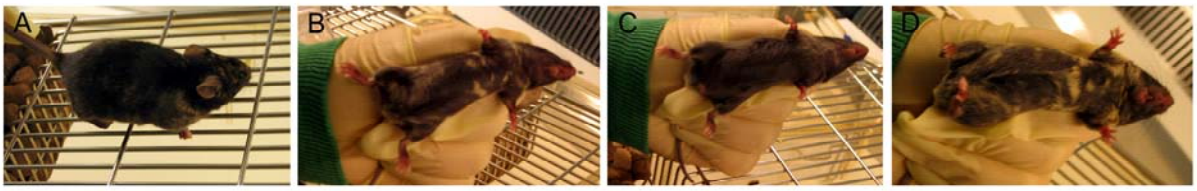

Fig. 4.23 Chimeric animals that resulted from microinjection of the CB2-eCFP MPI2 ES cell clones: (A-D)These animals exhibited a chimeric percentage ranging from 10% to 70%. These mice were obtained by microinjection of MPI 2 clones in the C57BL/6J blastocysts.

In Fig. 4.23 chimeric animals obtained from CB2-eCFP knock-in construct are shown. These animals show different chimeric percentage ranging from 5-70%. I had obtained 26 chimeric animals with CB2-eCFP knock-in construct of which 11 animals (8 male, 3 female) were of MPI2 background and 15 animals (11 male, 4 female) were of R1 background. With the similar knock-in construct of CB2-eGFP I had obtained 9 animals (6 male, 3 female) were of MPI2 background.

4.11 Germ line transmission of the *CB2-eCFP* and *CB2-eGFP* allele

Animals with a chimeric percentage more than 10% were mated to obtain germ line transmission of *CB2-eCFP* or *CB2-eGFP* allele. Chimeric animals obtained form MPI 2 ES cell line were bred with the C57BL/6J female mice (black skin) and those from R1 ES cell background with the CD1 female mice (white skin). The progenies were visually analyzed for fur color.

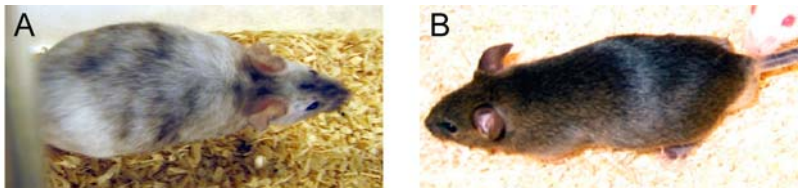

Fig. 4.24 Chimeric animals that resulted from microinjection of the CB2-eCFP R1 ES cell clones and its germ line offspring: A) This animal was obtained by microinjection of R1 clone in CD1 blastocysts. B) Germ line transmitted progeny obtained from the chimeric animal is shown.

Until now only three germ line transmissions of *CB2-eCFP-neo* allele in R1 ES cell background were obtained; two of them were found to be of wild type origin and the gene of interest was transmitted only in one animal shown in Fig. 4.24.

For the *CB2-GFP-neo* allele, three different homologous recombinated MPI 2 ES cell clones were injected into blastocysts. More than 15 chimeric animals were bred to obtain germ line transmission. No germ line transmission were yet obtained with the CB2-eGFP KI construct.

4.11.1 Southern blot analysis of germ line transmission

To test the genomic integration of the construct in mice, genomic DNA from the mouse tails was isolated and digested with *Xba I.* As shown in Fig. 4.17, the homologous recombinant locus yielded two fragments of 8.7 kb and 6.4 kb whereas the wild type locus yielded only a 6.4 kb fragment.

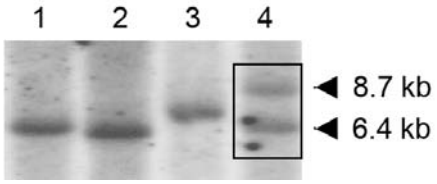

Fig. 4.25 Southern blot verification mouse tail DNA for the germ line transmission: Representative Southern blot analysis of *XbaI* digested genomic DNA from mice carrying the *CB2-CFP-neo* allele (lanes 4). Lane 1-3 indicates wild type mice.

As shown in Fig. 4.25, Southern blot analysis of genomic mouse tail DNA showed animal with the germ line transmission (lane 4), while the other animals only exhibited the wild type fragment. The heterozygous CB2-eCFP mouse was further bred to obtain homozygous animals.

4.12 PGK-Cre recombination

The heterozygous knock-in mice generated contained floxed neomycin cassette. This floxed cassette is directly located after the CB2-eCFP fusion protein and can

influence the stability and the expression of nearby genes. Thus to remove this, homozygous mice containing the *CB2-eCFP-neo* alleles were further bred with PGK-Cre mice (Lallemand, Luria et al. 1998). PGK-Cre mice showed a ubiquitous expression of Cre recombinase, which acts on the loxP sequences within the *CB2-eCFP* gene locus. After breeding CB2-eCFP homozygous knock-in animals with PGK-Cre mice, the neomycin cassette was ubiquitously removed in the resulting offspring, which were tested positive for the PGK-Cre sequence. Mice were genotyped by PCR. Heterozygous mice containing only *CB2-eCFP* allele were further bred to obtain homozygous mice.

Genotype	**Total**		**Males**		**Females**	
	Number	%	Total	% of males	Total	% of females
WT	24	30.7	13	33.3	13	33.3
Heterozygous	36	46.1	17	43.5	17	48.7
Homozygous	18	23	9	23	9	23
Total	78		39	50	39	50

Tab. 4.4 Representative table for generation of CB2-eCFP homozygous knock-in mice: Heterozygous mice were paired to generate homozygous mice.

The mating chart of 4 heterozygous male mice with the 7 heterozygous female mice is summerized in Tab. 4.4. The percentage of male and female offsprings obtained after the pairing was found to be equal. The mating resulted in 23% of homozygous animals and about 46% of heterozygous animals. This indicates that transmission of knock-in gene in these mice followed Mendelian inheritance.

4.13 Genotyping by CB2-eCFP mice with PCR

Southern blot determination is time consuming, so to determine the genotype of the mice quick and easy PCR genotyping method was established (Section 1.1.16). The genomic DNA was obtained from tail biopsies (Truett, Heeger et al. 2000). The common forward primer binds in the coding region of the CB2 receptor whereas the wild type reverse primer binds at the 3´ region outside the coding region of the wild type locus and in the coding region of the eCFP or eGFP in knock-in locus (Fig. 4.26).

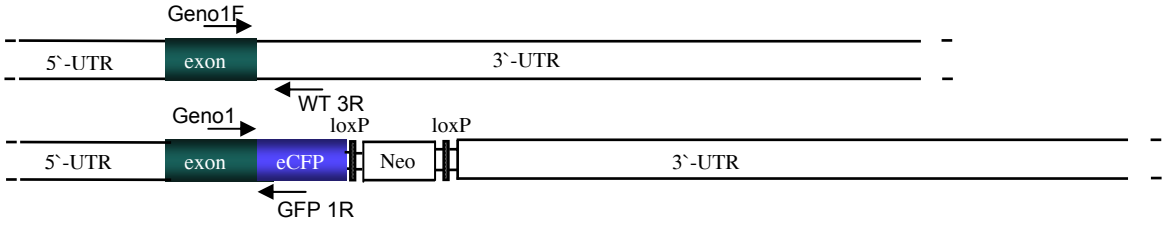

Fig. 4.26 Schematic diagram showing an allele specific genotyping strategy for the CB2-eCFP mice: Forward common primer (Geno 1F) binds in the coding region of CB2 and wild type primer (WT 3R) binds in the 3´ UTR. Knock-in primer (GFP 1R) binds in the eCFP coding region.

The PCR analysis resulted in the amplification of different fragments for the (600 bp) and the *CB2-CFP-neo* allele (390 bp). PCR products were analyzed by gel electrophoresis as shown in Fig. 4.27. As expected the *CB2-CFP-neo* heterozygous locus yielded fragments of 600 bp and 390 bp and homozygous *CB2-CFP-neo* locus yielded only a 390 bp fragment. Furthermore mice were tested for the presence of the PGK-Cre locus and for absence of neomycin by PCR.

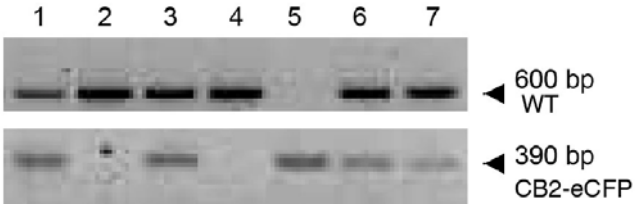

Fig. 4.27 Genotyping of *CB2-eCFP* knock-in animals: PCR analysis of genomic DNA from CB2-eCFP knock-in mice after breeding to PGK-Cre. Lane 2, 4 indicate wild type mice, lanes 1, 3, 6, 7 indicate heterozygous mice and lane 5 indicates homozygous mice.

4.13.1 Southern verification for the deletion of neomycin gene

After the breeding with the PGK-Cre mice, floxed neomycin cassette was removed which was verified by Southern blot analysis with the same DIG probe used for Southern screening of ES cells. The deleted locus will result in 7.1 kb fragment after digestion with *Xba I* enzyme. Other GFP binding DIG probe will bind to the CB2-eCFP region and should yield the same fragment of 7.1 kb size. Thus, genomic tail DNA from the offspring of CB2-eCFP knock-in mice and PGK-Cre mice was digested with *XbaI.* The Southern blots were screened with the DIG probe used previously for ES cell screening and GFP binding DIG probe.

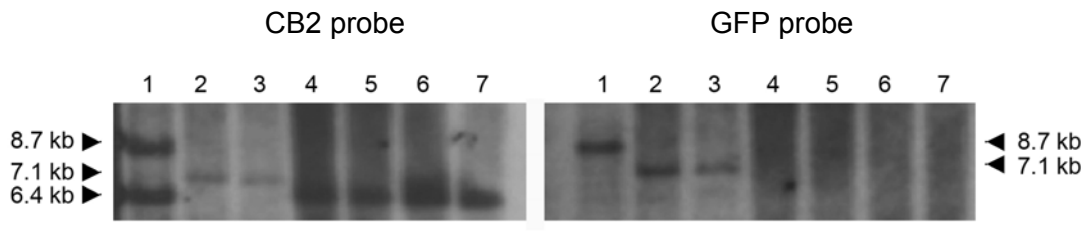

Fig. 4.28: Southern analysis of *CB2-eCFP* knock-in mice: Southern blot analysis of genomic tail DNA from CB2-eCFP knock-in mice after breeding to PGK-Cre where lane 4-7 indicates wild type mice, lane1 indicates heterozygous *CB2-CFP-neo* locus and lane 2 and 3 indicate homozygous *CB2-CFP* locus after deletion of neo. Probed with CB2 probe (left) and GFP probe (right).

As shown in Fig. 4.17, the homologous recombinant *CB2-eCFP-neo* allele yielded two fragments of 8.7 kb and 6.4 kb, whereas the wild type locus yielded only a 6.4 kb fragment. The homologous recombinant *CB2-eCFP* locus yielded a single fragment of 7.1 kb size. The results obtained were also verified with DIG probe binding in CFP coding region (Fig. 4.28). The results obtained from Southern blot analysis were in line with the PCR genotyping results. The CB2-eCFP knock-in mouse line was established using these homozygous mice as founders.

4.14 Expression analysis of homologous CB2-eCFP mice

After obtaining CB2-eCFP knock-in mice, the protein expression and the fluorescence were investigated. In order to visualize the eCFP tagged fluorescent CB2 receptor, the homozygous CB2-eCFP mice were analyzed macroscopically, microscopically, by FACS analysis, by protein isolation and at mRNA expression level.

4.14.1 Macroscopic visualization of CB2-eCFP

The CB2 receptor is primarily expressed in the immune system. It is highly expressed in organs like the spleen, thymus and lymph nodes. Thus the spleen from the homozygous CB2-eCFP knock-in mice was removed and washed with PBS solution. Expression of CB2-eCFP protein was visualized directly in fresh organ by Leica macroscope. eCFP fluorescence can be also visualized by using GFP filter set since the excitation and emission curve overlap with each other. Red filter observations were considered as a control for specific fluorescence (Fig. 4.29).

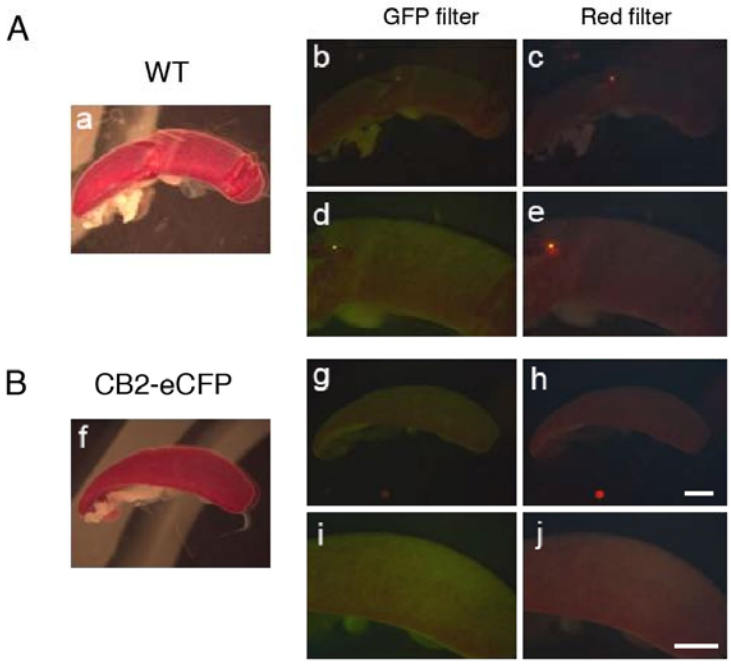

Fig. 4.29 Macroscopic visualization of spleen from CB2-eCFP and wild type mice: No specific eCFP fluorescence was seen in the spleen isolated from the homozygous mice (B) as compared to the wild type mice (A). Images a, b, g and h were taken at 1x magnification and d, e, i and j were taken at 2.5x magnification.

No specific fluorescence could be observed in spleen from CB2-eCFP homozygous animals. Organs of wild type mice showed a similar unspecific fluorescence (Fig. 4.29). Areas which showed green fluorescence also showed red fluorescence upon further observation with the red filter, indicating non specific fluorescence origin.
This result showed that at the macroscopic level, there was no difference in fluorescence between wild type control and CB2-eCFP mice, implying no expression of CB2-eCFP protein.

4.14.2 Microscopic visualization of CB2-eCFP

In order to analyze CB2-eCFP expression at cellular level, microscopic visualization of the tagged CB2 receptors was performed. Animals were perfused with PFA and then organs were soaked in sucrose solution overnight. Cryosections were made from these tissues. Organs such as spleen, lymph nodes and thymus were examined for the specific eCFP fluorescence under the fluorescent microscope Axioplan 2 imaging (Zeiss) as well as under Axiovert 40 CFL microscope (Zeiss) with specific eCFP filter set. Fig. 4.30 shows a representative spleen examination at different magnifications using a green filter for eCFP fluorescence visualization and a red filter for the non-specific fluorescence taken with Axioplan 2 imaging (Zeiss) microscope.

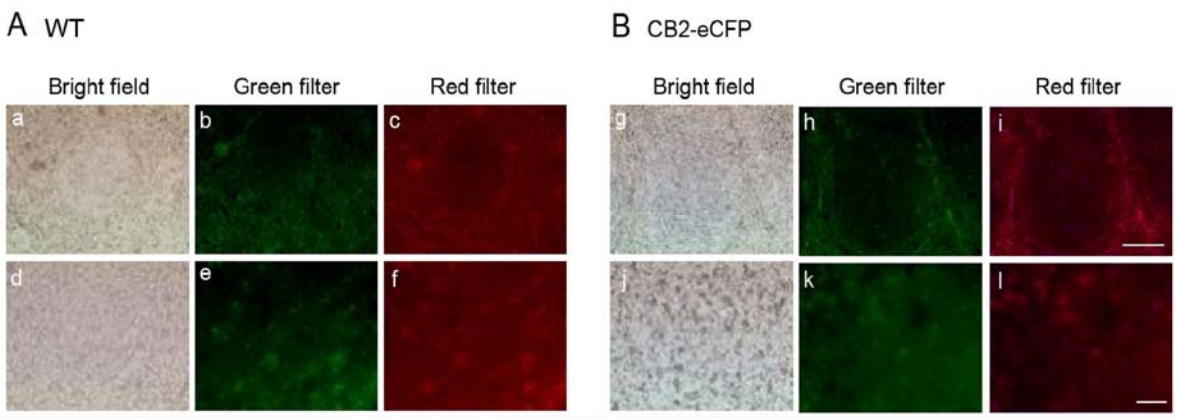

Fig. 4.30 Microscopic visualization of fluorescence in the spleen of CB2-eCFP and wild type mice: No eCFP specific fluorescence was seen in the spleen isolated from the homozygous CB2-eCFP knock-in mice (B). Images a, b, c, g, h and i were taken at 10x magnification and d, e, f, j, k and i were taken at 40x magnification. Scale bar =100 µm

As expected, wild type animals showed no significant signal for the eCFP (Fig.4.30 A). The homozygous CB2-eCFP knock-in mice also exhibited no specific eCFP fluorescence (Fig.4.30 B). In cell culture experiments with eCFP transfected cells and CB2-eCFP transfected cells can be observed under GFP filter and they do not show fluorescence when red filter is used to visualize. Comparison of the unspecific fluorescence signals using the red filter indicated that there is no difference between wild type and CB2-eCFP knock-in mice organs.

Spleen sections from wild type and CB2-eCFP knock-in homozygous animals were also visualized under the confocal microscope (Fig. 4.31).

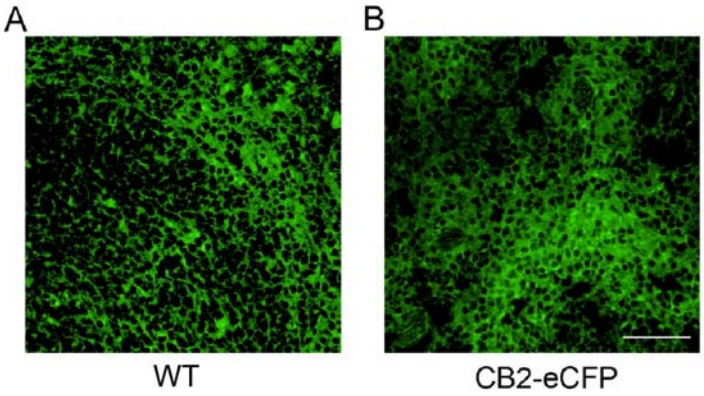

Fig. 4.31 Confocal visualization of spleens: Confocal images of a spleen of wild type (A) and CB2-CFP knock-in homozygous mice (B) under water emulsion and 40x magnification. No eCFP specific fluorescence was observed in spleen sections of knock-in mice as compared to wild type animals. However, there was a significant amount of autofluorescence observed in spleen of wild type mice. Scale bar =100 µm

However no specific fluorescence was observed in the CB2-eCFP knock-in homozygous spleen sections. Similarly no difference in thymus and lymph node sections was observed under confocal microscope.

4.14.3 FACS analysis of splenocytes from the CB2-eCFP knock-in mice

FACS analysis is more sensitive as compared to the macroscopic or microscopic analysis. I considered the possibly weak signal of the CB2-eCFP protein resulting into no microscopic detection of the CB2-eCFP protein. These cells could be detected with the FACS analysis. Thus, I analyzed cells with FACS analysis for the fluorescence. Freshly isolated splenocytes from CB2-eCFP knock-in mice were analyzed by the LSR-II FACS (BioRad) (Fig. 4.32) with a specific blue laser for eCFP protein.

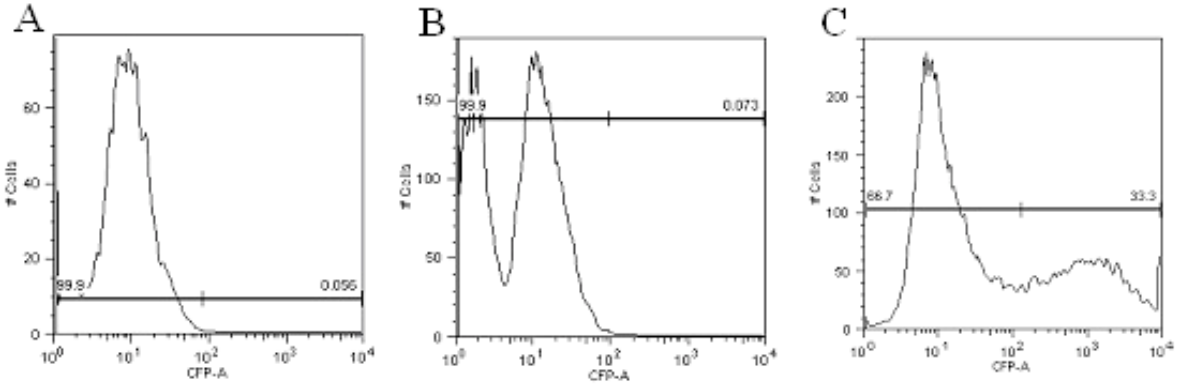

Fig. 4.32 FACS analysis of splenocytes from homozygous CB2-eCFP knock-in mice: FACS analysis of CB2-eCFP splenocytes showed no detectable eCFP positive cell population were present in spleen of homozygous CB2-eCFP animals. A) Splenocytes from wild type animals B) Splenocytes from heterozygous CB2-CFP knock-in mice C) CB2-eCFP HEK cells as positive control.

Unfortunately no specific fluorescence could be observed in the examined splenocytes (Fig 4.32,B). Similar observations were obtained when macrophages, thymus cells and lymph node cells analyzed by FACS analysis (data not shown). CB2-eCFP transfected HEK-293 cells, which were used as positive control, showed the population of the HEK-293 cells containing the fluorescent receptors (Fig 4.32,C). Wild type cells were used as a negative control (Fig 4.32,A).

4.14.4 Expression analysis of CB2-eCFP at protein level

Organs like spleen, thymus and lymph nodes from CB2-eCFP homozygous mice were lysed in protein lysis buffer and then fusion protein was immunoprecitated by using GFP antibody and detected with Western blot technique.

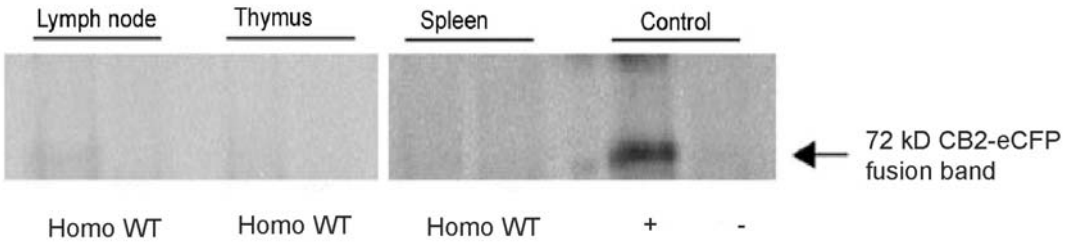

Fig. 4.33 CB2-eCFP protein expression analysis of CB2-eCFP mice: Immunoprecipitation of CB2-eCFP fusion proteins detected by GFP antibody lymph nodes, thymus and spleen from wild type (WT) and CB2-eCFP homozygous (Homo) mice respectively. CHO-K1, CB2-eCFP transfected, positive control (+) and untransfected CHO-K1 as negative control (-).

Western blot analysis showed no corresponding band for the fusion protein in the spleen, thymus and lymph nodes from CB2-eCFP knock-in homozygous animals (Fig. 4.33). Native HEK-293 cells and cells transfected with CB2-eCFP were used as positive and negative controls. A very weak band of 72 kD in lymph nodes was observed. However fluorescent expression analysis could not indicate any specific fluorescence in these organs.

Taken together, macroscopic, microscopic visualization, immuno precipitation results, and FACS analysis of CB2-eCFP expression displayed no specific signals of the fluorescence protein in the knock-in animals. Next, I wanted to determine whether the CB2-eCFP fusion transcript was expressed in these knock-in mice.

4.14.5 Detection of the CB2-eCFP fusion transcript by mRNA expression analysis.

Total RNA (tRNA) was isolated from spleen and thymus of wild type, homozygous and heterozygous CB2-eCFP knock-in mice. To avoid DNA contamination, tRNA was followed by additional DNAse digestion step. Further tRNA was analyzed by RT-PCR for expression of CB2-eCFP transcript.

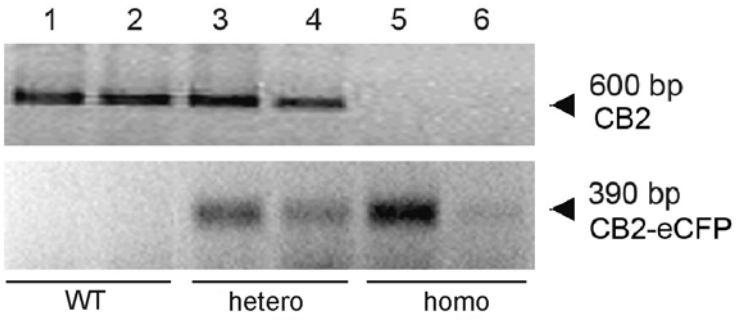

Fig. 4.34 Expression analysis of CB2-eCFP transcript: Allele specific semi quantitative RT-PCR analysis of cDNA from spleen and thymus tissue of wild type mice (WT) (lane 1,2), heterozygous (hetero) (lane 3,4) and homozygous (homo) (lane 5,6) CB2-CFP knock-in mice, respectively.

Gel electrophoresis of the RT-PCR analysis demonstrated that the CB2-CFP transcript was present in the spleen and thymus of heterozygous (Fig. 4.34, lane 3, 4) as well as in the homozygous mice in spleen and thymus (Fig. 4.34, lane 5,6). In the spleen and thymus of wild type control animals, only the CB2 transcript was observed (Fig. 4.34, lane 1, 2).

Although CB2-CFP protein was not detected in macroscopic and microscopic analysis, mRNA analysis for the expression of CB2-eCFP in homozygous and heterozygous CB2-eCFP knock-in animals using the allele specific primers revealed that the fusion transcript is present in spleen, thymus (Fig. 4.34) and in lymph nodes (data not shown) of these animals. One possibility could be the levels of CB2 are much below the detection levels. Thus models where CB2 expression is known to be highly up regulated may result in detection of CB2-eCFP protein.

The cannabinoid receptor 2 is reported to be highly up regulated in animal model systems such as, contact hypersensitivity (Karsak, Gaffal et al. 2007) and neuropathy pain model (data unpublished). Thus I used these systems where the CB2 expression was up regulated and possibly that increase in expression resulting into a detectable CB2-eCFP fluorescence.

4.14.6 Contact hypersensitivity model in CB2-eCFP knock-in mice

In the cutaneous contact hypersensitivity model, mice were challenged with the contact allergen DNFB to induce allergic response. Wild type and homozygous CB2-eCFP knock-in mice were treated with DNFB and the ear swelling was measured after the second challenge (Fig. 4.35).

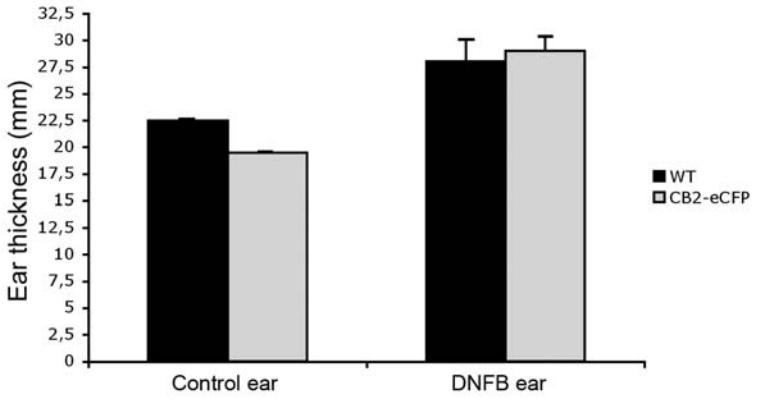

Fig. 4.35 Ear swelling in wild type and homozygous CB2-eCFP knock-in mice: Graph shows ear swelling after the second challenge with DNFB. Equal extents of ear swelling were observed in wild type (WT) and homozygous animals (CB2-eCFP).

I observed an increase in the ear swelling in wild type and CB2-eCFP knock-in mice after treatment with DNFB. The extent of ear swelling was not different in the two examined mouse strains, indicating that CB2-eCFP knock-in mice showed no altered allergic reaction in this contact hypersensitivity model. After the DNFB treatment mice were perfused with PFA and the DNFB treated ears were removed and additionally fixed with 4% PFA for 2 h. Ears were soaked in 30% sucrose solution over night before cryo sections were made and visualized for the CB2-eCFP fluorescence under Axioplan 2 imaging microscope (Zeiss).

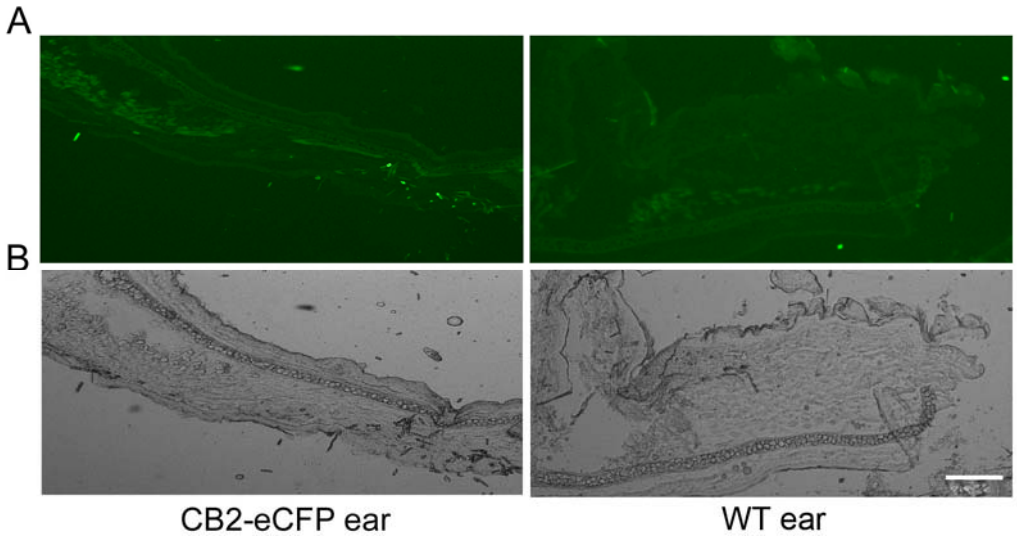

Fig. 4.36 Histological analysis of DNFB treated ears of CB2-eCFP and wild type mice: A) After the CHS was induced sections of ears of wild type and CB2-eCFP knock-in mice were observed under fluorescence microscope. B) Phase contrast images of the ears of wild type and CB2-eCFP knock-in mice. No specific fluorescence was observed in the sections of ears of homozygous animals after CHS. Scale bar =100 µm

No specific fluorescence was seen in the ears of the CB2-eCFP knock-in homozygous animals as compared to the wild type ears (Fig. 4.36).

4.14.7 Neuropathy pain model

A second known model used in our lab, where CB2 expression is up regulated, is the neuropathy pain model. In this model a neuropathic pain is induced by a partial sciatic ligation of nerve. This results in up regulation of CB2 expression in spinal cord region (data unpublished). The homologous CB2-eCFP knock-in and wild type mice were operated for a partial ligation. One week after surgery, the mice were sacrificed to examine the expression of CB2-eCFP. The spinal cord was removed and fixed with 4% PFA followed by 30% sucrose treatment before cryosections were made.

These sections were then observed for CB2-eCFP fluorescence under fluorescence microscope (Axioplan 2, Zeiss).

A punctuated green fluorescence pattern was seen (Fig. 4.37 A). Unfortunately this punctuated pattern was similar to that observed with the red filter, indicating non-specific fluorescence (Fig. 4.37 B). Moreover similar pattern was also present in wild type mice confirming the nonspecific origin (data not shown).

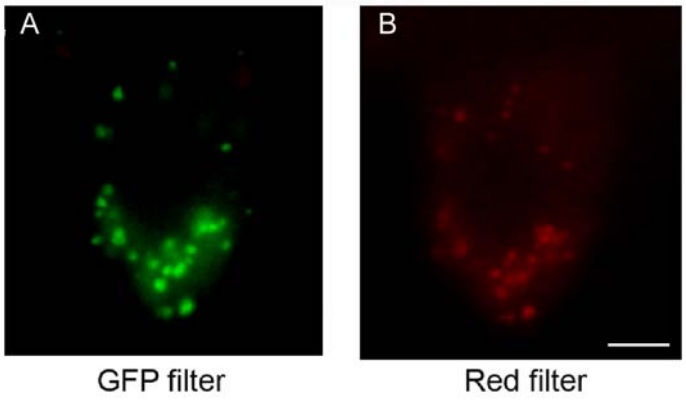

Fig. 4.37 CB2-eCFP expression in the neuropathy pain model: Spinal cord sections were analyzed by the fluorescence microscope. Spinal cord sections of 12 µm were studied with GFP (a) and red filters (b). No specific fluorescence was observed. Scale bar =50 µm

I have generated a CB2-eCFP knock-in mice and the expression of CB2-eCFP from these mice were analyzed macroscopically, microscopically, by FACS analysis and by protein immunoprecipitation. Unfortunately no protein expression was seen. However, CB2-eCFP transcript was present as detected by RT-PCR analysis. In models where CB2 expression is known to be up regulated also failed to detect the specific CB2-eCFP fluorescence.

5 Discussion

During the last decade, interest in the potential medicinal use of cannabinoid drugs has greatly increased. The endocannabinoid system performs various regulatory functions and has been implicated in a growing number of physiological roles, both in the central and peripheral nervous systems and in peripheral organs (Klein, Newton et al. 2001; Howlett, Barth et al. 2002; Mechoulam, Spatz et al. 2002; Howlett 2005).

To complement the pharmacological analysis of the cannabinoid system, our group and other researchers use a genetic approach such as targeted deletions of cannabinoid receptor genes CB1 (Ledent, Valverde et al. 1999; Zimmer, Zimmer et al. 1999; Marsicano, Wotjak et al. 2002; Robbe, Kopf et al. 2002), and CB2 (Buckley, McCoy et al. 2000) in mice.

Our group has also generated CB1-CB2 receptor double knock-out mice. Strikingly, these mice show severe wounds near metallic ear clippings (Fig. 4.1). These animals also scratch there ears more often compared to wild type animals. Cannabinoids exhibit immunomodulatory properties that influence several components of the immune-response machinery (Schatz, Lee et al. 1997; Berdyshev 2000). Moreover, previous work indicated that endocannabinoids promote wound closure in human colon injury (Wright, Rooney et al. 2005). In this study, the cannabinoid agonists, anandamide (AEA), noladin ether (NE) and arachidonylcyclopropyllamide (ACPA), showed increase in wound closure in *in vitro* scratch assay with human colonic epithelial cell lines, HT29 and DLD1. Cannabinoids have also shown to play a protective role in brain (Biegon and Joseph 1995; Panikashvili, Simeonidou et al. 2001; Mechoulam, Spatz et al. 2002; Kreutz, Koch et al. 2007), cardiac (Lagneux and Lamontagne 2001), ocular (Lalonde, Jollimore et al. 2006) ,liver (Julien, Grenard et al. 2005; Batkai, Osei-Hyiaman et al. 2007; Mallat, Teixeira-Clerc et al. 2007) injuries. These studies and our observations prompted us to address the possibility of impaired wound healing in the cannabinoid receptor double knock-out animals. To investigate the role of these receptors in wound healing, full thickness excision wound healing model was employed (Werner, Smola et al. 1994; Werner and Grose 2003). This model can be used to evaluate the ability of keratinocytes to stimulate wound healing. Keratinocytes synthesize numerous growth factors and cytokines that can influence wound healing. Keratinocytes are known to express CB1 receptors (Maccarrone, Di Rienzo et al. 2003). Both the CB1 and CB2 receptors are expressed

in normal epidermis and skin tumours of mice and humans (Casanova, Blazquez et al. 2003), as well as, shown to be expressed on sensory nerve fibres and adnexal structures in human skin (Stander, Schmelz et al. 2005). However, CB2 expression in these cells has been also debated (Ibrahim, Porreca et al. 2005; Oka, Wakui et al. 2006). Absence of these receptors in knock-out animals may lead to imbalance in regulation of endocannabinoid system and thus may result in wound impairment phenoytype in knock-out animals.

Wound healing is a natural process which involves regeneration of dermal and epidermal tissue. This complex process can be artificially categorized into three overlapping phases inflammatory, proliferative, and remodelling phase (Stadelmann, Digenis et al. 1998; Stadelmann, Digenis et al. 1998; Iba, Shibata et al. 2004). In mice inflammatory phase occurs within first 3 days where invasion of inflammatory cells, secretion of various inflammatory cytokines around site of injury takes place (Werner and Grose 2003). This is followed by proliferating phase (3-5 days) and finally leading to remodelling phase (5 day onwards) where activation of matrix metalloproteases (Pilcher, Wang et al. 1999; Wilson, Ouellette et al. 1999), secretion of various growth factors, migration of fibroblasts and keratinocytes, angiogenesis, wound contraction and finally remodelling of the scar tissue takes place (Martin 1997). Cannabinoid receptors and cannabinoids has been shown to influence migration of various immune related cells (Schatz, Lee et al. 1997; Berdyshev 2000; Jorda, Verbakel et al. 2002; Gokoh, Kishimoto et al. 2005; Ghosh, Preet et al. 2006). Thus I expected altered immune modulatory response in knock-out animals which might lead to observed phenotype. Therefore, I analyzed the wound healing in these mice on 5^{th} day and 13^{th} day. These double knock-out animals were of mixed genetic backgrounds of C57BL/6J and 129/Sv. I had also included single knock-out animals of C57BL/6J background with their control animals of C57BL/6J background.

However, no change in the wound healing properties in cannabinoid knock-out animals as compared to the wild type control animals was observed (Tab. 4.1 and Fig. 4.2), indicating that observed lesions are not due to impaired wound healing.

The phenotype was also lost when pure brass tags were used instead of high nickel tags. Alterations in tissue architecture, infiltration of mast cells, swelling of regional preauricular and submental lymph nodes in double knock-out mice showing wounds hinted towards an altered allergic response in these animals thus a cutaneous hypersensitivity model was further investigated (Karsak, Gaffal et al. 2007).

5.1 Role of cannabinoid system in contact hypersensitivity (CHS)

In this model system, we examined the possible involvement of cannabinoid receptors and its ligands in DNFB induced hypersensitivity. We found that upon repeated treatment with allergen DNFB, which induces a specific T-cell mediated allergic response, resulted in a remarked increase in the ear swelling in CB1/CB2 double knock-out mice (Fig. 4.3 A). Upon further investigations, we noted similar ear swellings were also observed in CB1 and CB2 single knock-outs (Fig. 4.3 B). This suggests a nonredundant role for each cannabinoid receptor in the allergic response to DNFB. This would also suggest that milder response originating from ear tags was only observed in mice lacking both receptors. The genetic blockade of the cannabinoid receptors resulted in allergic response. Further we examined the effect of pharmacological blockade using cannabinoid receptor antagonists on wild type mice after inducing DNFB induced CHS. We found upon subcutaneous treatment with these antagonists ear swelling was increased (Fig. 4.3 C). This further supports our assumption that endocannabinoid system is involved in the DNFB induced CHS. Studies by Ueda et al. reported effects of the CB2 receptor antagonists JTE-907 and SR144528 upon repeated topical application of DNFB on BALB/c female mice ear provoked ear swelling from 24 h after the 2nd application. These authors also reported significant and dose dependent inhibition of ear swelling upon acute oral administration of cannabinoid antagonists once a day for 6 days before and 1 and 23 h after the 4th exposure to DNFB (Ueda, Miyagawa et al. 2005). This suggests that CB2 antagonism may be initially beneficial but detrimental upon chronic blockade.

Thus both the pharmacological blockade as well as genetic blockade proved the role of these individual receptors in contact hypersensitivity.

We observed upregulation of CB2 mRNA after DNFB treatment (Karsak, Gaffal et al. 2007). Similar increase in CB2 mRNA was also observed after DNFB treatment in mouse ears by Ueda et al. supporting our observations (Ueda, Miyagawa et al. 2005; Ueda, Miyagawa et al. 2007). We also observed increase in the AEA and 2-AG levels after DNFB treatment in wild type and double knock-out animals which was more pronounced in later (Karsak, Gaffal et al. 2007). Similar increase in the endocannabinoid 2-AG was observed in another model system where 12-O-tetradecanoylphorbol 13-acetate (TPA) was used to induced acute inflammation in mouse ear (Oka, Wakui et al. 2006). These observations strongly indicate that endocannabinoid system is regulated in case of inflammation. It is possible,

therefore, that the involvement of the cannabinoid system is a common feature of inflammatory reactions.

Several investigators demonstrated that cannabinoids and the CB2 receptor exert suppressive effects on the inflammatory reactions and immune responses (Gokoh, Kishimoto et al. 2005; Gokoh, Kishimoto et al. 2005; Kishimoto, Muramatsu et al. 2005). For example, in rat peripherally administered cannabinoids inhibited carrageenan-induced edema, thermal hyperalgesia, and decrease in capsaicin induced edema and plasma extravazation (Richardson, Kilo et al. 1998).

In this study we also found that the topical and subcutaneous application of the Δ^9-THC reduced ear swellings induced by DNFB treatment (Fig. 4.4). Similarly ear swelling induced by TPA was also reduced upon Δ^9-THC treatment (Oka, Yanagimoto et al. 2005). Together these studies support the idea that the activation of endocannabinoid system may function to dampen the inflammatory response. In contrast, the specific CB2 receptor agonist HU-308 showed either no efficacy after s.c. application (Fig. 4.4 A) or even increased the allergic response after topical application (Fig. 4. 4 B). It has recently been shown that the CB2 receptor inverse agonist Sch.336 inhibits leukocyte chemotaxis and thus, HU-308 administration to the inflamed ear may have further increased leukocyte infiltration leading to more pronounced inflammatory response and might have resulted in increase in swelling (Lunn, Fine et al. 2006).

This opens up new avenues to treat the allergic diseases in humans like allergic contact dermatitis, which affects about 5% of men and 11% of woman in industrialized countries and is one of the leading causes for occupational diseases (Karsak, Gaffal et al. 2007). CHS is an inflammatory skin disorder associated with an itch. It has been reported in the human clinical studies that topical endocannabinoid application causes decrease in severity of itch (Szepietowski, Szepietowski et al. 2005; Stander, Reinhardt et al. 2006). To study exact mechanism of these processes and the role of cannabinoid receptors in *in vivo* system, it would be helpful to have mice model where distribution of these receptors can be easily analyzed.

However, we and other colleagues commonly encounter non- specific CB2 immuno-staining using cannabinoid receptor knock-out animals due to the scarcity of commercially available CB2 antibodies with substantial and/or authentic immunoreactivity. In addition to this problem, when compared to the relatively high expression of CB1 in the brain (≥ 1 pmol/mg) (Abood, Ditto et al. 1997), CB2

expression in immune cells or immune tissues is more moderate (10–300 fmol/mg (Gonsiorek, Fan et al. 2007). Thus, to overcome the technical difficulties in CB2 receptor detection, I wanted to generate a knock-in mouse strain where the CB2 receptor is tagged with the eCFP or eGFP protein, so that the CB2 receptor can be easily visualized and well studied.

Here, I report the generation of a novel CB2-eCFP and CB2-eGFP knock-in reporter mouse, which was aimed to allow the identification and isolation of viable fluorescent tagged CB2 receptor expressing cells *in vivo* and *in vitro*. Live cell observation potentiates a new type of experiment not previously possible using conventional techniques in which cells were required to be fixed prior to the visualization. This mouse would represent a useful tool to study various pathological conditions, where CB2 is involved. In addition, this fluorescent reporter system will also aid studies to understand the role of CB2 receptors in various tissues where the role of CB2 is still unknown or need to be elucidated. Therefore, I wanted to generate the tagged CB2 receptors, characterize them in *in vitro* and based on this generate knock-in mice expressing similar fusion.

5.2 Generation of fluorescent tagged CB2 knock-in mice

To allow direct visualization of the CB2 receptors, in this work eGFP and eCFP fluorescent tagged CB2 receptor were generated. Such fusion proteins are widely used to study protein trafficking (Lippincott-Schwartz and Smith 1997), and their usefulness is amply demonstrated for GPCRs (Kallal and Benovic 2000; Daly and McGrath 2003).

Expression of functional cannabinoid receptor 2 with C-terminal eGFP fusion has been reported in bone marrow and in the myeloid (32D/G-CSF-R) cells. The functionality of CB2-eGFP fusion in these cells was validated by assaying 2-AG induced transwell migration (Jorda, Lowenberg et al. 2003; Alberich Jorda, Rayman et al. 2004). Similarly, in neuroblastoma cells, C-terminal fusions with cannabinoid receptors (FLAG-CB1-IRES-EGFP and FLAG-CB2-IRES-EGFP retroviral construct) were successfully used in cAMP assay (Ishii and Chun 2002). Additionally, it has been shown that cannabinoid receptor 1 with similar C-terminal GFP fusion undergoes constitutive internalization and trafficking (Leterrier, Bonnard et al. 2004; Leterrier, Laine et al. 2006). Thus, I expected an unaltered functionality of the CB2 receptor after C-terminal fusion with eGFP or eCFP proteins. However, previous

studies with other receptors have reported that the C-terminal is important for receptor trafficking (Smyth, Austin et al. 2000). The truncation of the C-terminal may alter the tertiary structure of the receptor in a manner that changes its cellular trafficking, or specific determinants of the receptor sequestration. For example, mutation of a dileucine motif located in the C-terminal of the adrenergic receptor inhibits agonist-induced sequestration (Gabilondo, Hegler et al. 1997), but does not alter agonist-induced internalization of the thromboxane receptor (Parent, Labrecque et al. 1999; Parent, Labrecque et al. 2001). Thus, it is important to characterize the generated fusion protein.

In this study, I have established an *in vitro* expression system, based on C-terminal GFP and CFP fusion of CB2 receptors expressed in CHO-K1, HEK-293 and HeLa cell lines. Since CHO-K1 cells do not express endogenous CB2 receptors (Bouaboula, Desnoyer et al. 1999), this cell line have been commonly used for studying overexpressed cannabinoid receptors along with the CB2 expressing HEK-293 (NM_001841) and HeLa cell lines. This indicates the presence of a functional signalling cascade in the downstream pathways of the CB2 including several G protein alpha subunits (G alpha i/o) that are important for CB2 mediated response resulting in adenylate cyclase inhibition and phospholipase C activation. Thus these cells can be used as model system. Microscopic examination revealed predominant intracellular as well as plasma membrane localization of the CB2-eGFP or CB2-eCFP receptors (Fig. 4.10). Similar fluorescent expression pattern was observed by us (data unpublished) and by others with eGFP tagged CB1 receptor (Leterrier, Bonnard et al. 2004; Leterrier, Laine et al. 2006). Leterrier et al. have also reported that in CB1-eGFP HEK cells co-overexpressing angiotensin II AT1A and somatostatin SSTR2 receptors showed the same levels of transfected receptors with a predominant plasma membrane localization (Miserey-Lenkei, Lenkei et al. 2001), indicating that overexpression was not the cause for intracellular receptor accumulation.

A similar observation, of predominant intracellular and weak plasma membrane expression, was obtained in cell lines other than HEK-293, such as CHO-K1 and HeLa cells (Fig 4.10). Using a confocal microscope, it was observed that these receptors were also colocalized with the plasma membrane marker transferrin receptors (Fig 4.11 A). Transferrin receptor is found to be localized within lipid rafts and CB1 receptor has been shown to colocalize with it (Leterrier, Bonnard et al.

2004). It would be therefore interesting to study if CB2 receptor is also present within the lipid rafts. However, recently Bari et al. showed that in immune cells and neuronal cells only CB1 receptor signalling is controlled by lipid rafts, but not that of CB2 receptor (Bari, Spagnuolo et al. 2006; DeMorrow, Glaser et al. 2007). In order to find the origin of the strong intracellular signal different organelle markers were used. Only with α-giantin, which is a golgi marker, a complete interacellular Co-localization was observed (Fig. 4.11 B). This confirmed juxtanuclear subcellular distribution of CB2-eCFP fusion protein within golgi compartment. Cannabinoid receptors are known to undergo glycosylation (Song and Howlett 1995; Gonsiorek, Fan et al. 2007), which predominantly takes place in golgi apparatus. Golgi is also the site of receptor dephosphorylation and/or dissociation of the receptor/ligand/-arrestin complex to deliver a resensitized receptor to the cell surface for various other GPCRs (Zhang, Ferguson et al. 1996; Cornea, Janovick et al. 1999; Anborgh, Seachrist et al. 2000). Thus, it is not surprising that CB2 receptors are highly colocalized with a golgi marker.

Further, I wanted to detect the expression of intact fusion protein in this overexpression system. Theoretical calculated CB2 size is 45 kD and that of the fused eCFP or eGFP fluorescent proteins is 27 kD, thus fusion should result in CB2-eCFP or CB2-eGFP band of 45 kD + 27 kD that is of 72 kD size. I used anti-GFP antibody (Toyota, Shimamura et al. 2002; Gupta, Proia et al. 2007; Tsang, Chan et al. 2007) to test whether the complete CB2-fusion protein is expressed in cell culture system. As expected the anti-GFP antibody recognized a major diffuse 72 KD protein and an additional but defined 27 kD protein in the CB2-transfected (but not parental) CHO cells (Fig. 4.19). The appearance and size of these proteins was consistent with the predicted size for the C-terminal fusion for the CB2. Additionally, the faint 27 kD band may be due to the degradation of the fusion receptor since the band migrates at the similar distance to that expected for native GFP protein (Fig. 4.9).
The major diffuse appearance of the 72 kD receptor protein is consistent with the migration patterns of a glycoprotein (Hipkin, Sanchez-Yague et al. 1992; Gu and Schonbrunn 1997). The classification of CB2 as a glycoprotein was verified by its successful purification with wheat germ agglutinin chromatography prior to Western blot analysis (Gonsiorek, Fan et al. 2007). A minor band corresponding to a molecular weight of approximately 70 kD was observed, which could represent a

degraded receptor or another form of the receptor. Supporting observations were reported in studies by Carayon et al. and Gonsiorek et al. with transfected human HA-tagged CB2 receptor (Carayon, Marchand et al. 1998; Gonsiorek, Fan et al. 2007).

Next, I have also attempted to detect the fusion protein by using anti-CB2 antibody (Cayman chemical) for the re-verification of presence of 72 kD CB2 fusion protein. I had used spleen and brain tissue lysates from CB2 knock-out animal as negative control. However, I found a nonspecific CB2 band which was even present in protein lysates from brain as well as from spleen of CB2 knock-out mice (data not shown) showing nonspecificity of the CB2 antibody. Similar unsuccessful CB2 receptor detection attempts were also reported by a study in which various anti-CB2 antibodies (Calbiochem 209552 and 209554, ABR PA1–744 and PA1–746, Alexis) were tested using a panel of recombinant and tumour cell lines. The immunoreactive protein(s) were either too small or too large and/or were equally evident in samples from cells that do express CB2 (Gonsiorek, Fan et al. 2007). In this study immunoreactive bands were quite sharp, inconsistent with expected CB2 size (Hipkin, Sanchez-Yague et al. 1992; Gu and Schonbrunn 1997; Hipkin, Friedman et al. 1997). Taken together, these data indicate that CB2 antibodies are less than optimal for the immunodetection of authentic CB2 receptor (Gonsiorek, Fan et al. 2007).

After verifying the correct size of the fusion protein, I wanted to compare the functionality of the fusion protein to that of the native CB2 protein. I used CB2 receptor downstream signalling Erk-MAPK assay and internalization experiments to examine functionality of CB2 fused proteins.

MAP kinases, also known as extracellular signal-regulated kinases (Erks), act as an integration point for multiple biochemical signals, and are involved in a wide variety of cellular processes such as proliferation (Moniz, Verissimo et al. 2007; Wang, Lu et al. 2007), differentiation (Matsumoto, Hatanaka et al. 2006; Ge, Xiao et al. 2007), transcription regulation (Fitsialos, Chassot et al. 2007; Salim, Standifer et al. 2007) development (Fata, Mori et al. 2007; Scholl, Dumesic et al. 2007) and immunomodulation (Zhao, He et al. 2005). Many studies showed that the Erk-MAPK pathway is activated upon cannabinoid agonist stimulations mediated by both CB1 (Rubino, Vigano et al. 2006; Corbille, Valjent et al. 2007) and CB2 receptors (Bouaboula, Poinot-Chazel et al. 1996; Bouaboula, Dussossoy et al. 1999;

Shoemaker, Ruckle et al. 2005).

I compared the extent of agonist dependent phosphorylation of Erk-MAPK signalling pathway using CB2-eCFP and CB2 expression construct. I had also observed HU-308 concentration dependent Erk-MAPK´s activation in CB2 and CB2-eCFP tagged receptors (Fig. 4.13). Similar concentration dependent Erk-MAPK activation was observed by Shoemacker et al. in CB2 expressing CHO cells with cannabinoid agonist, CP55,940 (Shoemaker, Ruckle et al. 2005). I also studied the time dependent Erk-MAPK phosphorylation (Fig. 4.12) which was similar to that reported by Bouaboula et al. (Bouaboula, Poinot-Chazel et al. 1996). On the other hand, co-incubation with CB2 receptor antagonist AM-630 showed an equal decrease in Erk-MAPK activation state in both native and fused cells (Fig. 4.14). Thus the fusion protein showed as expected similar downstream MAPK signalling response.

After determining the unaltered functionality in downstream MAPK signalling, I wanted to observe internalization of the CB2-eCFP receptors. Compared to the large amount of information that has been gathered regarding the mechanisms of endocytosis and downregulation of other GPCRs, the knowledge on the routes and mechanisms of cannabinoid receptor endocytosis is still limited. Similar to that observed in case of other GPCRs (Ferguson 2001), CB1 is shown to be desensitized/internalized after binding with the ligand and again after the dephosphorylation step it can be trafficked back to the cellular membrane (Hsieh, Brown et al. 1999; Leterrier, Bonnard et al. 2004; Leterrier, Laine et al. 2006). This regulates the availability of the receptor on the membrane and hence the receptor-mediated action is tightly regulated. It has been shown that CB1 receptors undergo rapid internalization after activation with various cannabinoids like WIN 55,940, CP 55,940, HU-210. (Hsieh, Brown et al. 1999; Jin, Brown et al. 1999; Roche, Bounds et al. 1999; Coutts, Anavi-Goffer et al. 2001; Berghuis, Rajnicek et al. 2007). Also for the human CB2 receptor, Ser 352 phosphorylation dependent internalization has been put forth (Bouaboula, Desnoyer et al. 1999; Bouaboula, Dussossoy et al. 1999). However, the exact mechanisms underlying these phenomena have not yet been elucidated.

I studied in CB2-CFP expressing CHO-K1 cells, effects on internalization upon treatment with the cannabinoid receptor agonist HU-308. These cells showed internalization upon incubation with HU-308 and this can be reversed by the use of the cannabinoid receptor 2 antagonist AM-630 (Fig. 4.15). However, I could not

observe a rapid internalization in CHO-K1 or HEK-293 cells as reported for CB1 receptor internalization in AtT20 (Hsieh, Brown et al. 1999) and HEK-293 cells (Leterrier, Bonnard et al. 2004). Similar observations with slow internalization of CB2 receptors were also made in Prof. Ken Mackies lab with CB2 transfected HEK-293 cells or CHO-K1 cells (personal communication). These differences in the CB1 and CB2 receptor internalization could be receptor subtype specific and cell type dependant. Recently, developed commercial CB2 Redistribution® assay (BioImage Inc., Dec. 2007) employs a similar CB2 fusion with eGFP protein using a human osteosarcoma U2OS cell line (BioImage product). The authors of this assay used relatively long stimulation period for the internalization (1 h) further supporting my observations of slower internalization of CB2 receptors. In studies with human CB2-myc tagged receptor, the authors also incubated CHO cells for relatively long time (1-3 h) with agonists before investigating internalization by using FACS analysis (Bouaboula, Dussossoy et al. 1999). We can therefore conclude that CB2 receptor is not rapidly internalized as compared to that of CB1 receptor.

Thus in summary, I showed that my *in vitro* expression system expressed intact CB2-eCFP tagged protein. The fused receptors showed an equal extent of Erk-MAPK phosphorylation upon an agonist and antagonist treatment to that of CB2 receptors. Plasma membrane and intracellular CB2-eCFP fluorescent expression on was similar to that of reported expression pattern of CB1 receptors. The CB2-eCFP receptor undergoes agonist dependent internalization and co-incubation with CB2 receptor antagonist reversed this effect. Thus C-terminal tagging resulted into functional CB2 receptor, which may lead to a marker for microscopic visualization of cells and for studies involving this receptor. For example small molecules and the newly identified compounds can be easily screened for their efficacies using this system.

After confirming unaltered functionality in C-terminal tagged CB2 receptor, a similar knock-in constructs for CB2-eCFP and CB2-eGFP were generated (Fig. 4.19). I have used a homololougous 2.5 kb short arm of 5´ UTR sequence of CB2 sequence and a long arm of 6.4 kb of 3´ UTR region of CB2 for the homologous recombination in this construct. I kept the C-terminal fusion of the CB2 protein with eCFP or eGFP exactly identical to that I used for the cell culture studies.

After transfection of ES cells with the target construct CB2-eCFP and CB2-eGFP (Tab. 4.2) about 10% homologous recombinated clones were found. This frequency is relatively high as compared to the reported frequency (1-3%) for homologous

recombination (Capecchi 1989). Studies by Thomas and Capecchi have suggested an exponential relationship between target homology and targeting frequency with insertion and replacement vectors (Thomas and Capecchi 1987). However, another study observed a linear relationship between the length of homology and the targeting frequency (Shulman, Nissen et al. 1990). Although it is difficult to compare the results of the above experiments directly, the discrepancy might arise from a difference in the targeted genomic regions.

The amount of ES cell contribution to chimeric animal is largely dependent on the quality of cell line and can vary significantly between individual clones. It is also dependent on the genetic background of host embryo (Hogen, Beddington et al. 1994). Thus I had used 2 different ES cell origins as well as different positively recombinated ES cell clones for microinjection (Tab. 4.3).

I had obtained different chimeras with the R1 and MPI2 ES cell backgrounds in CD1 and C57Bl/6J animals respectively. The percentage of chimeras was in range of 5-70%, which shows that the ES cells used did not get effectively into every tissue. Inline with these observations, only in one chimeric animal with R1 ES cell background, CB2-eCFP germ line transmission was observed. Even in this chimeric animal the germ line transmission rate was very low. Only three germ line transmissions per 120 progenies were obtained. Out of these three germ line transmissions only one animal contained the desired gene of interest. Although majority of founders transmit the transgene to 50% of their offsprings, approximately 20-30% of the founders mosaics transmit the transgene at a lower frequency to 5-10% or not at all (Wilkie, Brinster et al. 1986; Longo, Bygrave et al. 1997; Suzuki, Kamada et al. 1997). It is known that in inbred mouse strains, such as C57BL/6J, ES cell lines colonize extensively, but in outbred strains such as CD1, ES cell poorly colonize (Zimmer 1992). However, until now, I had not obtained any other germ line transmission with the CB2-eGFP or CB2-eCFP chimeric animals. One possible reason for this could be that ES cells could have not colonized properly in mice strains.

To avoid possible influence of neomycin gene in knock-in mice containing Cnr2-eCFP-neo allele, these mice were paired with the transgenic mouse strain with early and uniform expression of the Cre site-specific recombinase. In this strain, PGK-Cre^{m}, the early acting PGK-1 promoter drives Cre, but, probably due to cis effects at the integration site, the recombinase is under dominant maternal control (Lallemand,

Luria et al. 1998). This resulted in the deletion of neomycin gene, which was verified using PCR and Southern blot analysis (Fig. 4.25, Fig. 4.27). Obtained heterozygous animals were further paired to generate homozygous animals. The transmission of the knock-in gene followed proper Mendelian population distribution (Tab. 4.5).

5.3 Expression analysis of CB2-eCFP knock-in mice

The generated knock-in mice were further analyzed for the expression of fusion proteins. Based on initial in situ hybridization studies, it was apparent that CB2 has a rather defined expression in peripheral immune cells and multiple lymphoid organs. CB2 mRNA is found in spleen, tonsils, bone marrow, mast cells, peripheral blood leukocytes, and a variety of hemopoietic cell lines, including the myeloid cell line U937 and HL-60 cells. Thus, I analyzed these tissues for CB2-eCFP fluorescence. I had used different fluorescent microscopes and confocal microscopes for visualization of tissue sections to rule out instrumental error or due to use of GFP filter set for visualization of eCFP. However, I could not observe specific fluorescence over the autofluorescence exhibited by these organs (Fig. 4.30-31).

Autofluorescence spectra are generally broad and encompass most of the visible spectral range, overlapping the emission wavelengths of green fluorescence protein and its many derivatives like eGFP and eCFP (Billinton and Knight 2001). When measuring fluorescence, the presence of autofluorescence often leads to low signal-to-noise ratios, and can even fail to detect or visualize at all. Autofluorescence also reduce the contrast and clarity of fluorescent-labelled structures. Natural fluorescence in organs is due in large part to substances like flavins, lipofuscins (Schnell, Staines et al. 1999), elastin (Deyl, Macek et al. 1980), collagens and porphyrins in organs (Svanberg, Kjellen et al. 1986). Moreover, autofluorescence can also arise due to cellular media or type of fixative method used (Stewart, Villasmil et al. 2007). Thus, I had used different methods of fixation, including the method used for the detection of eGFP tagged delta opioid receptor (Scherrer, Tryoen-Toth et al. 2006). Unfortunately, I could not observe specific CB2-eCFP fluorescence. Elowitz et al. found that a variety of GFPs, including eGFP, could undergo a photoconversion to a red fluorescent species upon irradiation with blue light, from an argon-ion laser or microscope lamp, under anaerobic conditions (Elowitz, Surette et al. 1997). The red fluorescent species thus formed absorbs green fluorescent light at 525 nm and fluoresces with a maximum at 600 nm. Thus GFP photoactivated in this way can be

viewed using a rhodamine filter set. Thus, I had also observed both the filters but found no difference in fluorescence pattern in wild type and CB2-eCFP tagged fluorescent mice.

Considering the possibility of very low-level expression and high autofluorescence, I used more sensitive FACS detection method for analysis. Even in the isolated splenocytes and in peritoneal and bone marrow derived macrophages from the homozygous mice revealed no presence of tagged CB2 receptors. All the findings point towards the absence of the fusion protein in these cells.

I further examined protein level expression of fusion protein using immunoprecipitation with GFP antibody. Unfortunately, in contrast to the cell culture overexpression studies (Fig. 4.9) I could not detect the CB2-eCFP fusion proteins in spleen and thymus (Fig. 4.33). Though, a very weak band of required size appeared in lymph nodes, which may indicate very low-level expression of protein. All these observations indicate that CB2 fusion receptor is not expressed in detectable level. Further, I wanted to observe the expression of the fusion transcript at RNA level. Thus, I analyzed bone marrow differentiated macrophages and dendritic cells, splenocytes, thymus and lymph nodes for the expression of CB2-eCFP transcripts (Fig. 4.34). I observed the presence of the fusion transcript in all tissues. Therefore, the lack of CB2-eCFP expression might be due to the change in CB2 reading frame or incorporation of stopcodon in knock-in locus. However, sequence analysis of amplified PCR product showed no mutations. CB2 fusion with fluorescent proteins by linker can also cause incorporation of the additional splice site. Analysis for additional splice sites did not reveal any additional splice sites incorporated, which could have affected protein translation. Additionally incorporated loxP site in 3' UTR region might interfere with the translation of CB2-eCFP protein. However, CB2-eCFP fusion transcript was present; hence, it is more likely that translation of the fusion protein in *in vivo* system was affected.

Another possible reason for not observing fluorescence could be caused by low level of CB2 receptor *in vivo*. In model systems, neuropathy pain (data unpublished) and contact hypersensitivity (Karsak, Gaffal et al. 2007) increased CB2 mRNA expression was observed. This increase may also result in the increase of CB2 protein. Thus, I had used these models for visualization of CB2-eCFP protein in CB2-eCFP homozygous mice. Unfortunately even in these models, I could not observe specific eCFP fluorescence.

In summary, absence or very low expression level of CB2-eCFP protein resulted into no specific fluorescence in the knock-in mice. This was verified by macroscopic and microscopic visualizations, by FACS analysis and immunoprecipitation with GFP antibody. However, in mRNA analysis CB2-eCFP transcript was observed. This indicates that CB2-eCFP was transcribed correctly. Amplified cDNA product for the CB2-eCFP fusion was sequenced and found to be identical to the expected sequence. Moreover, GFP immunoprecipation did not reveal CB2-eCFP fusion band in *in vivo* system. Together these observations indicate that either the CB2-eCFP mRNA translation or the stability of the fusion protein might have been affected in the knock-in mice.

Alternate approaches for stable expression of CB2 fusion protein in *in vivo* system would be to use additional promoter or Kozak sequence or CB2 poly-A sequence to CB2 sequence. One can also employ the monoallelic replacement of gene of interest by a fluorescent tagged protein (Alferink, Lieberam et al. 2003). However, such pseudo knock-out mice will help us to understand only the expression of CB2 protein but not the functionality of CB2 protein. Moreover, to study receptor mechanism in real time, fluorescent ligands can also be used. These ligands would also provide additional insights into the receptor mediated signal transduction and cellular biochemistry of endocannabinoid system. Recently, such ligands for the cannabinoid receptors have been synthesized by Prof. Alexandros Makriyannis laboratory (personal communication). Further, stability and detection of these ligands in living system needs to be investigated.

So far there are only two known eGFP tagged knock-in mice models reported for GPCRs, delta opioid receptor (Scherrer, Tryoen-Toth et al. 2006) and human rhodopsin (Chan, Bradley et al. 2004). During this work, chimeras with eGFP tagged CB2 receptor have also been generated. Since eGFP has about 3 times stronger fluorescence intensity to that of the eCFP, we expect these eGFP knock-in mice might yield a stronger and specific fluorescence and will help us to visualize CB2 receptor in *in vivo*.

6 Summary

The endocannabinoid system performs various regulatory functions and has been implicated in a growing number of physiological roles. In an animal model for cutaneous contact hypersensitivity (CHS), we show that mice lacking both known cannabinoid receptors display exacerbated allergic inflammation. Cannabinoid receptor antagonists increased allergic inflammation, whereas receptor agonists attenuated inflammation.

The results with CHS demonstrate a protective role of the endocannabinoid system in contact allergy in the skin and suggest a target for therapeutic intervention.

Unfortunately, it is difficult to assess CB2 receptor expression by immunostaining, because we still often observe immunostaining in tissues from CB2 knock-out mice. To overcome this problem the aim of this work was to generate mice with fluorescent tagged CB2 receptors.

During this work various cell lines expressing murine CB2, CB2-eCFP and CB2-eGFP receptors were generated. The cellular distribution and localization of the fusion proteins was analyzed by fluorescence microscopy. Furthermore, agonist dependent Erk-MAPK phosphorylation using CB2 and CB2-eCFP cell lines was also studied.

The fusion protein was found to be localized in the cell membrane as well as in intracellular compartments. This pattern was strikingly analogous to the one observed with a similar CB1-eGFP fusion protein, indicating that the fusion does not change cellular localization.

To determine whether downstream signalling pathways were affected by the C-terminal fusion, CB2 and CB2-eCFP expressing CHO cells were treated with increasing concentrations of the CB2 specific agonist HU-308. A similar pattern of phosphorylation was observed, indicating that the downstream signalling was not altered.

Having established that fluorescence tagging does not affect functionality of CB2 receptor; CB2-eCFP and CB2-eGFP knock-in mice were generated. Unfortunately, only a weak mRNA expression for CB2-eCFP in spleen, lymph nodes and thymus, and either no or a very low CB2-eCFP protein expression by immunoprecipitation was observed. No CB2-eCFP expression was found in peritoneal and bone marrow

derived macrophages, dendritic cells, splenocytes, and lymph node cells by FACS analysis, and also no specific fluorescence in tissue sections of spleen, lymph node, spinal cord, and thymus.

The in-vitro experiments indicate that the functionality of the CB2 receptor was not altered by eCFP fusion. Thus, the tagging strategy should to be useful for the detection of CB2 receptors in living cells or tissues. However, the very weak expression of CB2-eCFP receptors in knock-in mice indicates that the fusion affects expression at translation level and/or stability of the modified protein. During this work, CB2-eGFP knock-in mice were also generated, which are under current analysis.

7 References:

Abood, M. E., K. E. Ditto, et al. (1997). "Isolation and expression of a mouse CB1 cannabinoid receptor gene. Comparison of binding properties with those of native CB1 receptors in mouse brain and N18TG2 neuroblastoma cells." Biochem Pharmacol **53**(2): 207-14.

Adams, M. D., J. T. Earnhardt, et al. (1977). "A cannabinoid with cardiovascular activity but no overt behavioral effects." Experientia **33**(9): 1204-5.

Alberich Jorda, M., N. Rayman, et al. (2004). "The peripheral cannabinoid receptor Cb2, frequently expressed on AML blasts, either induces a neutrophilic differentiation block or confers abnormal migration properties in a ligand-dependent manner." Blood **104**(2): 526-34.

Alferink, J., I. Lieberam, et al. (2003). "Compartmentalized production of CCL17 in vivo: strong inducibility in peripheral dendritic cells contrasts selective absence from the spleen." J Exp Med **197**(5): 585-99.

Anborgh, P. H., J. L. Seachrist, et al. (2000). "Receptor/beta-arrestin complex formation and the differential trafficking and resensitization of beta2-adrenergic and angiotensin II type 1A receptors." Mol Endocrinol **14**(12): 2040-53.

Andersson, S., D. L. Davis, et al. (1989). "Cloning, structure, and expression of the mitochondrial cytochrome P-450 sterol 26-hydroxylase, a bile acid biosynthetic enzyme." J Biol Chem **264**(14): 8222-9.

Baker, D., G. Pryce, et al. (2006). "In silico patent searching reveals a new cannabinoid receptor." Trends Pharmacol Sci **27**(1): 1-4.

Baker, D., G. Pryce, et al. (2003). "The therapeutic potential of cannabis." Lancet Neurol **2**(5): 291-8.

Bamberger, C., A. Scharer, et al. (2005). "Activin controls skin morphogenesis and wound repair predominantly via stromal cells and in a concentration-dependent manner via keratinocytes." Am J Pathol **167**(3): 733-47.

Bari, M., P. Spagnuolo, et al. (2006). "Effect of lipid rafts on Cb2 receptor signaling and 2-arachidonoyl-glycerol metabolism in human immune cells." J Immunol **177**(8): 4971-80.

Basavarajappa, B. S. (2007). "Critical enzymes involved in endocannabinoid metabolism." Protein Pept Lett **14**(3): 237-46.

Batkai, S., D. Osei-Hyiaman, et al. (2007). "Cannabinoid-2 receptor mediates protection against hepatic ischemia/reperfusion injury." FASEB J **21**(8): 1788-800.

Beal, J. and N. Flynn (1995). "AIDS-associated anorexia." J Physicians Assoc AIDS Care **2**(1): 19-22.

Begg, M., P. Pacher, et al. (2005). "Evidence for novel cannabinoid receptors." Pharmacol Ther **106**(2): 133-45.

Ben-Shabat, S., E. Fride, et al. (1998). "An entourage effect: inactive endogenous fatty acid glycerol esters enhance 2-arachidonoyl-glycerol cannabinoid activity." Eur J Pharmacol **353**(1): 23-31.

Berdyshev, E. V. (2000). "Cannabinoid receptors and the regulation of immune response." Chem Phys Lipids **108**(1-2): 169-90.

Berghuis, P., A. M. Rajnicek, et al. (2007). "Hardwiring the brain: endocannabinoids shape neuronal connectivity." Science **316**(5828): 1212-6.

Bermudez-Siva, F. J., A. Serrano, et al. (2006). "Activation of cannabinoid CB1 receptors induces glucose intolerance in rats." Eur J Pharmacol **531**(1-3): 282-4.

Bidlack, J. M. and A. L. Parkhill (2004). "Assay of G protein-coupled receptor activation of G proteins in native cell membranes using [35S]GTP gamma S binding." Methods Mol Biol **237**: 135-43.

Biegon, A. and A. B. Joseph (1995). "Development of HU-211 as a neuroprotectant for ischemic brain damage." Neurol Res **17**(4): 275-80.

Bilkei-Gorzo, A., I. Racz, et al. (2005). "Early age-related cognitive impairment in mice lacking cannabinoid CB1 receptors." Proc Natl Acad Sci U S A **102**(43): 15670-5.

Billinton, N. and A. W. Knight (2001). "Seeing the wood through the trees: a review of techniques for distinguishing green fluorescent protein from endogenous autofluorescence." Anal Biochem **291**(2): 175-97.

Bisogno, T., D. Melck, et al. (1999). "Phosphatidic acid as the biosynthetic precursor of the endocannabinoid 2-arachidonoylglycerol in intact mouse neuroblastoma cells stimulated with ionomycin." J Neurochem **72**(5): 2113-9.

Boshart, M., F. Weber, et al. (1985). "A very strong enhancer is located upstream of an immediate early gene of human cytomegalovirus." Cell **41**(2): 521-30.

Bouaboula, M., B. Bourrie, et al. (1995). "Stimulation of cannabinoid receptor CB1 induces krox-24 expression in human astrocytoma cells." J Biol Chem **270**(23): 13973-80.

Bouaboula, M., N. Desnoyer, et al. (1999). "Gi protein modulation induced by a selective inverse agonist for the peripheral cannabinoid receptor CB2: implication for intracellular signalization cross-regulation." Mol Pharmacol **55**(3): 473-80.

Bouaboula, M., D. Dussossoy, et al. (1999). "Regulation of peripheral cannabinoid receptor CB2 phosphorylation by the inverse agonist SR 144528. Implications for receptor biological responses." J Biol Chem **274**(29): 20397-405.

Bouaboula, M., C. Poinot-Chazel, et al. (1996). "Signaling pathway associated with stimulation of CB2 peripheral cannabinoid receptor. Involvement of both mitogen-activated protein kinase and induction of Krox-24 expression." Eur J Biochem **237**(3): 704-11.

Bouaboula, M., M. Rinaldi, et al. (1993). "Cannabinoid-receptor expression in human leukocytes." Eur J Biochem **214**(1): 173-80.

Bradley, A. e. R., E.J.) (1987). Production and analysis of chimeric mice. In Teratocarcinomas and Embryonic Stem Cells: A Practical Approach.

Brauner-Osborne, H., P. Wellendorph, et al. (2007). "Structure, pharmacology and therapeutic prospects of family C G-protein coupled receptors." Curr Drug Targets **8**(1): 169-84.

Brozoski, D. T., C. Dean, et al. (2005). "Uptake blockade of endocannabinoids in the NTS modulates baroreflex-evoked sympathoinhibition." Brain Res **1059**(2): 197-202.

Buckley, N. E., D. Burbridge, et al. (2006). "Experimental methods to study the role of the peripheral cannabinoid receptor in immune function." Methods Mol Med **123**: 19-40.

Buckley, N. E., K. L. McCoy, et al. (2000). "Immunomodulation by cannabinoids is absent in mice deficient for the cannabinoid CB(2) receptor." Eur J Pharmacol **396**(2-3): 141-9.

Cadas, H., S. Gaillet, et al. (1996). "Biosynthesis of an endogenous cannabinoid precursor in neurons and its control by calcium and cAMP." J Neurosci **16**(12): 3934-42.

Capecchi, M. R. (1989). "Altering the genome by homologous recombination." Science **244**(4910): 1288-92.

Carai, M. A., G. Colombo, et al. (2006). "Investigation on the relationship between cannabinoid CB1 and opioid receptors in gastrointestinal motility in mice." Br J Pharmacol **148**(8): 1043-50.

Carayon, P., J. Marchand, et al. (1998). "Modulation and functional involvement of CB2 peripheral cannabinoid receptors during B-cell differentiation." Blood **92**(10): 3605-15.

Carlisle, S. J., F. Marciano-Cabral, et al. (2002). "Differential expression of the CB2 cannabinoid receptor by rodent macrophages and macrophage-like cells in relation to cell activation." Int Immunopharmacol **2**(1): 69-82.

Carrier, E. J., C. S. Kearn, et al. (2004). "Cultured rat microglial cells synthesize the endocannabinoid 2-arachidonylglycerol, which increases proliferation via a CB2 receptor-dependent mechanism." Mol Pharmacol **65**(4): 999-1007.

Casanova, M. L., C. Blazquez, et al. (2003). "Inhibition of skin tumor growth and angiogenesis in vivo by activation of cannabinoid receptors." J Clin Invest **111**(1): 43-50.

Chakrabarti, A., E. S. Onaivi, et al. (1995). "Cloning and sequencing of a cDNA encoding the mouse brain-type cannabinoid receptor protein." DNA Seq **5**(6): 385-8.

Chan, F., A. Bradley, et al. (2004). "Knock-in human rhodopsin-GFP fusions as mouse models for human disease and targets for gene therapy." Proc Natl Acad Sci U S A **101**(24): 9109-14.

Childers, S. R. and S. A. Deadwyler (1996). "Role of cyclic AMP in the actions of cannabinoid receptors." Biochem Pharmacol **52**(6): 819-27.

Collin, C., P. Davies, et al. (2007). "Randomized controlled trial of cannabis-based medicine in spasticity caused by multiple sclerosis." Eur J Neurol **14**(3): 290-6.

Corbille, A. G., E. Valjent, et al. (2007). "Role of cannabinoid type 1 receptors in locomotor activity and striatal signaling in response to psychostimulants." J Neurosci **27**(26): 6937-47.

Cormack, B. P., R. H. Valdivia, et al. (1996). "FACS-optimized mutants of the green fluorescent protein (GFP)." Gene **173**(1 Spec No): 33-8.

Cornea, A., J. A. Janovick, et al. (1999). "Simultaneous and independent visualization of the gonadotropin-releasing hormone receptor and its ligand: evidence for independent processing and recycling in living cells." Endocrinology **140**(9): 4272-80.

Cossu, G., C. Ledent, et al. (2001). "Cannabinoid CB1 receptor knockout mice fail to self-administer morphine but not other drugs of abuse." Behav Brain Res **118**(1): 61-5.

Coutts, A. A., S. Anavi-Goffer, et al. (2001). "Agonist-induced internalization and trafficking of cannabinoid CB1 receptors in hippocampal neurons." J Neurosci **21**(7): 2425-33.

Cravatt, B. F., D. K. Giang, et al. (1996). "Molecular characterization of an enzyme that degrades neuromodulatory fatty-acid amides." Nature **384**(6604): 83-7.

D'Ambra, T. E., K. G. Estep, et al. (1992). "Conformationally restrained analogues of pravadoline: nanomolar potent, enantioselective, (aminoalkyl)indole agonists of the cannabinoid receptor." J Med Chem **35**(1): 124-35.

Daly, C. J. and J. C. McGrath (2003). "Fluorescent ligands, antibodies, and proteins for the study of receptors." Pharmacol Ther **100**(2): 101-18.

Das, S. K., B. C. Paria, et al. (1995). "Cannabinoid ligand-receptor signaling in the mouse uterus." Proc Natl Acad Sci U S A **92**(10): 4332-6.

De Petrocellis, L., T. Bisogno, et al. (2002). "Effect on cancer cell proliferation of palmitoylethanolamide, a fatty acid amide interacting with both the cannabinoid and vanilloid signalling systems." Fundam Clin Pharmacol **16**(4): 297-302.

DeMorrow, S., S. Glaser, et al. (2007). "Opposing actions of endocannabinoids on cholangiocarcinoma growth: recruitment of Fas and Fas ligand to lipid rafts." J Biol Chem **282**(17): 13098-113.

Derocq, J. M., M. Segui, et al. (1995). "Cannabinoids enhance human B-cell growth at low nanomolar concentrations." FEBS Lett **369**(2-3): 177-82.

Devane, W. A., L. Hanus, et al. (1992). "Isolation and structure of a brain constituent that binds to the cannabinoid receptor." Science **258**(5090): 1946-9.

Deyl, Z., K. Macek, et al. (1980). "Studies on the chemical nature of elastin fluorescence." Biochim Biophys Acta **625**(2): 248-54.

Di Marzo, V. (1998). "'Endocannabinoids' and other fatty acid derivatives with cannabimimetic properties: biochemistry and possible physiopathological relevance." Biochim Biophys Acta **1392**(2-3): 153-75.

Di Marzo, V., C. S. Breivogel, et al. (2000). "Levels, metabolism, and pharmacological activity of anandamide in CB(1) cannabinoid receptor knockout mice: evidence for non-CB(1), non-CB(2) receptor-mediated actions of anandamide in mouse brain." J Neurochem **75**(6): 2434-44.

Di Marzo, V., A. Fontana, et al. (1994). "Formation and inactivation of endogenous cannabinoid anandamide in central neurons." Nature **372**(6507): 686-91.

Dinh, T. P., D. Carpenter, et al. (2002). "Brain monoglyceride lipase participating in endocannabinoid inactivation." Proc Natl Acad Sci U S A **99**(16): 10819-24.

Elowitz, M. B., M. G. Surette, et al. (1997). "Photoactivation turns green fluorescent protein red." Curr Biol **7**(10): 809-12.

Facci, L., R. Dal Toso, et al. (1995). "Mast cells express a peripheral cannabinoid receptor with differential sensitivity to anandamide and palmitoylethanolamide." Proc Natl Acad Sci U S A **92**(8): 3376-80.

Fata, J. E., H. Mori, et al. (2007). "The MAPK(ERK-1,2) pathway integrates distinct and antagonistic signals from TGFalpha and FGF7 in morphogenesis of mouse mammary epithelium." Dev Biol **306**(1): 193-207.

Felder, C. C., K. E. Joyce, et al. (1995). "Comparison of the pharmacology and signal transduction of the human cannabinoid CB1 and CB2 receptors." Mol Pharmacol **48**(3): 443-50.

Ferguson, S. S. (2001). "Evolving concepts in G protein-coupled receptor endocytosis: the role in receptor desensitization and signaling." Pharmacol Rev **53**(1): 1-24.

Fitsialos, G., A. A. Chassot, et al. (2007). "Transcriptional signature of epidermal keratinocytes subjected to in vitro scratch wounding reveals selective roles for ERK1/2, p38, and phosphatidylinositol 3-kinase signaling pathways." J Biol Chem **282**(20): 15090-102.

Fride, E. and R. Mechoulam (1993). "Pharmacological activity of the cannabinoid receptor agonist, anandamide, a brain constituent." Eur J Pharmacol **231**(2): 313-4.

Gabilondo, A. M., J. Hegler, et al. (1997). "A dileucine motif in the C terminus of the beta2-adrenergic receptor is involved in receptor internalization." Proc Natl Acad Sci U S A **94**(23): 12285-90.

Galiegue, S., S. Mary, et al. (1995). "Expression of central and peripheral cannabinoid receptors in human immune tissues and leukocyte subpopulations." Eur J Biochem **232**(1): 54-61.

Galve-Roperh, I., C. Sanchez, et al. (2000). "Anti-tumoral action of cannabinoids: involvement of sustained ceramide accumulation and extracellular signal-regulated kinase activation." Nat Med **6**(3): 313-9.

Ge, C., G. Xiao, et al. (2007). "Critical role of the extracellular signal-regulated kinase-MAPK pathway in osteoblast differentiation and skeletal development." J Cell Biol **176**(5): 709-18.

Gebremedhin, D., A. R. Lange, et al. (1999). "Cannabinoid CB1 receptor of cat cerebral arterial muscle functions to inhibit L-type Ca2+ channel current." Am J Physiol **276**(6 Pt 2): H2085-93.

Gerard, C., C. Mollereau, et al. (1990). "Nucleotide sequence of a human cannabinoid receptor cDNA." Nucleic Acids Res **18**(23): 7142.

Ghosh, S., A. Preet, et al. (2006). "Cannabinoid receptor CB2 modulates the CXCL12/CXCR4-mediated chemotaxis of T lymphocytes." Mol Immunol **43**(14): 2169-79.

Gokoh, M., S. Kishimoto, et al. (2005). "2-Arachidonoylglycerol, an endogenous cannabinoid receptor ligand, enhances the adhesion of HL-60 cells differentiated into macrophage-like cells and human peripheral blood monocytes." FEBS Lett **579**(28): 6473-8.

Gokoh, M., S. Kishimoto, et al. (2005). "2-arachidonoylglycerol, an endogenous cannabinoid receptor ligand, induces rapid actin polymerization in HL-60 cells differentiated into macrophage-like cells." Biochem J **386**(Pt 3): 583-9.

Gonsiorek, W., X. Fan, et al. (2007). "Pharmacological characterization of 2-Hydroxy-N,N- dimethyl-3-{2-[-[(R)-1-(5-methyl- furan-2-yl)-propyl]amino]-3,4-dioxo-cyclobut-1- enylamino}-benzamide (Sch527123), a potent allosteric CXCR1/CXCR2 antagonist." J Pharmacol Exp Ther.

Griffin, G., Q. Tao, et al. (2000). "Cloning and pharmacological characterization of the rat CB(2) cannabinoid receptor." J Pharmacol Exp Ther **292**(3): 886-94.

Grunberg, S. M. (1989). "Advances in the management of nausea and vomiting induced by non-cisplatin containing chemotherapeutic regimens." Blood Rev **3**(4): 216-21.

Gu, Y. Z. and A. Schonbrunn (1997). "Coupling specificity between somatostatin receptor sst2A and G proteins: isolation of the receptor-G protein complex with a receptor antibody." Mol Endocrinol **11**(5): 527-37.

Gupta, P. B., D. Proia, et al. (2007). "Systemic stromal effects of estrogen promote the growth of estrogen receptor-negative cancers." Cancer Res **67**(5): 2062-71.

Heim, R. and R. Y. Tsien (1996). "Engineering green fluorescent protein for improved brightness, longer wavelengths and fluorescence resonance energy transfer." Curr Biol **6**(2): 178-82.

Herkenham, M., A. B. Lynn, et al. (1990). "Cannabinoid receptor localization in brain." Proc Natl Acad Sci U S A **87**(5): 1932-6.

Hipkin, R. W., J. Friedman, et al. (1997). "Agonist-induced desensitization, internalization, and phosphorylation of the sst2A somatostatin receptor." J Biol Chem **272**(21): 13869-76.

Hipkin, R. W., J. Sanchez-Yague, et al. (1992). "Identification and characterization of a luteinizing hormone/chorionic gonadotropin (LH/CG) receptor precursor in a human kidney cell line stably transfected with the rat luteal LH/CG receptor complementary DNA." Mol Endocrinol **6**(12): 2210-8.

Hogen, B., R. Beddington, et al. (1994). "Manipulating the Mouse Embryo." Cold Spring Harbor Laboratory Press **2**.

Howlett, A. C. (2005). "Cannabinoid receptor signaling." Handb Exp Pharmacol(168): 53-79.

Howlett, A. C., F. Barth, et al. (2002). "International Union of Pharmacology. XXVII. Classification of cannabinoid receptors." Pharmacol Rev **54**(2): 161-202.

Howlett, A. C., T. M. Champion, et al. (1990). "Stereochemical effects of 11-OH-delta 8-tetrahydrocannabinol-dimethylheptyl to inhibit adenylate cyclase and bind to the cannabinoid receptor." Neuropharmacology **29**(2): 161-5.

Howlett, A. C., J. M. Qualy, et al. (1986). "Involvement of Gi in the inhibition of adenylate cyclase by cannabimimetic drugs." Mol Pharmacol **29**(3): 307-13.

Hsieh, C., S. Brown, et al. (1999). "Internalization and recycling of the CB1 cannabinoid receptor." J Neurochem **73**(2): 493-501.

Iba, Y., A. Shibata, et al. (2004). "Possible involvement of mast cells in collagen remodeling in the late phase of cutaneous wound healing in mice." Int Immunopharmacol **4**(14): 1873-80.

Ibrahim, M. M., F. Porreca, et al. (2005). "CB2 cannabinoid receptor activation produces antinociception by stimulating peripheral release of endogenous opioids." Proc Natl Acad Sci U S A **102**(8): 3093-8.

Idris, A. I., R. J. van 't Hof, et al. (2005). "Regulation of bone mass, bone loss and osteoclast activity by cannabinoid receptors." Nat Med **11**(7): 774-9.

Ishii, I. and J. Chun (2002). "Anandamide-induced neuroblastoma cell rounding via the CB1 cannabinoid receptors." Neuroreport **13**(5): 593-6.

Izzo, A. A. and A. A. Coutts (2005). "Cannabinoids and the digestive tract." Handb Exp Pharmacol(168): 573-98.

Jansen, E. M., D. A. Haycock, et al. (1992). "Distribution of cannabinoid receptors in rat brain determined with aminoalkylindoles." Brain Res **575**(1): 93-102.

Jarai, Z., J. A. Wagner, et al. (2000). "Cardiovascular effects of 2-arachidonoyl glycerol in anesthetized mice." Hypertension **35**(2): 679-84.

Jarai, Z., J. A. Wagner, et al. (1999). "Cannabinoid-induced mesenteric vasodilation through an endothelial site distinct from CB1 or CB2 receptors." Proc Natl Acad Sci U S A **96**(24): 14136-41.

Jin, W., S. Brown, et al. (1999). "Distinct domains of the CB1 cannabinoid receptor mediate desensitization and internalization." J Neurosci **19**(10): 3773-80.

Johns, D. G., D. J. Behm, et al. (2007). "The novel endocannabinoid receptor GPR55 is activated by atypical cannabinoids but does not mediate their vasodilator effects." Br J Pharmacol.

Johnson, M. R. a. M., L. S. (1986). "The discovery of nonclassical cannabinoid analgetics.

In Cannabinoids as Therapeutic Agents." CRC Press: 121 - 145.

Jorda, M. A., B. Lowenberg, et al. (2003). "The peripheral cannabinoid receptor Cb2, a novel oncoprotein, induces a reversible block in neutrophilic differentiation." Blood **101**(4): 1336-43.

Jorda, M. A., S. E. Verbakel, et al. (2002). "Hematopoietic cells expressing the peripheral cannabinoid receptor migrate in response to the endocannabinoid 2-arachidonoylglycerol." Blood **99**(8): 2786-93.

Juan-Pico, P., E. Fuentes, et al. (2006). "Cannabinoid receptors regulate Ca(2+) signals and insulin secretion in pancreatic beta-cell." Cell Calcium **39**(2): 155-62.

Julien, B., P. Grenard, et al. (2005). "Antifibrogenic role of the cannabinoid receptor CB2 in the liver." Gastroenterology **128**(3): 742-55.

Kallal, L. and J. L. Benovic (2000). "Using green fluorescent proteins to study G-protein-coupled receptor localization and trafficking." Trends Pharmacol Sci **21**(5): 175-80.

Kaplan, B. L., Y. Ouyang, et al. (2005). "Inhibition of leukocyte function and interleukin-2 gene expression by 2-methylarachidonyl-(2'-fluoroethyl)amide, a stable congener of the endogenous cannabinoid receptor ligand anandamide." Toxicol Appl Pharmacol **205**(2): 107-15.

Karsak, M., E. Gaffal, et al. (2007). "Attenuation of allergic contact dermatitis through the endocannabinoid system." Science **316**(5830): 1494-7.

Kishimoto, S., M. Muramatsu, et al. (2005). "Endogenous cannabinoid receptor ligand induces the migration of human natural killer cells." J Biochem (Tokyo) **137**(2): 217-23.

Klein, T. W., C. A. Newton, et al. (2001). "Cannabinoids and the immune system." Pain Res Manag **6**(2): 95-101.

Klein, T. W., C. A. Newton, et al. (1985). "The effect of delta-9-tetrahydrocannabinol and 11-hydroxy-delta-9-tetrahydrocannabinol on T-lymphocyte and B-lymphocyte mitogen responses." J Immunopharmacol **7**(4): 451-66.

Knop, J., R. Stremmer, et al. (1982). "Interferon inhibits the suppressor T cell response of delayed-type hypersensitivity." Nature **296**(5859): 757-9.

Koch, J. E. (2001). "Delta(9)-THC stimulates food intake in Lewis rats: effects on chow, high-fat and sweet high-fat diets." Pharmacol Biochem Behav **68**(3): 539-43.

Kostenis, E., M. Waelbroeck, et al. (2005). "Techniques: promiscuous Galpha proteins in basic research and drug discovery." Trends Pharmacol Sci **26**(11): 595-602.

Kreutz, S., M. Koch, et al. (2007). "Cannabinoids and neuronal damage: differential effects of THC, AEA and 2-AG on activated microglial cells and degenerating neurons in excitotoxically lesioned rat organotypic hippocampal slice cultures." Exp Neurol **203**(1): 246-57.

Lagneux, C. and D. Lamontagne (2001). "Involvement of cannabinoids in the cardioprotection induced by lipopolysaccharide." Br J Pharmacol **132**(4): 793-6.

Lallemand, Y., V. Luria, et al. (1998). "Maternally expressed PGK-Cre transgene as a tool for early and uniform activation of the Cre site-specific recombinase." Transgenic Res **7**(2): 105-12.

Lalonde, M. R., C. A. Jollimore, et al. (2006). "Cannabinoid receptor-mediated inhibition of calcium signaling in rat retinal ganglion cells." Mol Vis **12**: 1160-6.

Lambert, D. M. and V. Di Marzo (1999). "The palmitoylethanolamide and oleamide enigmas : are these two fatty acid amides cannabimimetic?" Curr Med Chem **6**(8): 757-73.

Ledent, C., O. Valverde, et al. (1999). "Unresponsiveness to cannabinoids and reduced addictive effects of opiates in CB1 receptor knockout mice." Science **283**(5400): 401-4.

Lee, D. K., K. R. Lynch, et al. (2000). "Cloning and characterization of additional members of the G protein-coupled receptor family." Biochim Biophys Acta **1490**(3): 311-23.

Leroy, D., M. Missotten, et al. (2007). "G protein-coupled receptor-mediated ERK1/2 phosphorylation: towards a generic sensor of GPCR activation." J Recept Signal Transduct Res **27**(1): 83-97.

Leterrier, C., D. Bonnard, et al. (2004). "Constitutive endocytic cycle of the CB1 cannabinoid receptor." J Biol Chem **279**(34): 36013-21.

Leterrier, C., J. Laine, et al. (2006). "Constitutive activation drives compartment-selective endocytosis and axonal targeting of type 1 cannabinoid receptors." J Neurosci **26**(12): 3141-53.

Lippincott-Schwartz, J. and C. L. Smith (1997). "Insights into secretory and endocytic membrane traffic using green fluorescent protein chimeras." Curr Opin Neurobiol **7**(5): 631-9.

Little, P. J., D. R. Compton, et al. (1989). "Stereochemical effects of 11-OH-delta 8-THC-dimethylheptyl in mice and dogs." Pharmacol Biochem Behav **32**(3): 661-6.

Liu, B. and D. Wu (2004). "Analysis of the coupling of G12/13 to G protein-coupled receptors using a luciferase reporter assay." Methods Mol Biol **237**: 145-9.

Longo, L., A. Bygrave, et al. (1997). "The chromosome make-up of mouse embryonic stem cells is predictive of somatic and germ cell chimaerism." Transgenic Res **6**(5): 321-8.

Lu, T., C. Newton, et al. (2006). "Role of cannabinoid receptors in Delta-9-tetrahydrocannabinol suppression of IL-12p40 in mouse bone marrow-derived dendritic cells infected with Legionella pneumophila." Eur J Pharmacol **532**(1-2): 170-7.

Lukas, S. E., J. H. Mendelson, et al. (1995). "Electroencephalographic correlates of marihuana-induced euphoria." Drug Alcohol Depend **37**(2): 131-40.

Lunn, C. A., J. S. Fine, et al. (2006). "A novel cannabinoid peripheral cannabinoid receptor-selective inverse agonist blocks leukocyte recruitment in vivo." J Pharmacol Exp Ther **316**(2): 780-8.

Maccarrone, M., M. Di Rienzo, et al. (2003). "The endocannabinoid system in human keratinocytes. Evidence that anandamide inhibits epidermal differentiation through CB1 receptor-dependent inhibition of protein kinase C, activation protein-1, and transglutaminase." J Biol Chem **278**(36): 33896-903.

Mackie, K. and B. Hille (1992). "Cannabinoids inhibit N-type calcium channels in neuroblastoma-glioma cells." Proc Natl Acad Sci U S A **89**(9): 3825-9.

Mackie, K., Y. Lai, et al. (1995). "Cannabinoids activate an inwardly rectifying potassium conductance and inhibit Q-type calcium currents in AtT20 cells transfected with rat brain cannabinoid receptor." J Neurosci **15**(10): 6552-61.

Mailleux, P., M. Parmentier, et al. (1992). "Distribution of cannabinoid receptor messenger RNA in the human brain: an in situ hybridization histochemistry with oligonucleotides." Neurosci Lett **143**(1-2): 200-4.

Mallat, A., F. Teixeira-Clerc, et al. (2007). "Cannabinoid receptors as new targets of antifibrosing strategies during chronic liver diseases." Expert Opin Ther Targets **11**(3): 403-9.

Mandavilli, A. (2003). "Marijuana researchers reach for pot of gold." Nat Med **9**(10): 1227.

Marsicano, G., C. T. Wotjak, et al. (2002). "The endogenous cannabinoid system controls extinction of aversive memories." Nature **418**(6897): 530-4.

Martin, M., C. Ledent, et al. (2000). "Cocaine, but not morphine, induces conditioned place preference and sensitization to locomotor responses in CB1 knockout mice." Eur J Neurosci **12**(11): 4038-46.

Martin, P. (1997). "Wound healing--aiming for perfect skin regeneration." Science **276**(5309): 75-81.

Mathre, M. L. (1997). "Cannabis in Medical Practice. A Legal, Historical and Pharmacological Overview of the Therapeutic Use of Marijuana." McFarland & Company, Inc,.

Matsuda, L. A., S. J. Lolait, et al. (1990). "Structure of a cannabinoid receptor and functional expression of the cloned cDNA." Nature **346**(6284): 561-4.

Matsumoto, E., M. Hatanaka, et al. (2006). "PKC pathway and ERK/MAPK pathway are required for induction of cyclin D1 and p21Waf1 during 12-o-tetradecanoylphorbol 13-acetate-induced differentiation of myeloleukemia cells." Kobe J Med Sci **52**(6): 181-94.

Mattes, R. D., K. Engelman, et al. (1994). "Cannabinoids and appetite stimulation." Pharmacol Biochem Behav **49**(1): 187-95.

Mechoulam, R., S. Ben-Shabat, et al. (1995). "Identification of an endogenous 2-monoglyceride, present in canine gut, that binds to cannabinoid receptors." Biochem Pharmacol **50**(1): 83-90.

Mechoulam, R., M. Spatz, et al. (2002). "Endocannabinoids and neuroprotection." Sci STKE **2002**(129): RE5.

Meiri, E., H. Jhangiani, et al. (2007). "Efficacy of dronabinol alone and in combination with ondansetron versus ondansetron alone for delayed chemotherapy-induced nausea and vomiting." Curr Med Res Opin **23**(3): 533-43.

Mihara, K., M. J. Smit, et al. (2005). "Human CXCR2 (hCXCR2) takes over functionalities of its murine homolog in hCXCR2 knockin mice." Eur J Immunol **35**(9): 2573-82.

Milligan, G. (2006). "G-protein-coupled receptor heterodimers: pharmacology, function and relevance to drug discovery." Drug Discov Today **11**(11-12): 541-9.

Miserey-Lenkei, S., Z. Lenkei, et al. (2001). "A functional enhanced green fluorescent protein (EGFP)-tagged angiotensin II at(1a) receptor recruits the endogenous Galphaq/11 protein to the membrane and induces its specific internalization independently of receptor-g protein coupling in HEK-293 cells." Mol Endocrinol **15**(2): 294-307.

Miyawaki, A., J. Llopis, et al. (1997). "Fluorescent indicators for Ca2+ based on green fluorescent proteins and calmodulin." Nature **388**(6645): 882-7.

Moniz, S., F. Verissimo, et al. (2007). "Protein kinase WNK2 inhibits cell proliferation by negatively modulating the activation of MEK1/ERK1/2." Oncogene.

Moore, R. J., R. Xiao, et al. (2000). "Agonist-stimulated [35S]GTPgammaS binding in brain modulation by endogenous adenosine." Neuropharmacology **39**(2): 282-9.

Moro, O., R. Ideta, et al. (1999). "Characterization of the promoter region of the human melanocortin-1 receptor (MC1R) gene." Biochem Biophys Res Commun **262**(2): 452-60.

Mukhopadhyay, S., S. Das, et al. (2006). "Lipopolysaccharide and cyclic AMP regulation of CB(2) cannabinoid receptor levels in rat brain and mouse RAW 264.7 macrophages." J Neuroimmunol **181**(1-2): 82-92.

Munro, S., K. L. Thomas, et al. (1993). "Molecular characterization of a peripheral receptor for cannabinoids." Nature **365**(6441): 61-5.

Natarajan, V., P. V. Reddy, et al. (1981). "On the biosynthesis and metabolism of N-acylethanolamine phospholipids in infarcted dog heart." Biochim Biophys Acta **664**(2): 445-8.

Nazzaro, P., M. Manzari, et al. (1999). "Distinct and combined vascular effects of ACE blockade and HMG-CoA reductase inhibition in hypertensive subjects." Hypertension **33**(2): 719-25.

Nelson, J. A., C. Reynolds-Kohler, et al. (1987). "Negative and positive regulation by a short segment in the 5'-flanking region of the human cytomegalovirus major immediate-early gene." Mol Cell Biol **7**(11): 4125-9.

Niiranen, A. and K. Mattson (1987). "Antiemetic efficacy of nabilone and dexamethasone: a randomized study of patients with lung cancer receiving chemotherapy." Am J Clin Oncol **10**(4): 325-9.

Ofek, O., M. Karsak, et al. (2006). "Peripheral cannabinoid receptor, CB2, regulates bone mass." Proc Natl Acad Sci U S A **103**(3): 696-701.

Offertaler, L., F. M. Mo, et al. (2003). "Selective ligands and cellular effectors of a G protein-coupled endothelial cannabinoid receptor." Mol Pharmacol **63**(3): 699-705.

Oka, S., K. Nakajima, et al. (2007). "Identification of GPR55 as a lysophosphatidylinositol receptor." Biochem Biophys Res Commun **362**(4): 928-34.

Oka, S., J. Wakui, et al. (2006). "Involvement of the cannabinoid CB2 receptor and its endogenous ligand 2-arachidonoylglycerol in oxazolone-induced contact dermatitis in mice." J Immunol **177**(12): 8796-805.

Oka, S., S. Yanagimoto, et al. (2005). "Evidence for the involvement of the cannabinoid CB2 receptor and its endogenous ligand 2-arachidonoylglycerol in 12-O-tetradecanoylphorbol-13-acetate-induced acute inflammation in mouse ear." J Biol Chem **280**(18): 18488-97.

Pacheco, M., S. R. Childers, et al. (1991). "Aminoalkylindoles: actions on specific G-protein-linked receptors." J Pharmacol Exp Ther **257**(1): 170-83.

Panikashvili, D., C. Simeonidou, et al. (2001). "An endogenous cannabinoid (2-AG) is neuroprotective after brain injury." Nature **413**(6855): 527-31.

Parent, J. L., P. Labrecque, et al. (2001). "Role of the differentially spliced carboxyl terminus in thromboxane A2 receptor trafficking: identification of a distinct motif for tonic internalization." J Biol Chem **276**(10): 7079-85.

Parent, J. L., P. Labrecque, et al. (1999). "Internalization of the TXA2 receptor alpha and beta isoforms. Role of the differentially spliced cooh terminus in agonist-promoted receptor internalization." J Biol Chem **274**(13): 8941-8.

Pertwee, R. G. (1997). "Pharmacology of cannabinoid CB1 and CB2 receptors." Pharmacol Ther **74**(2): 129-80.

Pettit, D. A., M. P. Harrison, et al. (1998). "Immunohistochemical localization of the neural cannabinoid receptor in rat brain." J Neurosci Res **51**(3): 391-402.

Pierce, K. L., R. T. Premont, et al. (2002). "Seven-transmembrane receptors." Nat Rev Mol Cell Biol **3**(9): 639-50.

Pilcher, B. K., M. Wang, et al. (1999). "Role of matrix metalloproteinases and their inhibition in cutaneous wound healing and allergic contact hypersensitivity." Ann N Y Acad Sci **878**: 12-24.

Pinsger, M., W. Schimetta, et al. (2006). "[Benefits of an add-on treatment with the synthetic cannabinomimetic nabilone on patients with chronic pain--a randomized controlled trial]." Wien Klin Wochenschr **118**(11-12): 327-35.

Ponti, W., T. Rubino, et al. (2001). "Cannabinoids inhibit nitric oxide production in bone marrow derived feline macrophages." Vet Immunol Immunopathol **82**(3-4): 203-14.

Prescott, S. M. and P. W. Majerus (1983). "Characterization of 1,2-diacylglycerol hydrolysis in human platelets. Demonstration of an arachidonoyl-monoacylglycerol intermediate." J Biol Chem **258**(2): 764-9.

Purnell, W. D. and J. M. Gregg (1975). "Delta(9)-tetrahydrocannabinol,, euphoria and intraocular pressure in man." Ann Ophthalmol **7**(7): 921-3.

Razvi, E. S. (2005). "G-Protein Coupled Receptors (GPCRs): Technical Overview, Emerging Technologies, Market Trends & Opportunities, 2nd Edition." Drug and Market Development Publishing 132.

Richards, M. H. and P. L. van Giersbergen (1995). "Human muscarinic receptors expressed in A9L and CHO cells: activation by full and partial agonists." Br J Pharmacol **114**(6): 1241-9.

Richardson, J. D., S. Kilo, et al. (1998). "Cannabinoids reduce hyperalgesia and inflammation via interaction with peripheral CB1 receptors." Pain **75**(1): 111-9.

Robbe, D., M. Kopf, et al. (2002). "Endogenous cannabinoids mediate long-term synaptic depression in the nucleus accumbens." Proc Natl Acad Sci U S A **99**(12): 8384-8.

Roche, J. P., S. Bounds, et al. (1999). "A mutation in the second transmembrane region of the CB1 receptor selectively disrupts G protein signaling and prevents receptor internalization." Mol Pharmacol **56**(3): 611-8.

Rockman, H. A., W. J. Koch, et al. (2002). "Seven-transmembrane-spanning receptors and heart function." Nature **415**(6868): 206-12.

Rodriguez de Fonseca, F., I. Del Arco, et al. (2005). "The endocannabinoid system: physiology and pharmacology." Alcohol Alcohol **40**(1): 2-14.

Rubino, T., D. Vigano, et al. (2006). "Changes in the expression of G protein-coupled receptor kinases and beta-arrestins in mouse brain during cannabinoid tolerance: a role for RAS-ERK cascade." Mol Neurobiol **33**(3): 199-213.

Ryberg, E., N. Larsson, et al. (2007). "The orphan receptor GPR55 is a novel cannabinoid receptor." Br J Pharmacol.

Salim, S., K. M. Standifer, et al. (2007). "Extracellular signal-regulated kinase 1/2-mediated transcriptional regulation of G-protein-coupled receptor kinase 3 expression in neuronal cells." J Pharmacol Exp Ther **321**(1): 51-9.

Sanchez, C., M. L. de Ceballos, et al. (2001). "Inhibition of glioma growth in vivo by selective activation of the CB(2) cannabinoid receptor." Cancer Res **61**(15): 5784-9.

Sawzdargo, M., T. Nguyen, et al. (1999). "Identification and cloning of three novel human G protein-coupled receptor genes GPR52, PsiGPR53 and GPR55: GPR55 is extensively expressed in human brain." Brain Res Mol Brain Res **64**(2): 193-8.

Schatz, A. R., M. Lee, et al. (1997). "Cannabinoid receptors CB1 and CB2: a characterization of expression and adenylate cyclase modulation within the immune system." Toxicol Appl Pharmacol **142**(2): 278-87.

Scherrer, G., P. Tryoen-Toth, et al. (2006). "Knockin mice expressing fluorescent delta-opioid receptors uncover G protein-coupled receptor dynamics in vivo." Proc Natl Acad Sci U S A **103**(25): 9691-6.

Schmid, P. C., P. V. Reddy, et al. (1983). "Metabolism of N-acylethanolamine phospholipids by a mammalian phosphodiesterase of the phospholipase D type." J Biol Chem **258**(15): 9302-6.

Schnell, S. A., W. A. Staines, et al. (1999). "Reduction of lipofuscin-like autofluorescence in fluorescently labeled tissue." J Histochem Cytochem **47**(6): 719-30.

Scholl, F. A., P. A. Dumesic, et al. (2007). "Mek1/2 MAPK kinases are essential for Mammalian development, homeostasis, and Raf-induced hyperplasia." Dev Cell **12**(4): 615-29.

Schwarz, A., S. Beissert, et al. (2000). "Evidence for functional relevance of CTLA-4 in ultraviolet-radiation-induced tolerance." J Immunol **165**(4): 1824-31.

Scutt, A. and E. M. Williamson (2007). "Cannabinoids stimulate fibroblastic colony formation by bone marrow cells indirectly via CB2 receptors." Calcif Tissue Int **80**(1): 50-9.

Selley, D. E., W. K. Rorrer, et al. (2001). "Agonist efficacy and receptor efficiency in heterozygous CB1 knockout mice: relationship of reduced CB1 receptor density to G-protein activation." J Neurochem **77**(4): 1048-57.

Shire, D., B. Calandra, et al. (1996). "Molecular cloning, expression and function of the murine CB2 peripheral cannabinoid receptor." Biochim Biophys Acta **1307**(2): 132-6.

Shire, D., C. Carillon, et al. (1995). "An amino-terminal variant of the central cannabinoid receptor resulting from alternative splicing." J Biol Chem **270**(8): 3726-31.

Shoemaker, J. L., M. B. Ruckle, et al. (2005). "Agonist-directed trafficking of response by endocannabinoids acting at CB2 receptors." J Pharmacol Exp Ther **315**(2): 828-38.

Showalter, V. M., D. R. Compton, et al. (1996). "Evaluation of binding in a transfected cell line expressing a peripheral cannabinoid receptor (CB2): identification of cannabinoid receptor subtype selective ligands." J Pharmacol Exp Ther **278**(3): 989-99.

Shulman, M. J., L. Nissen, et al. (1990). "Homologous recombination in hybridoma cells: dependence on time and fragment length." Mol Cell Biol **10**(9): 4466-72.

Slipetz, D. M., G. P. O'Neill, et al. (1995). "Activation of the human peripheral cannabinoid receptor results in inhibition of adenylyl cyclase." Mol Pharmacol **48**(2): 352-61.

Smart, D., K. O. Jonsson, et al. (2002). "'Entourage' effects of N-acyl ethanolamines at human vanilloid receptors. Comparison of effects upon anandamide-induced vanilloid receptor activation and upon anandamide metabolism." Br J Pharmacol **136**(3): 452-8.

Smyth, E. M., S. C. Austin, et al. (2000). "Internalization and sequestration of the human prostacyclin receptor." J Biol Chem **275**(41): 32037-45.

Song, C. and A. C. Howlett (1995). "Rat brain cannabinoid receptors are N-linked glycosylated proteins." Life Sci **56**(23-24): 1983-9.

Stadelmann, W. K., A. G. Digenis, et al. (1998). "Impediments to wound healing." Am J Surg **176**(2A Suppl): 39S-47S.

Stadelmann, W. K., A. G. Digenis, et al. (1998). "Physiology and healing dynamics of chronic cutaneous wounds." Am J Surg **176**(2A Suppl): 26S-38S.

Stander, S., H. W. Reinhardt, et al. (2006). "[Topical cannabinoid agonists. An effective new possibility for treating chronic pruritus]." Hautarzt **57**(9): 801-7.

Stander, S., M. Schmelz, et al. (2005). "Distribution of cannabinoid receptor 1 (CB1) and 2 (CB2) on sensory nerve fibers and adnexal structures in human skin." J Dermatol Sci **38**(3): 177-88.

Steffens, S., N. R. Veillard, et al. (2005). "Low dose oral cannabinoid therapy reduces progression of atherosclerosis in mice." Nature **434**(7034): 782-6.

Stewart, J. C., M. L. Villasmil, et al. (2007). "Changes in fluorescence intensity of selected leukocyte surface markers following fixation." Cytometry A **71**(6): 379-85.

Sugiura, T., T. Kodaka, et al. (1996). "2-Arachidonoylglycerol, a putative endogenous cannabinoid receptor ligand, induces rapid, transient elevation of intracellular free Ca2+ in neuroblastoma x glioma hybrid NG108-15 cells." Biochem Biophys Res Commun **229**(1): 58-64.

Sugiura, T., S. Kondo, et al. (1995). "2-Arachidonoylglycerol: a possible endogenous cannabinoid receptor ligand in brain." Biochem Biophys Res Commun **215**(1): 89-97.

Suzuki, H., N. Kamada, et al. (1997). "Germ-line contribution of embryonic stem cells in chimeric mice: influence of karyotype and in vitro differentiation ability." Exp Anim **46**(1): 17-23.

Svanberg, K., E. Kjellen, et al. (1986). "Fluorescence studies of hematoporphyrin derivative in normal and malignant rat tissue." Cancer Res **46**(8): 3803-8.

Szepietowski, J. C., T. Szepietowski, et al. (2005). "Efficacy and tolerance of the cream containing structured physiological lipids with endocannabinoids in the treatment of uremic pruritus: a preliminary study." Acta Dermatovenerol Croat **13**(2): 97-103.

Tam, J., O. Ofek, et al. (2006). "Involvement of neuronal cannabinoid receptor CB1 in regulation of bone mass and bone remodeling." Mol Pharmacol **70**(3): 786-92.

Thomas, K. R. and M. R. Capecchi (1987). "Site-directed mutagenesis by gene targeting in mouse embryo-derived stem cells." Cell **51**(3): 503-12.

Toyota, M., T. Shimamura, et al. (2002). "New bibenzyl cannabinoid from the New Zealand liverwort Radula marginata." Chem Pharm Bull (Tokyo) **50**(10): 1390-2.

Truett, G. E., P. Heeger, et al. (2000). "Preparation of PCR-quality mouse genomic DNA with hot sodium hydroxide and tris (HotSHOT)." Biotechniques **29**(1): 52, 54.

Tsang, K. Y., D. Chan, et al. (2007). "Surviving Endoplasmic Reticulum Stress Is Coupled to Altered Chondrocyte Differentiation and Function." PLoS Biol **5**(3): e44.

Tsou, K., S. Brown, et al. (1998). "Immunohistochemical distribution of cannabinoid CB1 receptors in the rat central nervous system." Neuroscience **83**(2): 393-411.

Twitchell, W., S. Brown, et al. (1997). "Cannabinoids inhibit N- and P/Q-type calcium channels in cultured rat hippocampal neurons." J Neurophysiol **78**(1): 43-50.

Ueda, Y., N. Miyagawa, et al. (2005). "Involvement of cannabinoid CB(2) receptor-mediated response and efficacy of cannabinoid CB(2) receptor inverse agonist, JTE-907, in cutaneous inflammation in mice." Eur J Pharmacol **520**(1-3): 164-71.

Ueda, Y., N. Miyagawa, et al. (2007). "Involvement of cannabinoid CB2 receptors in the IgE-mediated triphasic cutaneous reaction in mice." Life Sci **80**(5): 414-9.

Wade, D. T., P. M. Makela, et al. (2006). "Long-term use of a cannabis-based medicine in the treatment of spasticity and other symptoms in multiple sclerosis." Mult Scler **12**(5): 639-45.

Wagner, J. A., K. Varga, et al. (1999). "Mesenteric vasodilation mediated by endothelial anandamide receptors." Hypertension **33**(1 Pt 2): 429-34.

Wang, X., R. Lu, et al. (2007). "[Effects of extracellular signal-regulated kinase/mitogren-activated protein kinase signaling pathway activation on proliferation and cell cycle associated genes in human colon cancer cells]." Zhonghua Yi Xue Za Zhi **87**(14): 982-6.

Werner, S. and R. Grose (2003). "Regulation of wound healing by growth factors and cytokines." Physiol Rev **83**(3): 835-70.

Werner, S., H. Smola, et al. (1994). "The function of KGF in morphogenesis of epithelium and reepithelialization of wounds." Science **266**(5186): 819-22.

Wiley, J. L., J. J. Burston, et al. (2005). "CB1 cannabinoid receptor-mediated modulation of food intake in mice." Br J Pharmacol **145**(3): 293-300.

Wilkie, T. M., R. L. Brinster, et al. (1986). "Germline and somatic mosaicism in transgenic mice." Dev Biol **118**(1): 9-18.

Wilson, C. L., A. J. Ouellette, et al. (1999). "Regulation of intestinal alpha-defensin activation by the metalloproteinase matrilysin in innate host defense." Science **286**(5437): 113-7.

Wotherspoon, G., A. Fox, et al. (2005). "Peripheral nerve injury induces cannabinoid receptor 2 protein expression in rat sensory neurons." Neuroscience **135**(1): 235-45.

Wright, K., N. Rooney, et al. (2005). "Differential expression of cannabinoid receptors in the human colon: cannabinoids promote epithelial wound healing." Gastroenterology **129**(2): 437-53.

Xia, S., S. Kjaer, et al. (2004). "Visualization of a functionally enhanced GFP-tagged galanin R2 receptor in PC12 cells: constitutive and ligand-induced internalization." Proc Natl Acad Sci U S A **101**(42): 15207-12.

Zhang, J., S. S. Ferguson, et al. (1996). "Dynamin and beta-arrestin reveal distinct mechanisms for G protein-coupled receptor internalization." J Biol Chem **271**(31): 18302-5.

Zhao, Q., Z. He, et al. (2005). "2-Arachidonoylglycerol stimulates activator protein-1-dependent transcriptional activity and enhances epidermal growth factor-induced cell transformation in JB6 P+ cells." J Biol Chem **280**(29): 26735-42.

Zimmer, A. (1992). "Manipulating the genome by homologous recombination in embryonic stem cells." Annu Rev Neurosci **15**: 115-37.

Zimmer, A., A. M. Zimmer, et al. (1999). "Increased mortality, hypoactivity, and hypoalgesia in cannabinoid CB1 receptor knockout mice." Proc Natl Acad Sci U S A **96**(10): 5780-5.

Ziring, D., B. Wei, et al. (2006). "Formation of B and T cell subsets require the cannabinoid receptor CB2." Immunogenetics **58**(9): 714-25.

Zoratti, C., D. Kipmen-Korgun, et al. (2003). "Anandamide initiates Ca(2+) signaling via CB2 receptor linked to phospholipase C in calf pulmonary endothelial cells." Br J Pharmacol **140**(8): 1351-62.

Zygmunt, P. M., D. A. Andersson, et al. (2002). "Delta 9-tetrahydrocannabinol and cannabinol activate capsaicin-sensitive sensory nerves via a CB1 and CB2 cannabinoid receptor-independent mechanism." J Neurosci **22**(11): 4720-7.

Zygmunt, P. M., J. Petersson, et al. (1999). "Vanilloid receptors on sensory nerves mediate the vasodilator action of anandamide." Nature **400**(6743): 452-7.

8 Acknowledgements

I thank Prof. Dr. Andreas Zimmer who welcomed me to his research group, provided me the subject of this thesis and the facilities to accomplish this work under his supervision. His broad knowledge and professional insight were of great importance to accomplish this work. I also express my deep gratitude to Dr. Meliha Karsak for her supervision and total assistance throughout my work. I sincerely appreciate her constructive criticisms and apt suggestions.

I am very thankful to the speaker of Graduate College and my reviewer, Prof. Dr. Michael Famulok for his constant efforts for providing all of graduate students an excellent research atmosphere. I take this opportunity to thank all group leaders from Graduate College for conducting very informative workshops and seminars during the tenure of this program. This work would not have been possible without financial support from Graduate College 804. I would like to thank GRK-804 co-ordinator, Dr. Sven Jan Freudenthal for his constant support and encouragement.

I am grateful to Prof. Dr. Sabine Werner and Dr. Monica Krampert (ETH, Zurich) for their co-operation and inputs.

Pleasant company of my colleagues has made my stay in Bonn immensely enjoyable. I admire and thank each one of them for their help and understanding. Particularly, I thank Edda Erxlebe, Julia Essig, Anne Zimmer, Kerstin Michel, Angela Harmeth, Friederike Stamer, Charlotte Schick, Jürgen Schmidt and Maria Jaruszowiec for their excellent technical assistance. I deeply appreciate the secretarial help I received from Hedwig Gutschmidt, Tanja Sauerborn and Katja Krumnack.

I would also like to thank Dr. David Otte, Dr. Irfan Tamboli, Britta Schürmann, Jennifer Rehnelt and Hanna Vanderloop for their helpful advice during manuscript writing. I thank all my friends for their constant support.

My parents encouraged me to achieve my goals and always stood behind me. Their life has been greatest source of inspiration to me. I thank Vishal and Aparna for their love, compromises and support during all these years. In no words I can express my gratitude and love towards my family.

Finally, I salute my motherland. वन्दे मातरम् ।

9 Resume

Name: Date Rahul Anant

Address:

Birthdate:

Educational background:

06/1983 - 05/1986	Primary School in Shri Shivaji Maratha High School, Pune, India
06/1986 - 05/1993	Secondary School in Jnana Prabothini Prashala, Pune, India
06/1993 - 05/1995	Higher Secondary School in Abasaheb Garware College, Pune, India
06/1995 - 05/1998	Bachelor of Science (Chemistry), Pune University, Pune, India
06/1998 - 05/2000	Master of Science (Biochemistry), Pune University, Pune, India
Since 05/2004	PhD Student at Rheinischen Friedrich Wilhelms University, Bonn, Germany in ″Analysis of cellular functions by combinatorial chemistry and biochemistry″, GRK-804, under the guidance of Prof. Dr. Andreas Zimmer.

Work experience:

06/2004 - 06/2004	Research officer, Unilever research center, Bangalore, India
12/2004 - 04/2004	Research coworker, Heinrich Heine University, Duesseldorf, Germany

Publications:

* Attenuation of allergic contact dermatitis through the endocannabinoid system

Meliha Karsak, Evelyn Gaffal, **Rahul Date**, Lihua Wang-Eckhardt, Jennifer Rehnelt, Stefania Petrosino, Katarzyna Starowicz, Regina Steuder, Eberhard Schlicker, Benjamin Cravatt, Raphael Mechoulam, Reinhard Büttner, Sabine Werner, Vincenzo Di Marzo, Thomas Tüting, Andreas Zimmer
Science, Vol.316, no.5830 (2007), 1494 - 1497

* Oxidative modification of low-density lipoprotein: lipid peroxidation by myeloperoxidase in the presence of nitrite

T. Kraemer, I. Prakosay, **R.A. Date**, H. Sies and T. Schewe
Biological Chemistry, Volume 385, Issue 9 (2004), 809-818

Bonn, 21/11/2007

10 Publication

Part of this work has been previously published in the following peer reviewed journal:

- Attenuation of allergic contact dermatitis through the endocannabinoid system

Meliha Karsak*, Evelyn Gaffal*, **Rahul Date**, Lihua Wang-Eckhardt, Jennifer Rehnelt, Stefania Petrosino, Katarzyna Starowicz, Regina Steuder, Eberhard Schlicker, Benjamin Cravatt, Raphael Mechoulam, Reinhard Büttner, Sabine Werner,Vincenzo Di Marzo, Thomas Tüting, Andreas Zimmer

Science, Vol.316, no.5830 (2007), 1494 - 1497

* Equal contributors